Adaptive Changes in the Morphology of Natural Materials Due to Alterations in Mechanical Stress

by

Katharine I. Hsu

BACHELOR OF SCIENCE IN CIVIL AND ENVIRONMENTAL ENGINEERING
UNIVERSITY OF CALIFORNIA, LOS ANGELES, 1995

Submitted to the Department of Civil and Environmental Engineering
in Partial Fulfillment of the Requirements for the Degree of

MASTER OF SCIENCE IN CIVIL AND ENVIRONMENTAL ENGINEERING
at the
MASSACHUSETTS INSTITUTE OF TECHNOLOGY

February 1997

Author _____
Department of Civil and Environmental Engineering
January 19, 1997

Certified By _____
Lorna J. Gibson
Professor of Civil and Environmental Engineering
Thesis Supervisor

Accepted By _____
Joseph M. Sussman
Professor of Civil and Environmental Engineering
Chairman, Departmental Committee on Graduate Studies

Adaptive Changes in the Morphology of Natural Materials Due to Alterations in Mechanical Stress

by

Katharine I. Hsu

Submitted to the Department of Civil and Environmental Engineering
On January 19, 1997
In Partial Fulfillment of the Requirements for the Degree of
Master of Science in Civil and Environmental Engineering

Abstract

Natural materials have shown their ability to adapt their geometry in response to mechanical stress. In examining their shape and structure, it becomes apparent that the major strategic function of structural materials and systems involves mechanical support under changing load. This comparison study examines how the morphology of four biological materials (bone, wood, plant stems, and blood vessels) is influenced by environmental loading conditions. As these materials remodel their shape through adaptive growth, they seek to maintain an optimal structure that is able to sustain a particular mechanical support requirement.

Bone and wood adapt to increased mechanical load by increasing their density while plant stems and blood vessels develop thicker vessel walls. For bone, trabecular bone density and cortical bone thickness are increased with load in order to maintain a roughly constant peak functional strain; wood and blood vessels remodel their shape under elevated levels of stress in order to maintain a constant surface stress and constant circumferential stress, respectively. In addition, plant stems and blood vessels which develop thicker vessel walls due to mechanical stressing show a tendency to reduce their elastic modulus so that they could overcome their stiffness and become more flexible, preventing rupture. The examination of these materials suggests that natural materials remodel functions to maintain a constant stress or strain, giving a constant factor of safety.

Thesis Supervisor: Lorna J. Gibson
Title: Professor of Civil and Environmental Engineering

Acknowledgments

I would like to express my gratitude to Professor Lorna J. Gibson for her guidance throughout this project. It has been a great privilege for me to learn from you.

My graduate school life experience would not have been complete without the shared moments with friends from Boston Chinese Evangelical Church's Graduate Student Small Group. Thank you for sympathizing with me and sharing in my joys as we all learned what it was like to "drink from a fire hose". Your friendship will be treasured. To MIT Chinese Christian Fellowship - you have touched my life through your sincerity and genuine love for our Lord. I will never forget the joy that I see in your hearts.

E-Mail has served as my lifeline to the support of my friends back home. Thank you all for your friendship, laughter, compassion, and long-distance prayers. I especially cherish the honesty, understanding, and prayers of my fellow junk-food aficionado. Your friendship is very precious to me; God is good!

I would have been difficult to persevere without the love and encouragement of my family. Mom and Dad - I appreciate all of your sacrifices. You have always served as godly examples for me. Michael - you have become more than a brother to me, but also a friend. Know that I am always praying for you.

I give my utmost to my Lord, Jesus Christ, who is my strength in weakness. May my small achievements be a reflection of your endless grace. You deserve all praise and glory. I continue to find joy in obedience and contentment in each day because You are the strength of my heart.

Because of the Lord's great love we are not consumed,
for his compassions never fail.
They are new every morning;
great is your faithfulness.

Lamentations 3:22-23

Table of Contents

Chapter 1: Introduction

Biological systems often have efficient designs because their structure has been able to evolve and adapt to its environment over time. One example can be seen in wood, which has a strength per unit weight comparable to steels. Antlers, shell and bone have a toughness an order of magnitude greater than engineering ceramics. Many engineering designs look to nature as an inspiration because of its tendency for optimum structural or material design. The Crystal Palace built in London for the 1851 Exhibition was designed by Sir Joseph Paxton who conceived the link-work construction by examining a leaf of a water lily. Sir Marc Brunel studied a ship worm when designing a tunneling shield for the construction of the Wapping Tunnel. It has also been suggested that the 1915 patent by Junkers for a honeycomb or sandwich airplane structure was based on the internal structure of a pheasant feather. Science has come full circle as more and more scientists are looking towards nature's materials for clues about how to make stronger composites, improve building materials, and build more efficient structures. [Ashby *et al.* 1995, Cowin 1986, Gibson *et al.* 1995]

Natural materials have evolved to fulfill the needs arising from the ways animals and plants function. Many of these needs involve mechanical adaptation: the need to support static and dynamic loads created by organism mass, the need to store and release elastic energy, the need to resist fracture. Adaptive optimization has lead to the formation of exceptionally efficient materials as this process seeks to minimize the mass of material required for some mechanical requirement (i.e. stiffness, strength, toughness) to minimize the metabolic energy required for synthesizing materials. Natural materials are able to adapt their geometry in response to mechanical stresses. As the material experiences modifications in the type of loading it experiences, the material can change or *remodel* its structure such that the general function of the material is maintained. Functional analysis ventures to describe the way an organic structure or process contributes to the maintenance and survival of an organism.

Biomechanics attempts to understand the mechanics of living systems. The term "mechanics" is used to describe force, motion, and strength of materials. In general,

mechanics is utilized in the analysis of a dynamic system, and the biological world has become an object of inquiry. Biology can provide insights into the structure and function of certain materials and how biological systems work to support one another; for example, how the shape of a bone accommodates the type of loading it experiences, how external environmental conditions influence the growth of a tree, how a body's circulation system obliges elevations in blood pressure.

The focus of this comparative study will be to examine how the shape of biological materials is influenced by the loading conditions of their environment. Studies on bone, wood, plant stems, and blood vessels have all shown morphological adaptations when subjected to a change in mechanical loading. In each of these materials, there is a consistent finding that with increased loading, tissue deposition is increased to adapt to such a change. This thesis will examine what the mechanical criteria are for such remodeling behavior and attempt to determine if there are any similarities in the remodeling of the above materials.

The following chapters will investigate the following natural materials: bone, wood, plant stems, and blood vessels. Each chapter will first look at the basic structure and composition of the material. Subsequently, experiments which focus on morphological adaptations to mechanical loading will be reviewed so as to understand the effects of loading on the material, followed by an evaluation of how the materials' general form is optimized for the given loading condition. The concluding chapter compares the functional adaptive changes in morphology of the four materials.

References

Ashby, M.F., L.J. Gibson, U. Wegst, and R. Olive. 1995. The Mechanical Properties of Natural Materials - I: Material Property Charts. *Proc. R. Soc. Lond. A.*, v. 450, pp. 123-140.

Cowin, S.C. 1986. Wolff's Law of Trabecular Architecture at Remodeling Equilibrium. *Journal of Biomechanical Engineering*, v. 108, pp. 83-88.

Gibson, L.J., M.F. Ashby, G.N. Karam, U. Wegst, and H.R. Shercliff. 1995. The Mechanical Properties of Natural Materials - II: Microstructures of Mechanical Efficiency. *Proc. R. Soc. Lond. A.*, v. 450, pp. 141-162.

Chapter 2: Bone

2.1. *Introduction*

It has been recognized that there exists a relationship between the intensity of mechanical loading to which a skeleton is exposed during daily activities and the mass and strength of the bone. Through casual observation, one notices that large, heavy individuals who are more physically active are inclined to have denser and stronger bones compared to frail, sedentary individuals. Along with bone density variations which appear in different individuals, there are also complex distributions of *bone apparent density* (bone mass per unit volume) within the bone of a specific person or animal. This is a result of bone's ability to adapt to the changes in its loading pattern. It is able to adjust its density to accommodate increasing or decreasing load such that its strength is maintained if not improved.

Remodeling in the context of adaptation to a mechanical environment is used to describe any adaptive changes in bone. Internal remodeling usually refers to trabecular bone remodeling and occurs in a process of activation, resorption, and formation. Remodeling of the endosteal and periosteal surfaces of cortical bone tend to involve more modeling, where formation and resorption of bone tissue may occur more independently, or repair processes. In this chapter, observations in long bone in both trabecular and cortical bone, will be examined based on the theories and experiments put forth in recent publications. This study will look at bone structure and see how this natural material responds to loads through its modeling process.

2.2. *Bone Composition and Structure*

Bone is described as a connective tissue which supports the various structures of the body by supporting it against gravity, acting as a lever system for muscular action, and serving as a protective covering for vital internal organs. Bone is also a metabolic tissue in that it serves as a supply for calcium which is essential for nerve conduction, clot

formation, and cell secretion. In mechanical terms, bone can be considered a composite material with solid and fluid phases.

2.2.1. *Bone Composition on a Molecular Level*

On the molecular level, bone is a composite material composed of a fibrous protein, known as collagen, and stiffened by the dense filling of calcium phosphate. Some of its other components include water, amorphous polysaccharides, proteins, and living cells and blood vessels. Collagen acts as a structural protein; the protein molecule, tropocollagen, consists of three polypeptides of the same length and combines to form the microfibrils of collagen. Tropocollagen molecules are approximately 260 *nm* long and are staggered along side each other by one-fourth their length. They possess the tendency to combine together to form microfibrils by bonding head to tail with molecules of neighboring fibrils. There is a small gap or *hole region* between the head of one molecule and the tail of the next, and because the tropocollagen molecules are stacked side by side, these gaps produce a 67 *nm* periodicity. On the whole, the microfibril is stabilized by intermolecular crosslinks as microfibrils gather to form fibrils. The collagen microfibrils, together with glycosaminoglycans, form the organic phase of bone's extracellular matrix. The high collagen content (90%) in the organic phase assists bone in resisting tensile stresses. The inorganic or mineral phase consists mainly of calcium phosphate crystals and gives the bone its exceptional resistance to compressive stresses. It comprises approximately 50% of bone by volume and 75% by weight. The inorganic material in bone corresponds fairly closely to hydroxyapatite, $3Ca_3(PO_4)_2 \bullet Ca(OH)_2$, with small quantities of other ions. It exists as tiny crystals about 200 $\mathring{A}$ long with an average cross-section of about 2500 $\mathring{A}^2$. These hydroxyapatite crystals are arranged along the length of the collagen fibrils. Thus, bone is essentially a composite material made up of collagen and hydroxyapatite. The apatite crystals are very strong and stiff while collagen is not; thus the Young's modulus of cortical bone (18 *GPa* in tension in the human femur) is between that of apatite and collagen. As a composite material, bone's strength is higher

than that of apatite or collagen alone because its softer components prevent the stiff ones from brittle cracking and the stiff components prevent the soft ones from yielding.

Bone cells which are embedded in the extracellular matrix include osteoblasts (bone-forming cells), osteoclasts (bone-destroying cells), and osteocytes (bone-maintaining cells). *Osteoblasts* **[Figure 2.1]** are cuboidal cells with a single, rounded nucleus surrounded by an extensive rough endoplasmic network associated with the production of protein (collagen and proteoglycan in the organic phase). Osteoblasts also maintain a Golgi[1] apparatus for packaging and changing proteins for secretion. In general these cells can be found as a continuous layer on bone surfaces during active deposition. *Osteoclasts* **[Figure 2.2]** are characterized as large, multinucleated cells with a ruffled, membrane border located along the bone surface. These particular cells can have a diameter up to 100 μ and can contain up to 50 nuclei. Like osteoblasts, osteoclasts have well-developed Golgi bodies which produce lysosomes that aid in the breakdown of underlying bone while mitochondria[2] are also abundant in the cytoplasm of osteoclasts. *Osteocytes*, the bone-maintaining cells, **[Figure 2.3]** are actually osteoblasts trapped in small spaces called lacunae in surrounding osteoid. These cells tend to be flattened with few cellular organelles and a single nucleus. Osteocytes maintain an extensive network of interaction with other cells through cellular processes within openings in the bone known as canaliculae. Gap junctions which join the processes from adjacent cells provide a pathway for metabolic diffusion and are essential for maintaining viable bone. If there is an interference in the canalicular network, it may result in osteocyte death, and that portion of bone becomes necrotic and removed by osteoclasts.

Osteocytes are the remains of osteoblasts which have secreted bone around themselves and become isolated from the extracellular matrix. Approximately 10% of the osteoblasts which deposit bone carry on as osteocytes while the others disappear. It has been observed that osteoblast and osteocyte orientations are parallel to collagen fibers. The result is a fibrous, oriented-composite matrix with cells that can sense stress directions

[1] A Golgi body is an organelle consisting of layers of flattened sacs that take up and process secretory and synthetic products from endoplasmic reticulum. It then either releases the finished products into various parts of cell cytoplasm or secretes them to the outside of the cell.
[2] Mitochondria are organelles in the cytoplasm of cells that function in energy production.

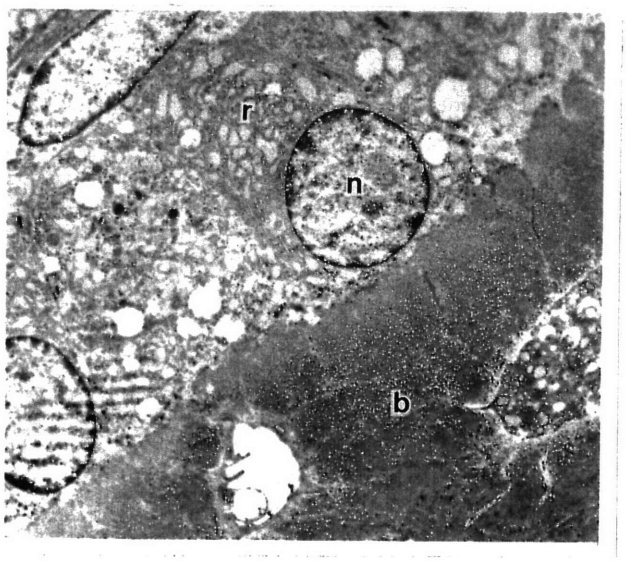

Figure 2.1: Osteoblasts on Bone Surface (x 3640). (*b*) = bone; (*n*) = nucleus; (*r*) = rough endoplasmic reticulum. [Bouvier 1989]

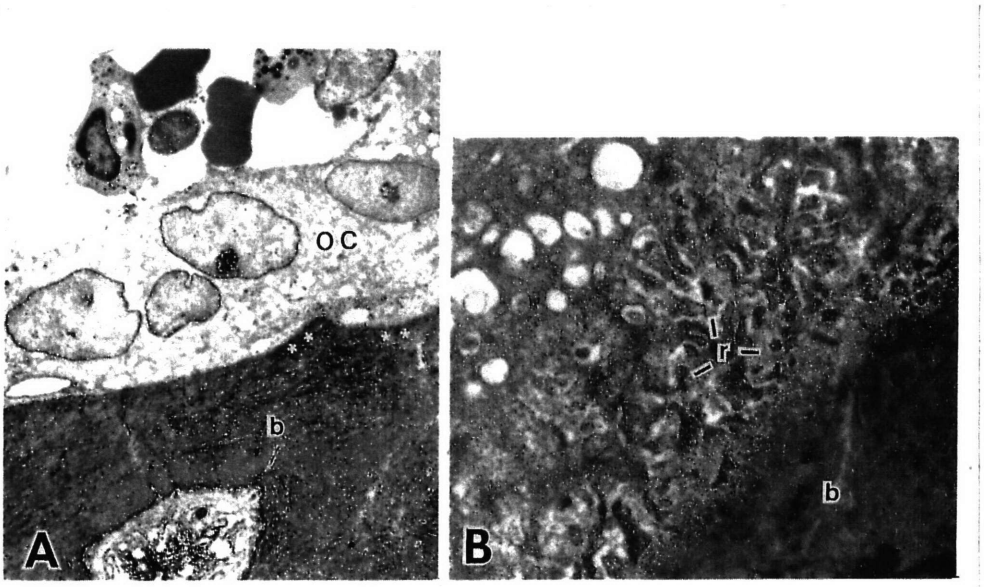

Figure 2.2: Electron Micrograph of Osteoclast. (A) Osteoclast (*OC*) with 4 Nuclei (*) on Bone Surface (x 3090). (B) Ruffled Border (*r*) of Osteoclasts (x 15,465). [Bouvier 1989]

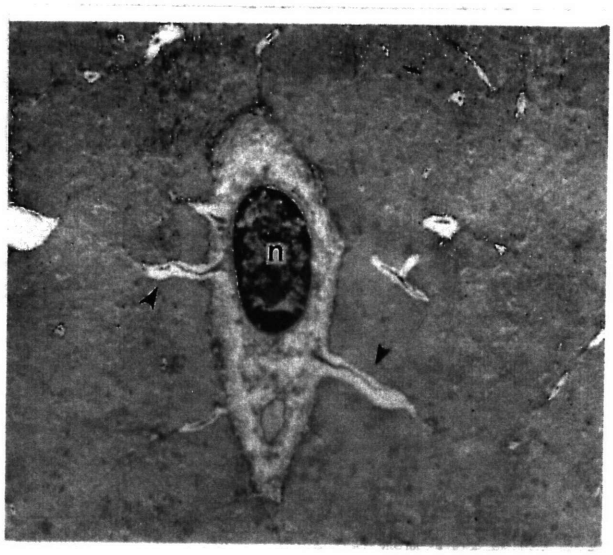

Figure 2.3: Osteocyte with Lacuna (x 5200). (*n*) = nucleus. [Bouvier 1989]

and gradients. Collagen fibers parallel osteocyte lacunae orientation, and this formation has the tendency to reduce any stress concentrating effects that may occur in voids.

After the initial deposition of bone, the tissue is usually subjected to secondary reconstruction also known as remodeling which takes the form of osteons that are formed in two basic steps. The osteoclast creates a small tunnel which is invaded by blood vessels and filled by osteoblasts. These osteoblasts fill in the osteoclast resorption canals by laying down a cement line (characterized by low collagen content) and concentric rings of bone tissue. This then leaves a small opening in the center for nerves and blood vessels.

As bone adapts to mechanical loading, a decrease in load causes bone resorption while an increase causes bone formation. The osteoclasts and osteoblasts are responsible for this resorption and formation. It is hypothesized that bone contain cells (osteocytes) which are sensitive to mechanical signals such that there is a way of measuring mechanical loading in the bone for it to adapt to changes in mechanical requirements. At the same time, there is the assumption that bone mass regulation takes place at a local level, where there exists a steady state or remodeling equilibrium. As mechanical loading is altered, the bone tissue responds accordingly. [Bouvier 1989, Currey 1984, Fung 1981, Martin *et al.* 1989]

2.2.2. *Bone Microstructure: Woven Bone, Primary Bone, Secondary Bone*

The basic cellular and chemical components of bone are similar in all types of bone, however their differing properties are related to their varying organization and control of these components. Bone can produce two types of tissue, a regularly orientated and highly organized tissue and a randomly orientated and poorly organized tissue. As bone matures, its microstructure changes, and these changes in microstructure can be divided into three general categories: woven-fibered bone, primary bone, and secondary bone.

The initial bone that is laid down is *woven bone*. **[Figure 2.4]** This particular type of bone is the only kind that can be deposited without any previous hard tissue or cartilage model, also termed *de novo*. It is associated with periods of rapid formation as in accelerated growth or fracture repair. Woven bone is quickly laid and most

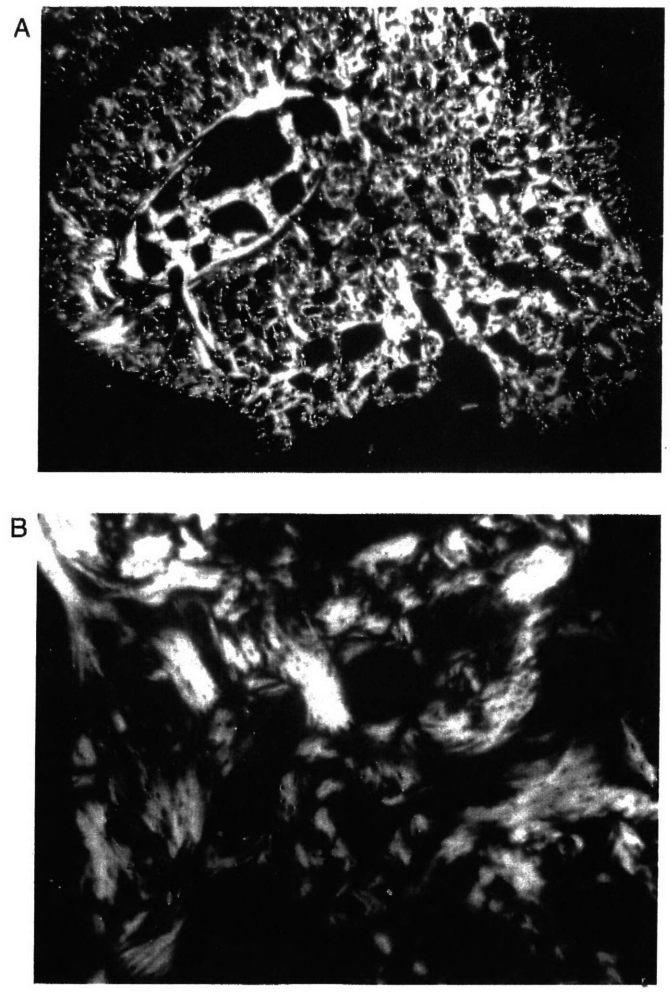

Figure 2.4: (A) Ulna from Dog Showing Woven Bone Formation along Surface (Original Magnification x 3.12). (B) Higher Magnification of Same Bone (Original Magnification x 25). [Martin *et al.* 1989]

characteristically found in the fetus and in the callus, or thick tissue, produced during fracture repair. Collagen of woven bone is randomly orientated and fine-fibered with a diameter of approximately 0.1 μm; its random orientation makes it difficult to discern any preferred directions over distances greater than a few micrometers. Woven-fibered bone is generally less dense than other types of bone and can become highly mineralized and brittle. Its reduced density is a function of the loose packing of collagen fibers and large porosities. Like all bone, woven bone contains osteocytes located in the lacunae and blood vessels. The spaces surrounding the blood vessels are quite extensive which differs from the structure of lamellar bone. The primary function of woven bone is mechanical where it provides both temporary strength and scaffolding where lamellar bone can be deposited since other bone tissues cannot be formed de novo.

The second type of bone microstructure is *primary bone* which varies during its developmental process. Primary bone cannot be deposited de novo like woven bone, but must be placed on a preexisting substrate. It is also more slowly forming and has a higher mineral content compared to that of woven bone. There are three types of primary bone: primary lamellar **[Figure 2.5]**, plexiform **[Figure 2.6]**, and primary osteons **[Figure 2.7]**. These are all morphologically distinct from one another and offer different mechanical and physiological properties for different functions. Primary bone is generally characterized by its more precise arrangement and thin layers, approximately 200μ in thickness for each laminae, with collagen fiber orientated at right angles to the laminae. Collagen fibers in any one lamella are parallel to each other, but the fibers in successive lamellae are at about right angles to each other. *Primary lamellar bone* is organized circumferentially around the inner and outer surface of the whole bone. It is very dense with few vascular channels and discontinuities. *Plexiform bone*, on the other hand, is rapidly deposited like woven bone, but achieves better mechanical properties. This type of primary bone is especially necessary in growing animals whose skeletal system must keep up with rapid growth and also reduce the potential of bone fracture. Plexiform bone possesses the appearance of intertwining vascular network throughout the bone. It is highly oriented and begins to form from buds from the subperiosteal or subendosteal bone surface and grows perpendicularly from the surface for a short distance. They are then reoriented and grow

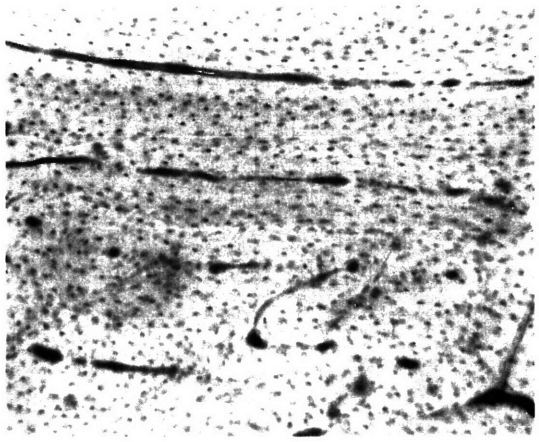

Figure 2.5: Primary Lamellar Bone from Dog Radius (Original Magnification x 25). [Martin *et al.* 1989]

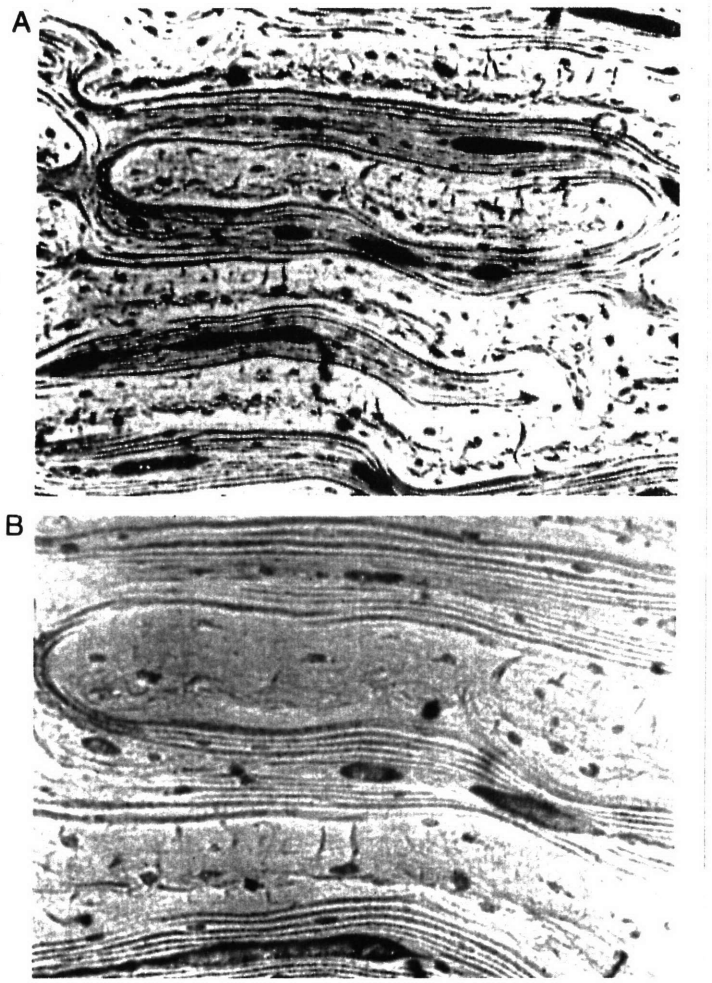

Figure 2.6a: Bovine Plexiform Bone Containing a Core of Nonlamellar Bone with Spaces Inbetween Containing Blood Vessels Surrounded by Primary Lamellar Bone. (A) Original Magnification x 21; (B) Original Magnification x 35.2. [Martin *et al.* 1989]

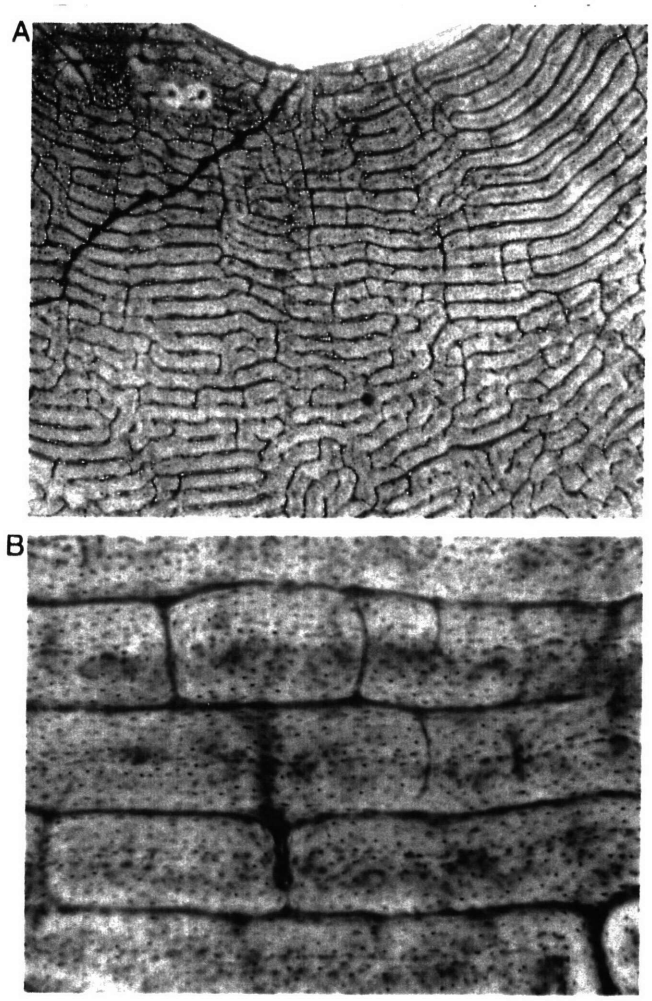

Figure 2.6b: Fully Formed Plexiform Bone in Adult Sheep at: (A) Original Magnification x 6.25, (B) Original Magnification x 25. [Martin *et al.* 1989]

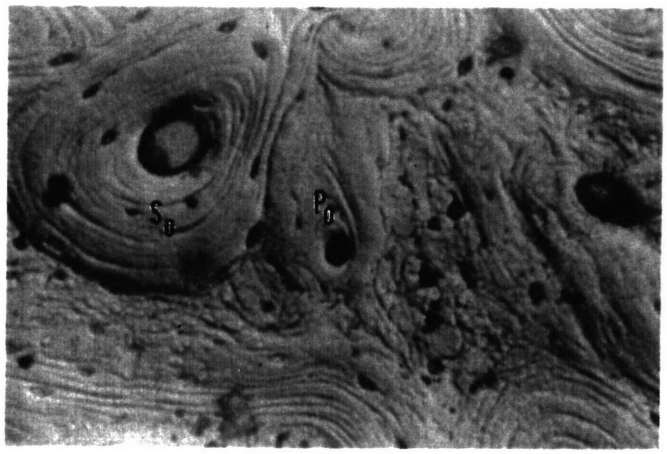

Figure 2.7: Transverse Section of Bovine Bone showing Primary (P_o) and Secondary (S_o) Osteons (Original Magnification x 35.2). [Martin *et al.* 1989]

parallel to the surface. Plexiform bone is primarily found in larger, rapidly growing animals such as elephants, cows, some dinosaurs, and larger breeds of dogs. It has also been found in humans - in growing children around the time of major growth spurts. Some of the advantages of plexiform bone include creating large amounts of surface area which are covered by vascular connective tissues, and thus increasing the area for formation and storage of red blood cells. Plexiform bone also improves the strength of bone by providing twice the amount of surface area for bone matrix deposition with the parallel buds of bone. At the same time, most of this bone formation is seen on the periosteal surface of the long bone diaphysis which is an ideal place to add bone because it is furthest from the neutral axis in bending, and consequently small additions of bone significantly add to the bone's structural rigidity.

The third type of primary bone is arranged concentrically around individual vascular channels and not around the entire bone cortex. A set of these concentric lamellae range from a few to as many as 20, and with the osteocytes and central vascular channel, they compose the *primary osteon*. **[Figure 2.7]** The main distinction between primary and secondary osteons (which will be defined below) is the absence of a cement line or reversal line characterized by its low collagen content. This absence of the cement line is a result of the fact that the bone is not a product of remodeling. In general, primary osteons are modified vascular channenels as a consequence of sequential layering of bone. These osteons are found within well-organized primary lamellar bone and can also function as storage space for exchangeable calcium ions.

When bone is a product of the resorption of previously existing tissue or a product of deposition of new bone tissue in its place, it is defined as *secondary bone*, the last category of bone microstructure. The qualifying distinction between primary bone and secondary bone is that primary bone is completely new while secondary bone is "replacement" bone. Secondary bone is initiated by the resorption of whole bone by osteoclasts and subsequent formation by osteoblasts is a secondary osteon. The secondary osteon has a central vascular channel with a diameter of 50-90 μm, and this is known as the Haversian canal. It is surrounded by a series of concentric lamellae with osteocytes arranged in a circular pattern. The lamellae spiral around the osteon in layers giving the

secondary osteon a diameter of approximately 200-300 μm in human bone. The Haversian canal contains blood vessels, nerves, and a variety of cell types depending on the age of the osteon. Osteonal vessels average a diameter of 15 μm, but grow wider near the endosteal surface. These vessels contain no smooth muscle, but rather are capillaries lined with a layer of endothelial cells. The area between the vessel and canal wall contains a variety of different cells, and it is frequently possible to observe osteoblasts in the process of surrounding themselves with bone matrix. Adjacent to the Haversian canal are the lining cells which are the resting osteoblasts that provide a pool of potential bone-forming cells. [Martin *et al.* 1989]

2.2.3. *Cortical Bone and Trabecular Bone*

At the next higher level of bone structure is bone tissue which exists in two fundamental forms: cortical bone and trabecular bone. *Cortical bone* is a dense material with a specific gravity of approximately *2*. It is solid with spaces only for osteocytes, canaliculi, capillaries, or sites of erosion. Cortical bone's smooth outer surface is called the periosteal surface while its internal surface is identified as the endosteal surface. **[Figure 2.8]** On the periosteal surface, numerous layers of lamellar bone accumulate forming a thick cortical plate. *Trabecular bone*, also known as cancellous bone, exists in the metaphyseal region of long bones such as the femur, humerous, radius, ulna, and tibia, and within the bounds of cortical bone coverings of smaller flat and short bones such as the vertebrae. **[Figure 2.9]** It is composed of short struts (approximately 0.1 *mm* in diameter and extending for about 1 *mm*) of bone material called trabeculae which can be idealized as rod- and plate-shaped. The connected trabeculae give cancellous bone a spongy appearance; it is quite porous often with half the bone volume associated with pore volume. No blood vessels exist within the trabeculae, but vessels adjacent to the tissue weave in and out of the large spaces between the struts. The material composing trabecular bone is usually primary lamellar bone and sometimes fragments of Haversian bone. In young mammals, it can also be made of woven-fibered bone.

The structure of trabecular bone varies both in microscopic and macroscopic anisotropy as well as in its porosity which is proportional to the total volume unoccupied

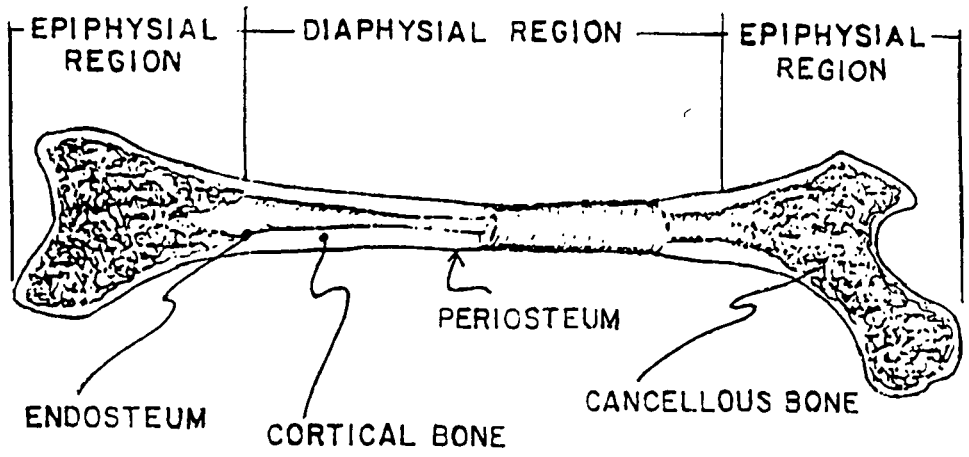

Figure 2.8: Sketch of Longitudinal Section of Femur Illustrating Trabecular and Cortical Bone Types. [Cowin 1981]

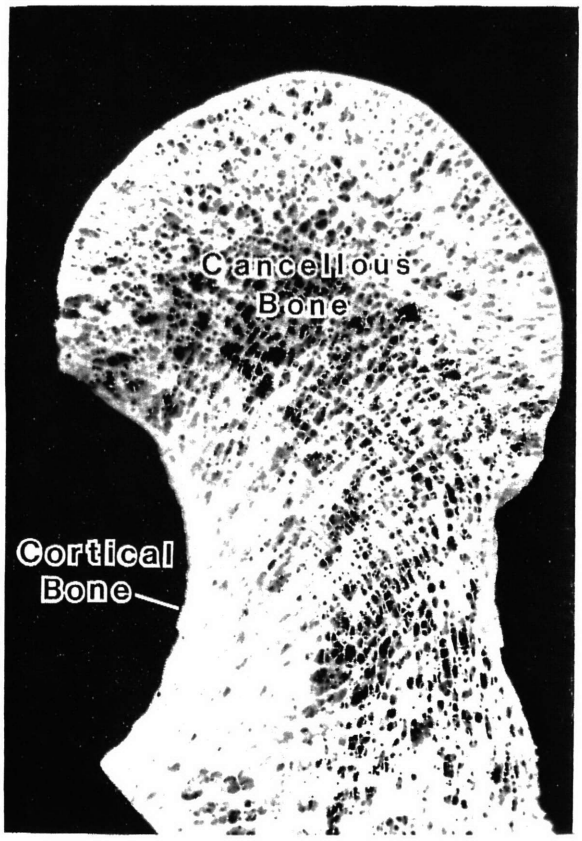

Figure 2.9: Femoral Head showing Trabecular and Cortical Bone. [Bouvier 1989]

by bone tissue. Different variations of the trabeculae pattern are found in characteristically different places. In general the struts with no preferred orientation are found deep in the bone away from loaded surfaces. More oriented struts tend to be observed underneath loaded surfaces where stress patterns are more reasonably constant. Trabecular bone predominates in the epiphyseal region while there is usually very little in the diaphyseal region. As the bone tissue grows on preexisting surfaces, it is often the case that cortical bone is formed in a region where trabecular bone already exists. Where this occurs, the trabecular bone is not replaced, but rather new bone surrounds the preexisting trabeculae struts resulting in a ambiguous structure pattern with no obvious and distinctive grain. **[Figure 2.10]** [Bouvier 1989, Cowin 1986, Currey 1984]

2.2.4. *Long Bone Anatomy*

The structure of long bone consists of a shaft, known as the diaphysis, with a metaphysis or expansion on each end. **[Figure 2.11]** In developing, immature bone the metaphysis is surrounded by an epiphysis which is joined to the metaphysis by a cartilaginous growth plate. The growth plate is where calcification of cartilage takes place, and upon the completion of growth, the epiphysis which is composed of trabecular bone becomes fused with the metaphysis. At the extremity of each epiphysis there is a special covering of articular cartilage which forms a gliding surface for the joint. The coefficient of dry friction between the articular cartilage of the joints can be as low as 0.0026, making the cartilage covering a very effective and efficient joint.

On the outer shell of the metaphyses and epiphyses lies a thin layer of cortical bone that is continuous around the long bone contour and compact around the diaphysis. The diaphysis is basically a hollow tube with walls composed of dense cortical bone that is thick throughout the extent of the shaft. This thickness then tapers off to form the thin shell of the metaphysis. The center space within the diaphysis known as the medullary cavity contains bone marrow. A thin layer of highly active cells which produce circumferential enlargement and remodeling of growing bone is the periosteum which covers the entire external surface of mature long bone. The outer layer of the periosteum is fibrous and comprises almost the entire periosteum of mature bone, and after maturity,

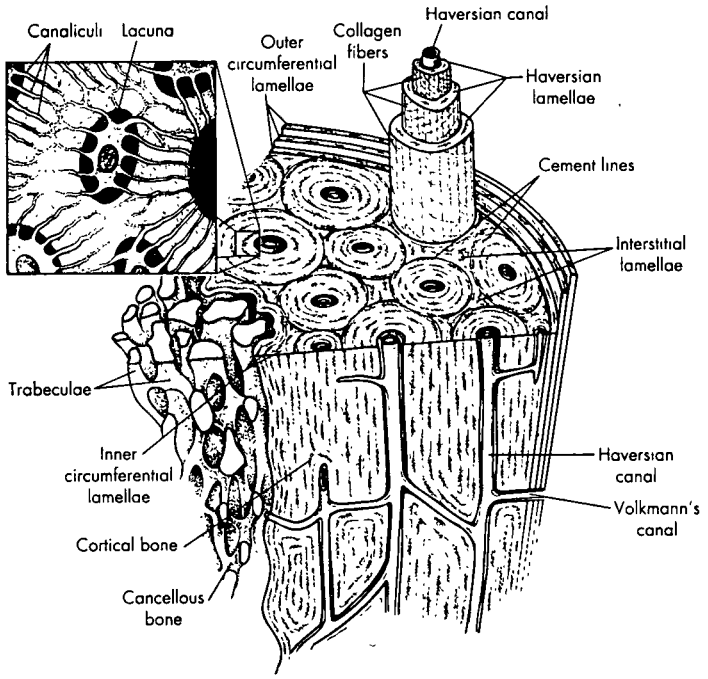

Figure 2.10: Schematic Drawing of Shaft of Long Bone Showing Cortical and Trabecular Bone. [Anderson *et al.* 1994]

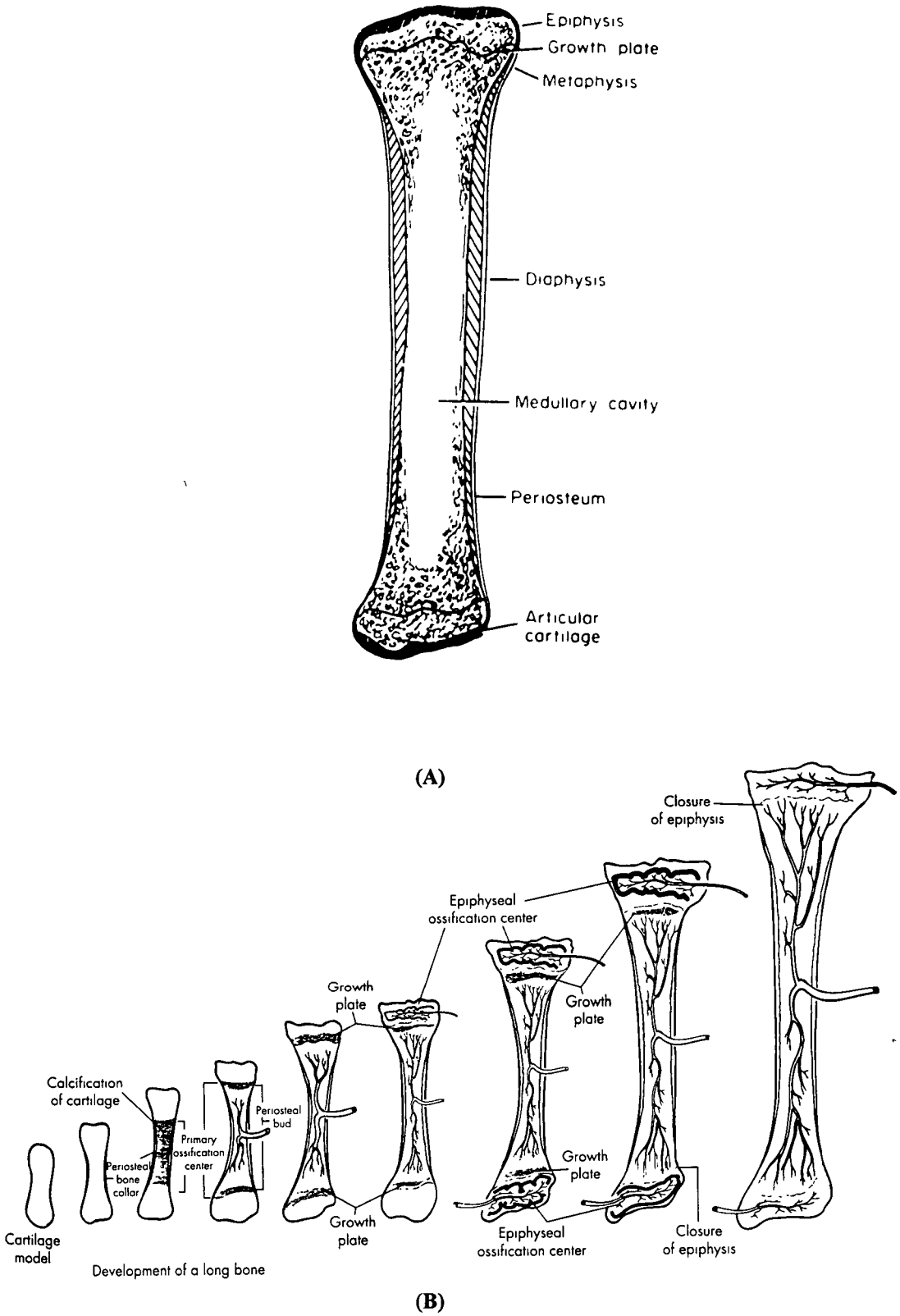

Figure 2.11: (A) Long Bone Anatomy. [Fung 1981];
(B) Development of Long Bone. [Anderson *et al.* 1994]

this layer of active cells becomes mainly composed of a capillary blood vessel network. In most of the diaphyseal region, the periosteum is thin and loosely attached, and thus the blood vessels are capillary vessels. In contrast, at the expanded ends of the long bone, ligaments are attached firmly and convey larger blood vessels. [Fung 1981]

2.2.5. *Remodeling*

Studies of cortical and trabecular bone structure have been performed in conjunction with bone remodeling. Bone remodeling is viewed as a process which adapts bone tissue to the mechanical environment at each point in the structure. In theory, this process optimally adjusts tissue distribution within the bones as a result of the load the bone must bear. The natural remodeling process arranges the given amount of material to support occurring loads with a safety factor.

Living bone is continually undergoing changes of growth, reinforcement, and resorption. This remodeling occurs in two basic ways, external and internal. External remodeling or surface bone remodeling refers to the changes in the shape of the bone caused by movement of external bone surfaces. With increased loads, bone's external surface will move so that the cross-sectional area transverse to the increased load is increased. The reverse will occur with reduced loading. Internal bone remodeling involves changing of the bulk density of bone tissue with stress. When loading applied to the bone is increased, the bulk density of bone tissue will also increase with time. This tissue will also increase stiffness and strength. Conversely, if the loading is decreased, bone tissue density will be reduced as it becomes less strong and less stiff.

There are two ways in which concentric cylinders are formed in bone that can be recognized in the formation of the secondary osteon and primary osteon. When the blood vessel is surrounded by preexisting bone, osteoclasts resorb the bone around the blood vessel, and the edges of the cavity are removed while the cement sheath is laid. The cavity then begins to be filled by lamellar bone, and the result is a mature secondary osteon. Here, the course of the preexisting lamellae is interrupted by the osteon. A similar process occurs in the formation of the primary osteon, however, it can only take place on the growing surface. With the primary osteon, the lamellae are uninterrupted by the osteon

and there is no cement sheath. As stated previously, osteons are able to sense direction and gradients of stress. This is evident with observations in the preferred orientation of osteoblasts and osteocytes parallel to collagen fibers, and as remodeling occurs, bone structure is efficiently adapted to changes in mechanical loading and stress-concentrating effects are reduced. [Fung 1981, Currey 1984, Martin *et al.* 1989]

2.3. *Bone Remodeling*

The adaptation of trabecular and cortical bone to alterations in their mechanical environment has been of great interest, especially in biomechanics. Reduction in bone density has been observed in periods of disuse in prolonged immobilization. At the same time, increases in bone density have been found in athletes and animals under heavy exercise. As bone grows in response to the mechanical loading it experiences, evidence of this adaptive phenomenon can be observed in various forms through bone atrophy and hypertrophy. Clinical studies show such evidence in situations such as paralysis and convalescence during chronic disease states. The exposure of astronauts to weightlessness during space travel has also resulted in a density reduction of the skeletal system. Such findings indicate the response of bone tissue to reduced strain is characterized by a loss of bone tissue mass. Studies have also shown constant peak strain during periods of activity such as exercise.

Keaveny *et al.* (1994) examined the tensile and compressive strengths of bovine tibial trabecular bone and found that strength depends on the density of trabecular bone. **[Figure 2.12]** while yield strains were independent of modulus. **[Figure 2.13]** At the same time, they determined that the difference between tensile and compressive strengths increases with increasing modulus **[Figure 2.14]** while the difference between yield strains remains independent of modulus. This conclusion reflects the modulus-dependent difference between tensile and compressive strengths in trabecular bone and explains some of the seemingly conflicting conclusions drawn on tensile and compressive strengths previously put forth because of variations in the mean modulus. Although Keaveny *et al.*'s study has its limitations due to the fact that it tested tibial specimens which were only

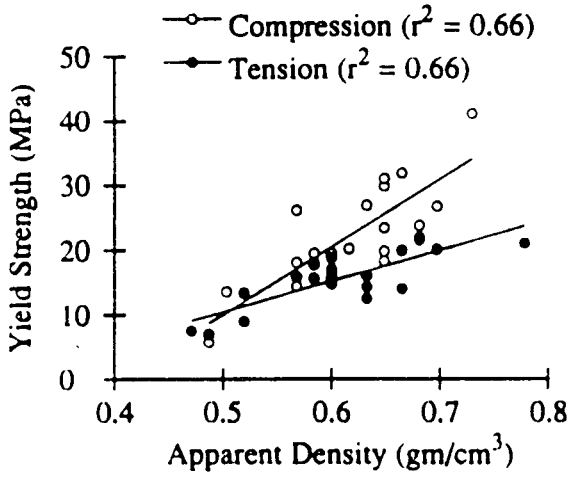

Figure 2.12: Yield Strength versus Apparent Density for Tensile and Compressive Loading of Bovine Proximal Tibia. [Keaveny *et al.* 1994]

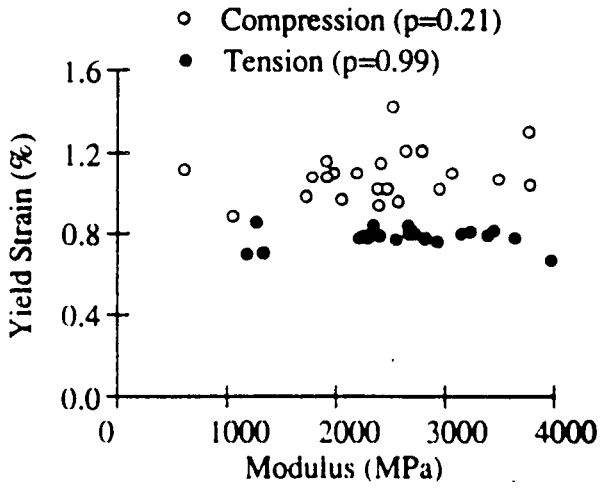

Figure 2.13: Plot of Yield Strain versus Modulus for Tensile and Compressive Loading of Bovine Proximal Tibia. [Keaveny *et al.* 1994]

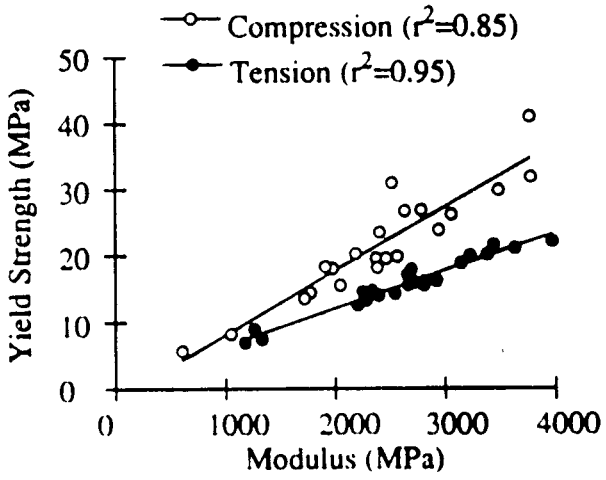

Figure 2.14: Yield Strength versus Modulus for Tensile and Compressive Loading of Bovine Proximal Tibia. [Keaveny *et al.* 1994]

loaded in line with principal trabecular orientation, the main stated above conclusions should prove to be valid for most cases of trabecular bone strength.

In general, trabecular bone plays a key role in the function of bone joints since it serves to transmit large contact stresses at the articular surfaces to the cortical bone of the cortical shaft. Through the observations of both trabecular and cortical bone, one can track the morphological changes that bone undergoes in order to accommodate its induced stress requirements.

2.3.1. *Historical Remarks*

The first attempts to explain trabecular bone structure began in the 19th century when in 1867, G. H. Meyer presented line drawings of the structure he had observed in various bones. He proposed that the spongy material (trabecular bone) in the bone showed a "well motivated architecture which is closely connect with the statics and mechanics of bone." [Roesler 1981] When C. Culmann, a Swiss mathematician, saw Meyer's drawings, he noticed that the lines of the drawings resembled curves of principal stress trajectories in a crane-like curved bar loaded similarly to that of a human femur. In comparing the drawings of Culmann to his own, Meyer found similarities in the idealized structure of the trabecular bone in the proximal end of the femur and in the Culmann crane. This lead him to believe that the structure of trabecular bone was influenced by principal stresses.

In 1869, Julius Wolff published his ideas of bone transformation which he describes as under the influence of "pathological alteration of the external form and under the load on bones, following mathematical rules." [Roesler 1981] In essence he proposed that mechanical stresses affect the remodeling process of bone. Wolff emphasized the idea that the modeling of trabecular bone follows these mathematical rules and later compared the correspondence of the principal stress trajectories of Culmann to the structure of the femur. Both show the crossing at right angles of lines from the drawings and planes from the bone structure that he made at corresponding sections. Wolff's theory became known as the trajectory theory or *Wolff's Law*. **[Figure 2.15]** He went on to conclude that

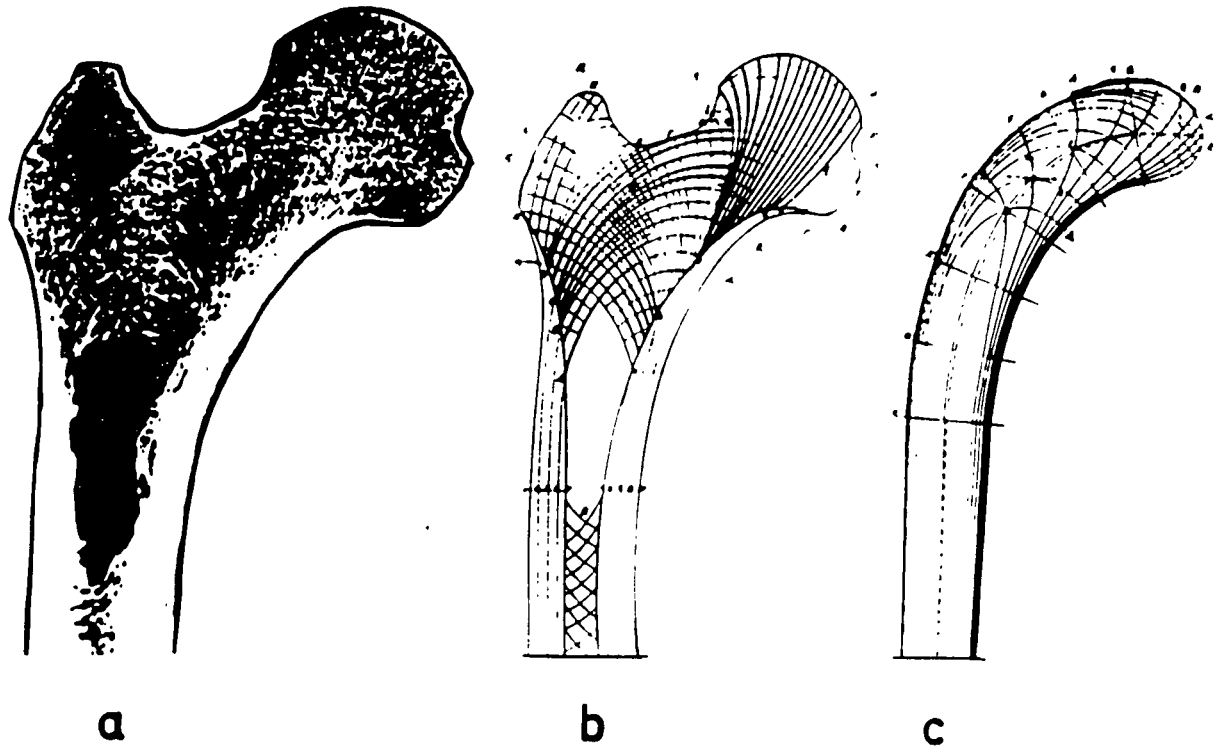

Figure 2.15: (a) Frontal Section Through Proximal End Femur, (b) Line Drawing of Trabecular Structure, (c) Culmann's Crane Copied from Wolff. [Roesler 1989]

nature found the most appropriate form and greatest efficiency for bone with minimum material consumption.

W. Roux, in 1885, also proposed a trajectorial architecture of trabecular bone to describe its geometry to explain how its organization provides maximum strength with a minimum amount of material. These same ideas were also echoed by F. Pauwels (1948) who conducted photoelastic experiments toward this theory, and J.C. Koch (1917) who performed detailed strength of materials analysis of the human femur and the architecture of trabecular bone within it. Koch concluded that trabeculae in the proximal femur were arranged in tensile and compressive systems aligned in the principal stress directions while the spacing and thickness of the trabeculae vary with stress magnitudes. [Hayes *et al.* 1981]

2.4. *Experiments and Morphological Changes*

When attempting to verify the validity of the concepts established by Wolff's Law, experiments on bone tissue are executed to evaluate the influence of loading history alterations on bone remodeling. The response of bone can be generalized as the arrangement of a new bone matrix and/or the resorption of existing bone. As a result common ways to assess the remodeling of bone tissue are to look at the effect of bone atrophy and hypertrophy. Most of the experiments that have been performed looked at the changes of cortical bone and trabecular bone density with changing load.

2.4.1. *Bone Remodeling: Assumptions*

When attempting to predict and understand the response of bone to changes in mechanical load, it is important to understand the way the changes are sensed in the bone itself. Alterations in bone function are induced by changes in loading and loading pattern. If bone remodeling is to be considered site specific, a local and physically measurable display of the modified loading must exist at varying points in bone.

For Hookean materials, mechanical stress and strain are often used interchangeably since they are proportional. Bone is linear elastic, but its modulus depends on morphology

because it is a nonhomogeneous, anisotropic material. Through results in many in vivo strain gauge experiments, it has been concluded that bone senses change in functional use by measuring strain. This conclusion is reinforced with the finding of nearly constant peak functional strains of bones with the same function in a wide variety of animals and by Keaveny *et al. 's.* finding of a constant strain to failure in trabecular bone.

Experiments have shown that the peak strain at functionally equivalent sites in growing bone are constant throughout the growth period. Regardless of bone size and activity in each of the different species, peak functional strains in the bones of different animals with similar function were all within the range of 2000-3000 με as can be seen in **Table 2.1**. In contrast, evidence shows that peak stresses in bone during various activities differ greatly in different animals and are correlated with body mass. Thus it seems that strain equilibrium is achieved by adaptive response. Strain history, being the probably mechanical source that regulates the adaptive response of bone, embodies all past strain variations such as:

- *Magnitude*
- *Strain Mode* (tension, compression shear in a particular plane)
- *Strain Rate* (bone deformation rate)
- *Strain Frequency* (deformation cycles per second)
- *Stimulus Duration* (total number of deformation cycles or time over cycles applied)
- *Strain Distribution* (pattern of strain magnitude across bone section)
- *Strain Energy* (elastic energy stored or dissipated during deformation)
- *Strain Direction* (principal strain direction relative to bone surface)

Looking at the data from Keaveny *et al.*, the authors show that the trabecular bone of the bovine proximal tibia achieves a compressive yield strain of approximately 1.0% while the tensile yield strain reaches approximately 0.8%. **[Figure 2.13]** S.C. Cowin (1989) also reports for cortical bone tissue of bovine femoral bone an average compressive yield strain in the axial direction of 2.53% and an average axial tensile yield strain of 3.24%. Comparing these data and with the peak compressive functional strains of 0.2-0.3%, we can see that trabecular and cortical bone maintain a safety factor of 4 and 10, respectively, inherent in their remodeling so as to prevent failure.

Table 2.1: Peak Functional strains in animals. [Martin *et al.* 1989]

Bone	Activity	Peak Strain ($\mu\varepsilon_c$)
Horse radius	Trotting	-2800
Horse tibia	Galloping	-3200
Horse metacarpal	Acceleration	-3000
Dog radius	Trotting	-2400
Dog tibia	Galloping	-2100
Goose humerus	Flying	-2800
Cockerel ulna	Flapping	-2100
Sheep femur	Trotting	-2200
Sheep humerus	Trotting	-2200
Sheep radius	Galloping	-2300
Sheep tibia	Trotting	-2100
Pig radius	Trotting	-2400
Fish Hypural	Swimming	-3000
Macaca mandible	Biting	-2200
Turkey tibia	Running	-2350

Another assumption to take into account when considering remodeling is the concept of a steady-state range. This remodeling equilibrium can be characterized as the bone loading situation where bone tissue is being simultaneously resorbed and deposited while maintaining no net change in its macroscopic properties or geometry. Because bone functions cover a wide spectrum of activities, it is likely that the strain values that compose equilibrium are site specific and bone specific. Remodeling equilibrium can also be changed due to processes such as aging or changes in hormonal, genetic, and metabolic activity. These changes usually introduce complexity in remodeling theories concerned with mechanical adaptation processes and are usually assumed constant during net remodeling behavior where mechanical input is the chief stimulus.

Since it has been established that strain is the mechanical parameter that is sensed, the question now remains as to the mechanism by which strain influences the remodeling process. There have been several proposed mechanisms which include diffusion effects and damage accumulation. One hypothesis is that material strains directly affect osteocyte (bone-maintaining cells) cell membranes or their extracellular components. Another possible mechanism for bone remodeling in cancellous bone is the continuous repair of microfractures in the trabeculae. Experiments performed on rabbit tibia subject to intermittent loading showed microfractures with greater disorganization and greater remodeling activity as well as significant stiffening of the trabeculae. It can be said that the trabecular bone acts as a shock absorber with microfractures as the mechanism for energy absorption, and subsequently the microfractures remodel into stronger tissue that is more dense. It is likely that a combination of these effects and others influence the remodeling of trabecular bone. [Cheal 1986, Martin *et al.* 1989, Hart *et al.* 1989]

2.4.2. *Experiments: Bone Atrophy*

Evidence that is most often cited as an indicator of the effect of mechanical loading on bone from regulation is bone atrophy where normal functioning loads are eliminated. This condition is known as disuse osteoporosis, or more accurately, osteopenia. Assuming an equilibrium point between tissue deposition and resorption mediated by some mechanical forces (and several other biological factors which also come into play), atrophy

due to a drastic reduction in mechanical forces leads to decreased bone mass. Bone atrophy also encompasses the effects of noncatastrophic, long term decreases in strain experienced by bone which were previously uninvestigated have become of great intrigue. Long term success of an implant is dependent on its compatibility. In the case of hip implants, a decreased stress is experienced in the proximal end of the femur because the load is transmitted through the implant stem to the midshaft. **[Figure 2.16]** As a result, bone resorption may occur because of the reduced loading experienced and cause a subsequent loosening of hip implants. From this example, one can see the alterations of stress influence the stress distribution around the implants, and this has been one of the motivating factors to better characterize the relationship between loading history and bone remodeling.

Immobilization studies are the most effective in providing insight to the effects of decreased loading. Some of the first studies done on bone atrophy by Allison and Brooks (1921) on dogs, by Geiser and Treuta (1958) on rabbits, and by Kazarian and Von Gierke (1961) on monkeys note a loss of trabecular tissue when load reductions were imposed on various bones. In the case of Kazarian and Von Gierke, bone loss was characterized as a decrease in the number and thickness of trabeculae as the adult monkeys were subjected to total body casting. At the same time cortical volume was also decreased as its thickness was reduced 15%. [Meade 1989]

More recent studies were done by Uhthoff *et al.* (1978) and Jaworski *et al.* (1980) who examined long term immobilization effects on young and old beagle dogs. These studies showed the responses of animals of different age groups when experiencing a change in load history. The initial bone volume of the young adult dogs (weighing 7-13 *kg*) and the older adult dogs (age 7-8, weighing 11-16 *kg*) is expressed as the ratio of cortical bone area to the total area of the cross-section at mid-diaphysis. As shown in **Table 2.2**, there was a 5-12% reduction in initial bone volume of the older dogs compared to the younger. Forelimbs of both dogs were immobilized by a plaster cast and then sacrificed between 2-40 weeks after initiation. The experimental animals showed decrease in bone density and increase in medullary canal after 32-40 weeks while the outside diameters did not change significantly for the older dogs, but did experience a noteworthy

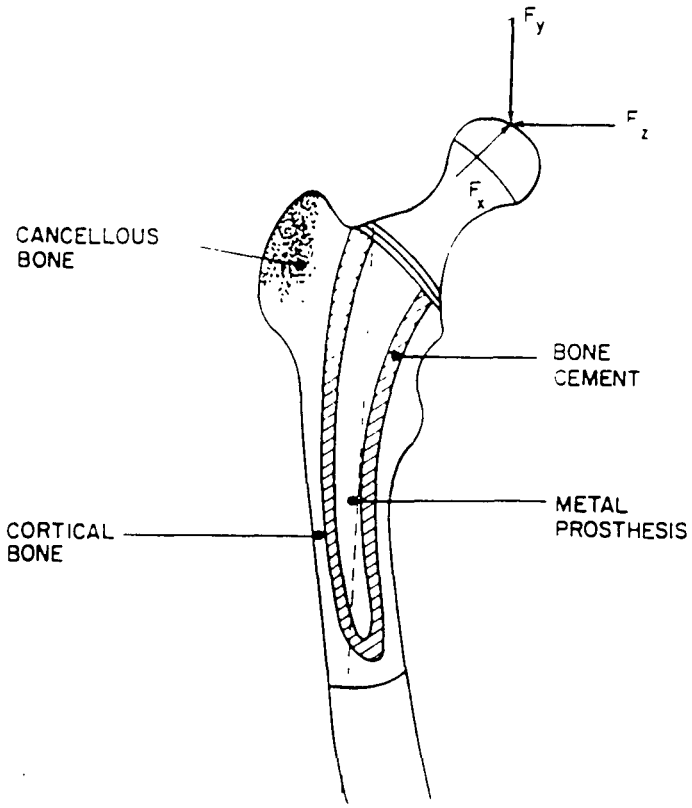

Figure 2.16: Femoral Component of Total Hip Replacement and Applied Joint Force Components. [Cowin 1989]

Table 2.2: Bone Volume as Cortical Bone Area to Total Area of Cross-Section of Four Bones in Young Adult and Older Beagle Dogs Before Immobilization. [Jaworski *et al.* 1980]

Bone	Male			Female		
	Young	Old	% Difference	Young	Old	% Difference
Third Metacarpal	86± 0.9	79± 2.9	8.14	86± 0.5	80± 0.5	6.98
Ulna	80± 0.5	75± 1.2	6.25	80± 0.8	76± 1.4	5.00
Radius	80± 1.3	71± 2.0	11.25	81± 0.7	75± 1.0	7.41
Humerus	68± 2.2	63± 1.1	7.35	70± 2.9	62± 2 0	11.43

reduction on the periosteal envelope in the younger dogs. Cross-sectional measurements were taken at 40 weeks of the mid-diaphysis of the third metacarpal, radius, ulna, and humerus **[Figure 2.17]** showing a reduction in cortical bone thickness due to expansion of the medullary cavity. The pattern of bone loss was studied with respect to the duration of immobilization. Their findings were consistent with others showing trabecular bone loss at mid-diaphysis of the immobilization bone, however, losses fluctuated throughout the experiment without any development of a discernible pattern. **[Figure 2.18] Tables 2.3-2.6** show the histomorphometric details of the aforementioned bones for the older dogs while **Tables 2.7-2.10** reveal the results of the young adult dogs for each of these bones. At the end of bone experiments, the greatest bone loss was experienced in the third metacarpal and the least in the humerus.

The pattern of bone loss for the young adult and older dogs is characterized in three stages: rapid bone loss followed by reversal, gradual and more sustained bone loss, and stabilization of bone loss. Although the older dogs began the experiment with less bone mass than the younger dogs, they seemed to lose less bone during the 40-week experimental period while their stages of bone loss appeared less distinct. Another interesting observation was that the periosteal envelope contributed to most of the bone loss in younger dogs while the endosteal surface did so for the older dogs. The differences in the behavior of these bone envelopes which encase the cortex of the diaphysis seem to vary more than trabecular bone which only has one surface, the endosteal surface. For the young adult dogs who had just completed growth, their bones'

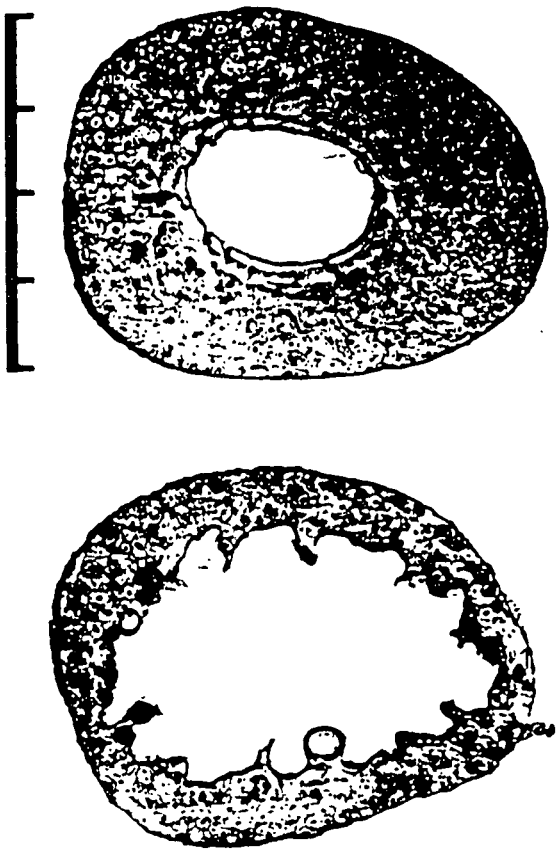

Figure 2.17: Cross-section of Third Metacarpal at 40 weeks. (Top) Control; (Bottom) Experimental Side Showing Expansion of Medullary Cavity and Thinning of Cortex. Scale is in millimeters. [Jaworski *et al.* 1980]

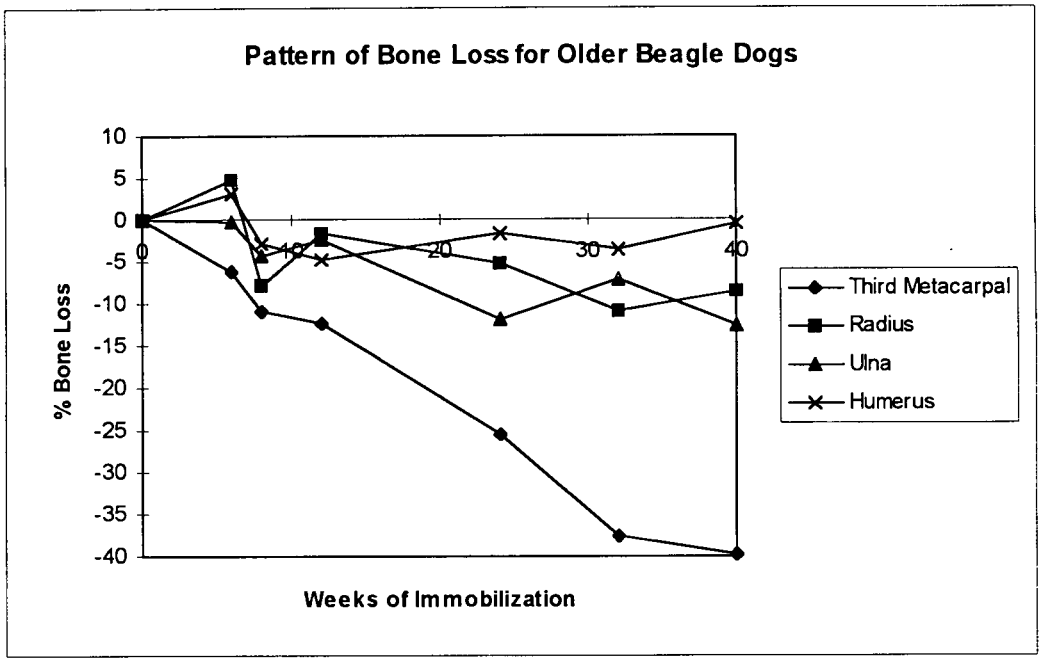

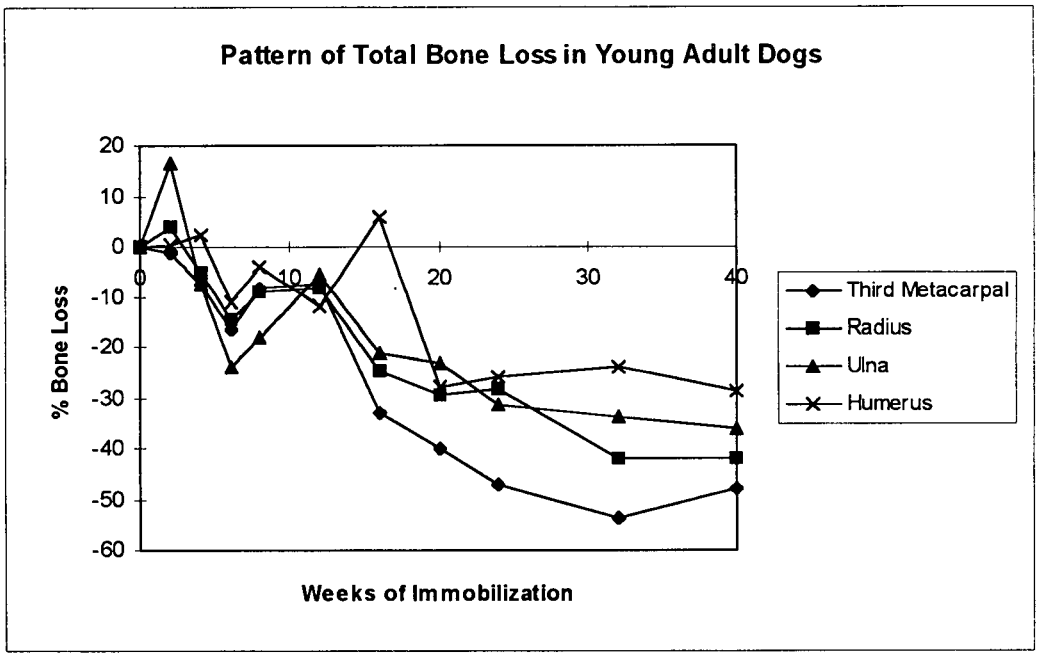

Figure 2.18: Graph Relating Bone Loss Pattern to Immobilization Duration Expressed as Percentage of Control. [Jaworski *et al.* 1980, Uhthoff *et al.* 1978]

Table 2.3: Histomorphic Data for Third Metacarpal of Old Beagle Dog [Jaworski *et al.* 1980]

Weeks in Cast	Tot Cross-Sectional Area (mm^2) Experimental	Control	Medullary Canal Area (mm^2) Experimental	Control	Difference mm^2	%	Area of Porosity (mm^2) Experimental	Control	Difference mm^2	%	Total Percent Difference
6	13.25	13.00	2.25	1.50	-0.75	-6 54	0.27	0.05	-0.22	-1.92	-6.28
8	15.61	16.23	3.21	3.13	-0.08	-0.61	0.82	0.08	-0.74	-5.68	-11.05
12	19.60	19.60	4.57	3.41	-1.16	-7.30	1.09	0.29	-0.80	-5.03	-12.33
24	14.10	14.93	3.81	1.58	-2.23	-16.73	0.36	0.02	-0.34	-2.55	-25.51
32	15.07	16.60	6.96	4.20	-2.76	-22.64	0.51	0.21	-0.30	-2.46	-37.65
40	18.88	18.73	8.86	2.69	-6.17	-37.15	0.54	0.28	-0.26	-1.65	-39.85

Table 2.4: Histomorphic Data for Radius of Old Beagle Dog [Jaworski *et al.* 1980]

Weeks in Cast	Tot Cross-Sectional Area (mm^2) Experimental	Control	Medullary Canal Area (mm^2) Experimental	Control	Difference mm^2	%	Area of Porosity (mm^2) Experimental	Control	Difference mm^2	%	Total Percent Difference
6	31.75	30.38	5.88	5.63	-0.25	-1.02	0.08	0.16	+0.08	+0.33	+4.88
8	39.34	41.71	9.54	9.59	+0.05	+0.16	0.38	0.21	-0 17	-0.53	-7.83
12	56 30	56.70	13.80	14.30	+0.50	+1.20	1.58	0.74	-0.84	-2.02	-1.78
24	42.06	42.78	11.19	10.29	-0 90	-2.78	0.11	0.06	-0.05	-0.15	-5.15
32	45.39	47.03	12.70	10.50	-2.20	-6.05	0.28	0.12	-0.16	-0.44	-11.00
40	48.67	50.08	12.50	11.25	-1.25	-3.29	1.41	0.82	-0.59	-1.55	-8.55

Table 2.5: Histomorphic Data for Ulna of Old Beagle Dog [Jaworski *et al.* 1980]

Weeks in Cast	Tot Cross-Sectional Area (mm^2) Experimental	Control	Medullary Canal Area (mm^2) Experimental	Control	Difference mm^2	%	Area of Porosity (mm^2) Experimental	Control	Difference mm^2	%	Total Percent Difference
6	30.13	28.00	6.38	4.00	-2.38	-9.86	0.08	0.26	+0.18	+0.75	-0.29
8	33.07	34.19	7.04	7.38	+0.34	+1.29	0.75	0.39	-0.36	-1.36	-4.31
12	51.70	51.30	12.33	11.50	-0.83	-2.20	1 68	1.22	-0.46	-1.22	-2.36
24	30.06	33.38	6.07	6.07	0	0	0 09	0.16	+0.07	+0.26	-11.97
32	44.09	44.04	11.73	9.76	-1.97	-5.84	1.02	0.53	-0.49	-1.45	-7.14
40	42.17	47.42	9.00	10.17	+1.17	+3.22	1.39	0.92	-0.47	-1.29	-12.56

Table 2.6: Histomorphic Data for Humerus of Old Beagle Dog [Jaworski *et al.* 1980]

Weeks in Cast	Tot Cross-Sectional Area (mm^2) Experimental	Control	Medullary Canal Area (mm^2) Experimental	Control	Difference mm^2	%	Area of Porosity (mm^2) Experimental	Control	Difference mm^2	%	Total Percent Difference
6	72.00	70.50	22.25	22.25	0	0	0.18	0.17	-0.01	-0.02	+3.10
8	91.69	92.07	38.25	37.44	-0.81	-1.50	0.82	0.51	-0.31	-0.57	-2.77
12	116.00	114.00	44.20	39.40	-4.80	-6.45	0.83	0.76	-0.07	-0.09	-4.66
24	82.11	85.14	27.29	30.09	+2.80	+5.13	1.22	0.48	-0.74	-1.36	-1.78
32	89.50	88.40	31.20	28.10	-3.10	-5.21	0.89	0.81	-0.08	-0.13	-3.49
40	106.70	106.90	36.50	36.63	+0.13	+0.19	1.49	1.19	-0.30	-0.43	-0.53

Table 2.7: Histomorphic Data for Third Metacarpal of Young Beagle Dog [Uhthoff *et al.* 1978]

Weeks in Cast	Tot Cross-Sectional Area (mm^2)		Medullary Canal Area (mm^2)				Area of Porosity (mm^2)				Total Percent Difference
	Experi-mental	Control	Experi-mental	Control	Difference mm^2	Difference %	Experi-mental	Control	Difference mm^2	Difference %	
2	18.8	19.1	2.3	2.3	0	0	0.1	0.3	+0.2	+2.0	-1.0
4	16.8	17.7	3.0	3 0	0	0	0.2	0	-0.2	-1.4	-7.5
6	17.2	19.3	3.2	2.7	-0.5	-3.0	0.2	0.1	-0.1	-0.6	-16.4
8	17.9	18.9	2.5	2.2	-0.3	-1.8	0.13	0	-0.13	-0.3	-8.1
12	14.1	14.4	2.2	2.3	+0.1	+0.9	0.7	0	-0.7	-5.8	-7.4
16	21.5	28.2	6.8	7.1	+0.3	+1.4	0 7	0.2	-0.5	-2.4	-33.0
20	12.3	17.9	2.8	3.2	+0.4	+2.7	0.7	0	-0.7	-4.8	-40.1
24	13.7	20.9	4.0	2.8	-1.2	-6.6	0.1	0	-0 1	-0.6	-46.9
32	10.1	18.0	3.1	2.9	-0.2	-1.4	0	0	0	0	-53.6
40	14.3	24.0	4.8	5.7	+0.9	+4.8	0	0	0	0	-48.0

Table 2.8: Histomorphic Data for Radius of Young Beagle Dog [Uhthoff *et al.* 1978]

Weeks in Cast	Tot Cross-Sectional Area (mm^2)		Medullary Canal Area (mm^2)				Area of Porosity (mm^2)				Total Percent Difference
	Experi-mental	Control	Experi-mental	Control	Difference mm^2	Difference %	Experi-mental	Control	Difference mm^2	Difference %	
2	53.0	50.0	13.5	11.9	-1.6	-4.3	0.2	0.3	+0 1	+0.3	+4.0
4	49.5	52.0	8.6	10.2	+1.6	+3.9	1.3	0.1	-1 2	-2.9	-5.0
6	48.3	50.8	12.8	0.3	-12.5	-8.4	0	0	0	0	-14.5
8	54 0	56.3	13.3	11.7	-1.6	-3.6	0.2	0	-0.2	-0.4	-9.1
12	41.7	42.9	9.8	8.5	-1.3	-3 8	0.4	0	-0.4	-1.0	-8 4
16	103.5	121.8	42.2	42.9	+0.7	+0.8	2.3	0.7	-1.6	-2.0	-24.6
20	49.4	57.8	20.0	16.2	-3.8	-9.1	0.1	0.1	0	0	-29.4
24	50.7	54.5	19.9	11.6	-8.3	-19.3	0	0	0	0	-28.2
32	35.2	55.1	11.2	13.7	+2.5	+6.0	0	0	0	0	-42.0
40	59.8	77.4	29.2	24.8	-4.4	-8.4	0.2	0.3	+0.1	+0.2	-41.9

Table 2.9: Histomorphic Data for Ulna of Young Beagle Dog [Uhthoff *et al.* 1978]

Weeks in Cast	Tot Cross-Sectional Area (mm^2)		Medullary Canal Area (mm^2)				Area of Porosity (mm^2)				Total Percent Difference
	Experi-mental	Control	Experi-mental	Control	Difference mm^2	Difference %	Experi-mental	Control	Difference mm^2	Difference %	
2	39.9	32.9	9.6	6.7	-2.9	-11.3	0.5	0.6	+0.1	+0.4	+16.4
4	32.8	34.4	6.4	6.6	+0.2	+0.7	0.7	0.1	-0.6	-2.2	-7.3
6	31.0	36.7	8.3	7.0	-1.3	-4.5	0.3	0.3	0	0	-24.1
8	41.6	49.0	9.3	9.5	+0.2	+0.5	0.1	0.4	+0.3	+0.3	-18.1
12	29.2	32.0	6.2	7.0	+0.8	+2.0	0.2	0	-0.2	-0.5	-5 6
16	87.5	115.2	27.8	40.2	+12.4	+16 8	1.4	1.2	-0.2	-0.3	-21.0
20	41.4	40.8	16.3	8.4	-7.9	-24.6	0.3	0.2	-0.1	-0.3	-23.0
24	38.2	46.2	12.9	9.6	-3.3	-9.1	0.1	0	-0.1	-0.3	-31.3
32	32.8	41.7	10.3	7.6	-2.7	-7.9	0	0.1	+0.1	+0.3	-33.8
40	43.8	54.1	16.0	11.2	-4.8	-11.3	0.6	0.3	-0.3	-0.7	-36.2

Table 2.10: Histomorphic Data for Humerus of Young Beagle Dog [Uhthoff *et al.* 1978]

Weeks in Cast	Tot Cross-Sectional Area (mm^2)		Medullary Canal Area (mm^2)				Area of Porosity (mm^2)				Total Percent Difference
	Experi-mental	Control	Experi-mental	Control	Difference mm^2	Difference %	Experi-mental	Control	Difference mm^2	Difference %	
2	91.1	92.9	30.1	31.1	+1.0	+2.0	0.6	0.7	+0.1	+0.2	+0.2
4	106.8	101.6	40.2	36.6	-3.6	-5.6	0	0	0	0	+2 5
6	98.4	105.0	35.4	34.6	-0.8	-1.1	0.3	0.1	-0.2	-0.3	-10.8
8	97.8	201.8	32.8	33.3	+0.5	+0.7	0	0	0	0	-3.8
12	83.2	85.9	32.2	28.3	-3.9	-6.8	0.1	0	-0.1	-0.2	-11.7
16	203.1	205.1	105.8	102.1	-3.7	-3.6	0.5	0 2	-0.3	-0.3	+5.8
20	100.3	105.3	51.2	37.1	-14.1	-20.7	0.7	0.13	+0.6	+0.1	-27.9
24	105.6	129.1	46.2	48.8	+2.6	+3 2	0	0	0	0	-26.0
32	92.9	105.9	41.5	38.4	-3.1	-4.6	0.13	0.17	+0.04	0	-23.9
40	141.7	157.9	81.6	73.6	-8.0	-9.5	0.37	0.38	+0.01	0	-28.8

periosteal surface seem more sensitive to remodeling due to alterations in physical activity. In contrast, the older beagle dogs show an expansion of their medullary cavity as a result of the combination of age-related thinning and immobilization. Examining these observations, the experiments suggest that the rate and amount of bone loss is age-related in long-term immobilization as older dogs appear to lose less bone than young dogs. It is also interesting to note that trabecular bone revealed recovery when remobilization occurred after 6-12 weeks of inactivity. This usually took place during the biphasic stage of rapid bone loss and reversal, or the stage of more gradual, sustained bone loss when resorption is quite active. These two stages both show more reversible bone atrophy. In general, more extensive recovery was shown in the younger dogs compared to the older during short immobilization periods. At the same time, trabecular bone which makes up about 20% of the total bone volume, but possesses 90% of the surface area experiences greater losses because of the greater surface to volume ratio of the tissue. [Meade 1989, Jaworski *et al.* 1980, Uhthoff *et al.* 1978]

Another resorptive phenomena experienced in adaptive bone remodeling is a result of stress shielding often seen after the implantation of a prosthesis. When this occurs the surrounding bone is partially "shielded" from carrying load and starts to resorb. A prosthetic stem shields the bone from stress because it shares the load that is normally taken by bone alone. The results are reduced bone stresses and a reduction of bone mass due to resorption.

The implantation of prosthetic components are expected to alter stresses in surrounding trabecular bone. As bone stress and stress-shielding patterns depend on the material, geometrical, and bonding characteristics of the implant, bone resorption patterns have been presumed to also depend on these characteristics. Thus when an implant stem is less stiff, stress-shielding becomes less severe, and bone resorption is reduced. One of the suggestions to avoid resorption has been the press-fitted stem without any coating. Using this method, the tapered stem is wedged into the medullary canal and "press-fitted" as the endosteal cortex becomes compressed continuously by the hip-joint force. Endosteal compression generates hoop stresses such that it causes the bone to maintain its mass.

There is also reduced rigidity because the stem is not bonded, and therefore it allows for more bending deformation and less stress shielding in bone.

Bone resorption and remodeling around prosthetic hip stems threaten the integrity of the stiff and noncemented implants. Reduced cortical thickness and increased porosity have caused loosening, stem failure, or even bone fracture. Van Reitbergen *et al.* (1993) investigated the postoperative morphology around a press-fitted stem and compared it to previously studied bonded (porous ingrowth) stems. Adult male mongrel dogs underwent total hip replacement receiving a cemented ultrahigh molecular weight polyethylene acetabular component and a cementless, titanium alloy femoral component. **Figure 2.19** shows the two-year remodeling pattern from four sections of one of the eleven dogs in the experimental group. In general, the bone-implant interface included a membrane which consisted of collagen fibers and fibrocytes parallel to the implant, intimate bone contact, and marrow. Membrane thickness increased during the period from six months to two years proximally, but not distally while in most places, the membrane was separated from the marrow by a shell of trabecular bone. After six months, differences between the treated and control femurs were not significant. In contrast, at two years the differences were more noteworthy at the proximal end of the bone with 20-23% reduction in cortical bone area.

When comparing these results with experiments using the bonded stems, it was found that similar amounts of resorption of the proximal cortex occurred. Van Reitbergen *et al.* investigated how similar amounts of resorption could develop under completely different stress conditions using a finite element model. It is determined that proximal bone resorption is similar in the press-fitted implants, bonded and unbonded, and it can be explained with adaptive bone remodeling. The smooth press-fitted stems produce high proximal stresses from its wedging effects that occur immediately postoperatively. This results in trabecular densification, and consequently proximal bone stresses reduce with time stress patterns changes due to bone adaptations until the stem eventually becomes distally jammed in the intramedullary canal. Thus the proximal bone is bypassed and resorption takes place until a new equilibrium is found. In the long term case, bonded and unbonded press-fitted stem resorption can be explained with Wolff's Law. While the

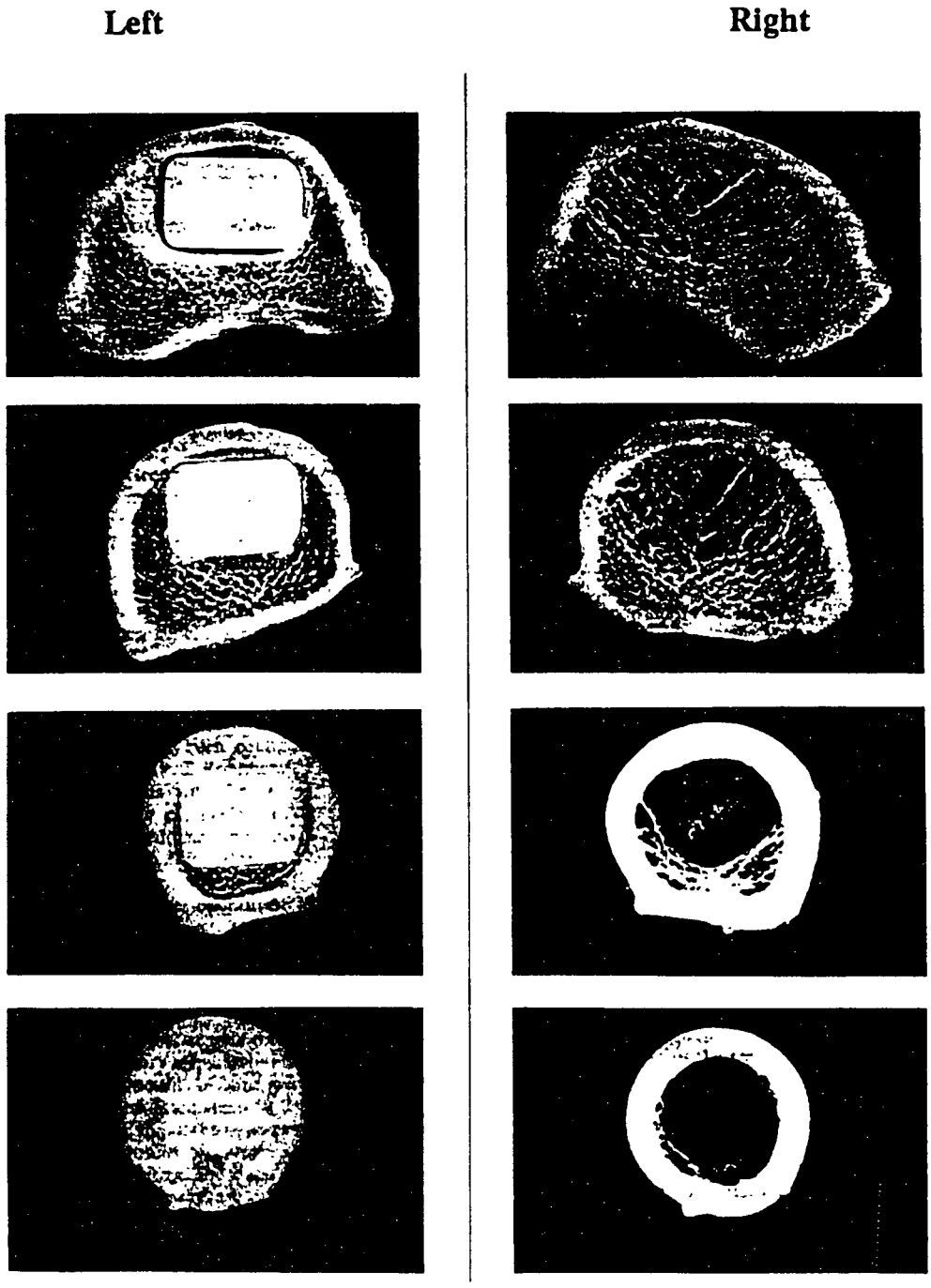

Figure 2.19: Radiographs of 4 Sections of the 2-year Postoperative Dog Femurs. Operated Femur Shown on Left and the Contralateral Control Femur Shown on Right. [Van Reitbergen *et al.* 1993]

bonded stem induces a steady resorption until a new equilibrium is determined, the unbonded resorption process is not monotonic. [Van Reitbergen *et al.* 1993]

2.4.3. *Experiments: Bone Hypertrophy*

Another means of assessing the response of bone due to mechanical loading involves examining hypertrophy. This phenomenon tends to be overlooked in comparison to bone atrophy, but in recent years it has been of noteworthy interest with the development of prosthetic joint replacements and sports and rehabilitative medicine. Increasing interest in fitness and the development of sports medicine has also been a catalyst for further investigation of the effects of exercise (which impose magnified loading on specified limbs) on the skeletal system. Another development that has given incentive to understand bone remodeling is in the case of osteoporosis. Evidence by Aloia *et al.* (1978) and Krolner *et al.* (1983) show moderate amounts of exercise can retard and in some cases reverse this degenerative process when increasing calcium intake.

Evidence of bone hypertrophy is apparent in various exercise studies. Investigations have shown the effects of exercise and training in the long bones of humans. One such example is by Jones *et al.* (1977) who used x-ray studies of the humeri of professional tennis players, and the results showed that cortical thickness of the playing side was increased by 34.9% in men and 28.4% in women when compared with the contralateral control. Another similar hypertrophic investigation was done where a non-surgical experiment examined the effects of heightened level of exercise on the density of bone tissue of the limbs involved. Weight-bearing or activity-level are increased over a period of time in such ways which are expected to alter bone loading. A study by Dalin and Olsson (1974) compared three groups of people: cross country runners ages 50-59 who had been involved with the sport for at least 25 years, previously inactive male office workers who underwent a three-month exercise program, and age and weight matched controls for the sedentary group. The bone density of the subjects were assessed at different locations. No significant differences were observed in bone density between the short term exercise group and the inactive control group. However, the long term runners displayed a bone density much higher than the controls. Interestingly, the density

increased were not only found in the legs, but equally in the arms. [Meade 1989, Bertram *et al.* 1991]

An exercise study by Woo *et al.* (1981) examined year-old, skeletally immature pigs who were subject to 12 months of daily one hour runs at 6 *km/hr*. The controls for this experiment were same age pigs which were kept sedentary for an equal period of time. In this particular study, morphological changes in bone in addition to biomechanical properties of bone tissues were examined to determine the effects of long-term physical activity. The flexural modulus of elasticity (E), ultimate bending stress (σ_f), and structural properties of bone strips cut from the diaphysis of the swine femur represented by maximum load (P_{max}) and maximum stored energy (A_{max}) were used as comparison values for the control and experimental subjects. E and σ_f were found to be nearly similar for both the control and exercised groups, but a comparison of the bone's structural properties of bone strips revealed significant increases in P_{max} and A_{max} after training. The maximum load (P_{max}) and maximum stored energy (A_{max}) for the exercised animals were 35% and 32% greater than the controls, respectively. **[Figure 2.20]** When the cortical bone was also examined, results demonstrated an average increase of 17% for the exercised animals with significant increases in thickness around the posterior, medial, and lateral portions of the bone. This seemed to indicate that running on level grade had less of an influence on the anterior quadrant of the femur of the swine compared to other regions. **[Figure 2.21]** In addition, while periosteal diameters in the anteroposterior and mediolateral direction did not change significantly, the endosteal diameters decreased 8% and 11% in these two regions, respectively, marking a reduction in the medullary canal area and increase in cortical thickness. Comparison of dry, ash, and calcium weights also exhibited significant differences in the control and exercised groups as the exercised animals showed a consistently higher tissue-component weight. Since the composition of the bone remained unchanged, these weight increases are therefore related to increases in bone volume, which leads to an increased cortical thickness.

As exercise training increases the stresses in the bone internally, bone responds by increasing its cortical thickness and reducing the medullary cavity. The increases in cross-sectional area allow the bone to carry more load and absorb more energy before failure

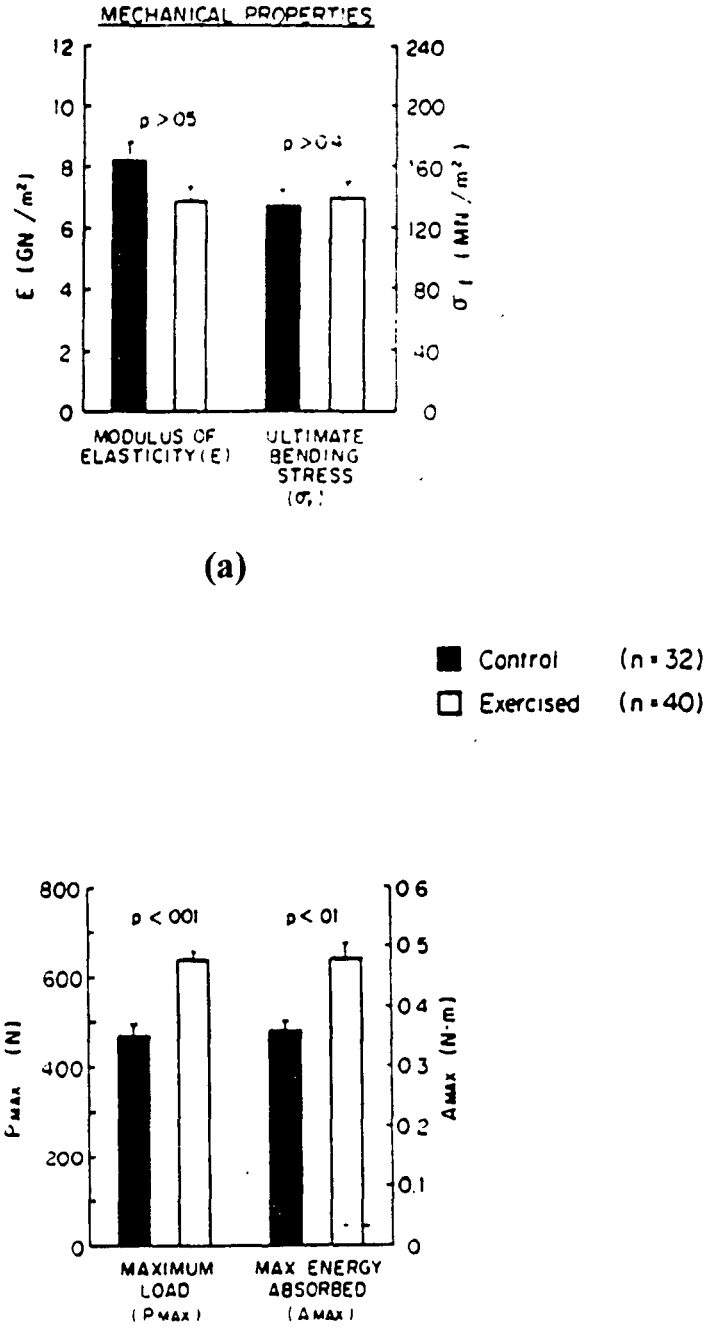

Figure 2.20: Comparison of Mechanical Properties of Swine Bone: (a) Modulus of Elasticity and Ultimate Bending Stress, (b) Maximum Load and Maximum Stored Energy. [Woo *et al.* 1981]

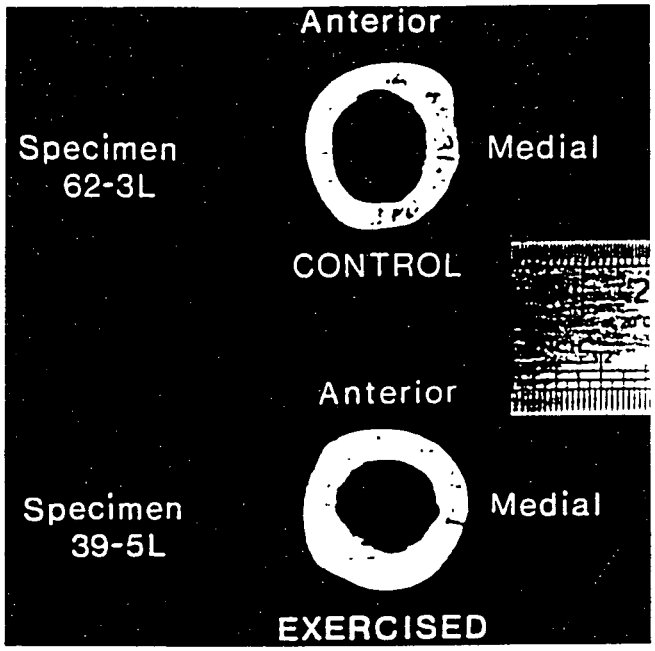

Figure 2.21: Photographs of Cross-Section of Proximal End of Femur in Swine. [Woo *et al.* 1981]

occurs, and this is evident in **Figure 2.20(b)**. Further analysis of bone density and biochemical content of both groups were similar. **[Figure 2.22]** Thus, it appeared that increase in bone strength following exercise was due to bone mass increase rather than a change in composition or mechanical properties. From this study, prolonged exercise had a significant effect on the quantity of bone, and the findings also provided strong evidence that surface remodeling is a principal response to long-term exercise while it had a positive effect on the structural strength of the bone. [Woo *et al.* 1981]

L.E. Lanyon and C.T. Rubin (1984) performed experimental studies on the ulnae of rooster and turkeys when investigating bone hypertrophy and cortical bone. A portion of the ulna was severed and a steel cap was placed over the cut end to protect the diaphysis of naturally occurring loads. Pins were then externalized from the caps to allow mechanical loading. **[Figure 2.23]** These experiments showed that both hypertrophy and atrophy of the ulna were dependent on the magnitude of the load, rate of application, and number of cycles. For instance, when loaded at 4 cycles per day, bone mass was maintained; when loaded at 36 cycles per day, bone mass increased. These studies indicate that skeletal elements are sensitive to a change in stress pattern. [Bertram *et al.* 1991]

In their experiments testing the effects of static and dynamic loading on bone remodeling, Lanyon *et al.* (1984) assessed remodeling activity in turkey ulnae under the conditions of disuse alone, disuse with superimposed continuous compressive load, and disuse interrupted by short daily periods of intermittent loading. After an eight week period, bone sections from the midpoint were examined. The non-loaded bones showed no remodeling activity on the periosteal surface while the endosteal surface showed evidence of resorption as the enclosed endosteal area increased by 11%. Percentage porosity also increased from a mean of 0.52% to a mean of 2.1% which was an increase between 0.61%-4.82% in all of these animals. The total combined changes of the unloaded turkeys provided a total reduction in bone area of 13%. The animals which were subjected to static loading experienced similar remodeling changes as in the disuse or non-loaded situation. A widened endosteal area and increased intracortical porosity also resulted in a total area difference of approximately 13%. For each bird in the dynamically

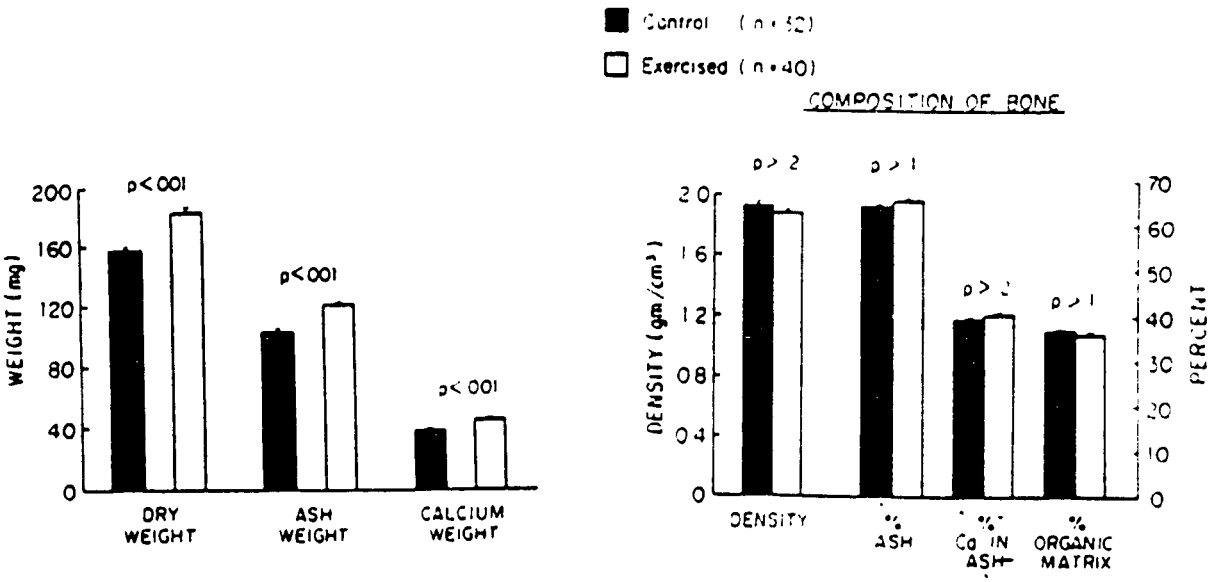

Figure 2.22: Biochemical Contents of Swine Bone. [Woo *et al.* 1981]

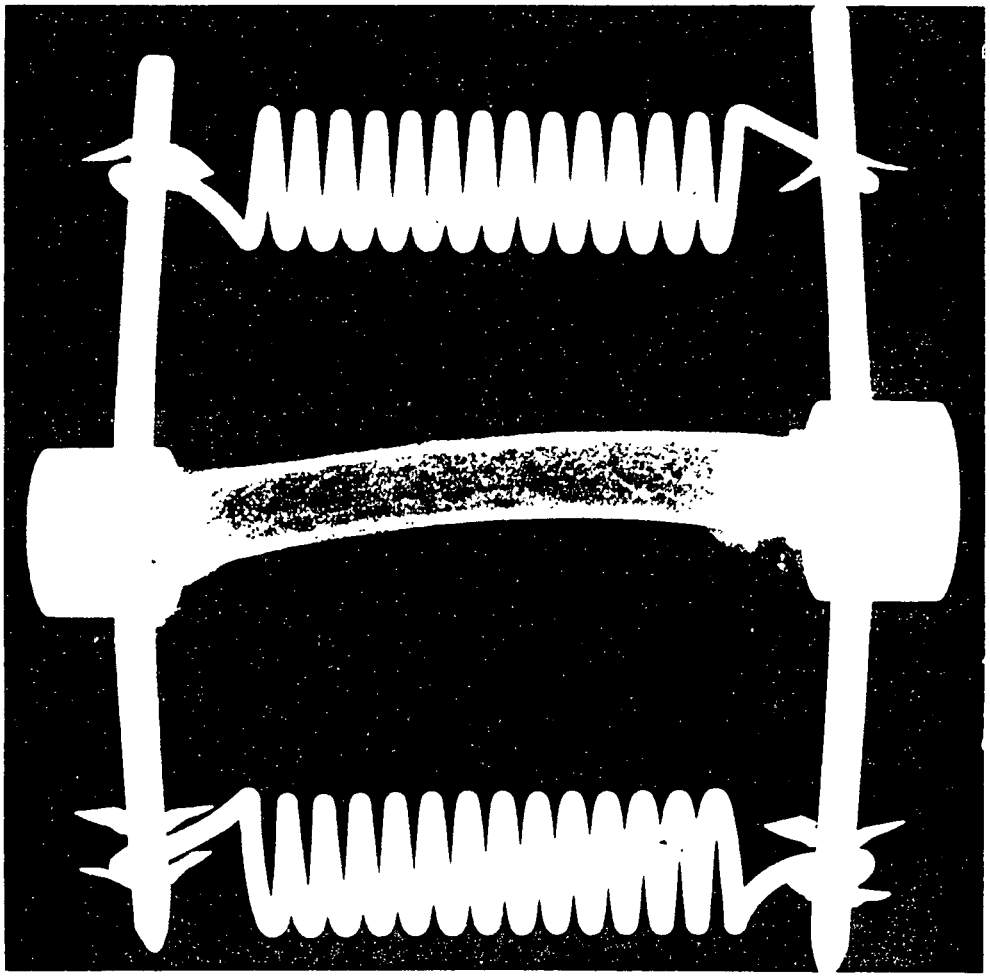

Figure 2.23: A Radiograph of Avian Ulnar Preparation Showing the Bone's Diaphysis with Caps and Transfixing Pins. The Pins were Joined by Loading Springs Situated Outside the Wing. [Lanyon *et al.* 1984]

loaded group, the cross-sectional area increased an average of 24% as a result of new bone formation primarily on the periosteal surface. **[Figure 2.24]** From these results, Lanyon *et al.* concluded that in this particular experiment, static loads which are sufficient enough to produce strains in the functional dynamic strain range have no effect on bone remodeling. However, when the similar load is applied intermittently for short daily periods as in the dynamic loading case, the bone may experience an increase in mass. This reinforces the notion that bone adaptation may be dependent on, not only magnitude of load, but also the rate of application and number of cycles. [Lanyon *et al.* 1984]

2.5. *Optimization*

2.5.1. *Bone Density*

Reviewing the results of the aforementioned experiments, it can be concluded that bone indeed does undergo morphological changes with variations in loading. Bone is able to optimize its shape by altering its bone density through osteoclastic bone resorption and osteoblastic bone formation as greater mechanical loads lead to increased bone density while reduced mechanical loads exhibit a decrease in bone density. While the majority of remodeling studies have been primarily concerned with changes in cortical bone, it is important to note that direct comparisons between cortical and trabecular bone remodeling are difficult and should be carefully questioned.

Bone density has been shown to be the most important structural variable. Research investigating bone atrophy show a loss of trabecular tissue as well as a reduction in trabeculae strut thickness with limb immobilization. In some cases, as with the experiments on dogs by Uhthoff *et al.* (1978) and Jaworski *et al.* (1980), the younger animals subjected to shorter periods of immobilization recovered their bone tissue loss after remobilization. These results show evidence of bone's adaptation to the mechanical stresses to which it is subjected. In the same studies, changes in cortical bone thickness were also experienced with immobilization as bone density decreased and the diameter of the medullary canal increased. The adaptive remodeling process for these two experiments were characterized in stages which included (1) rapid bone loss followed by

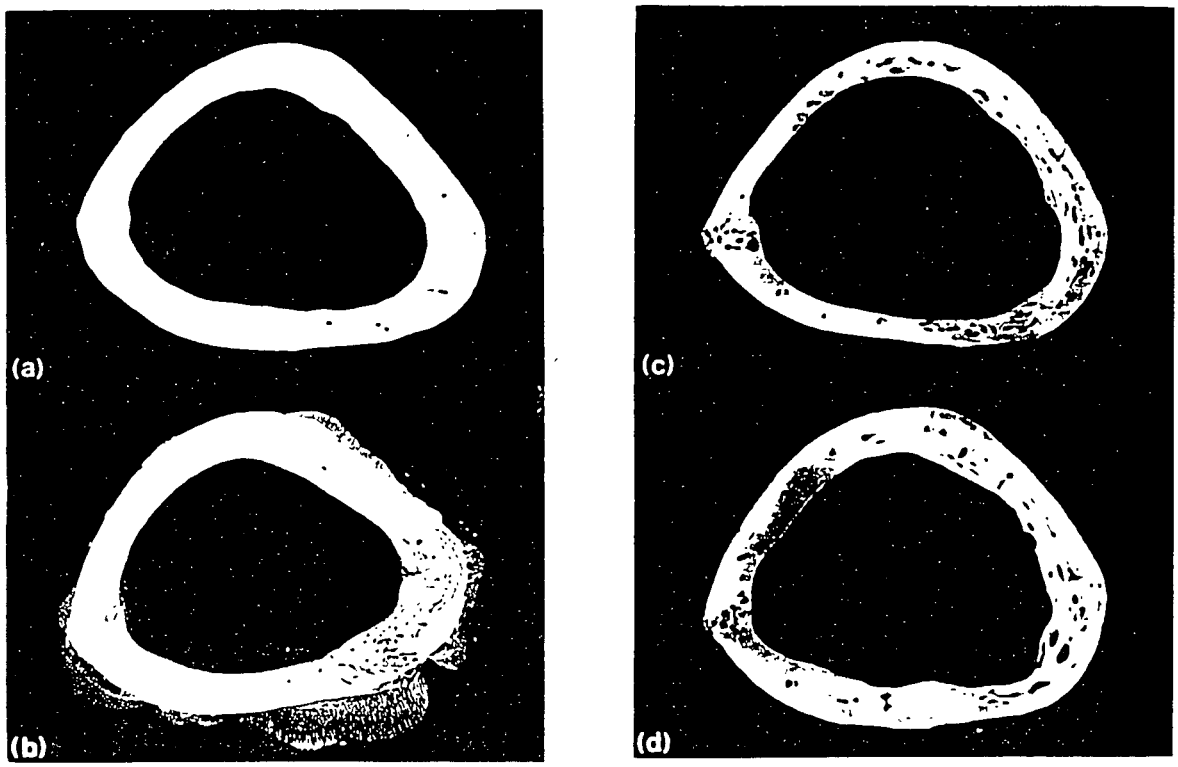

Figure 2.24: **Transverse Sections Taken from Turkey Ulna Midshaft at end of Experimental Period.**
(a) Intact Right Ulna from Bird #10.
(b) Prepared Left Ulna from Bird #10 Subjected to 100 cycles/day of intermittent loading.
(c) Prepared Ulna from Bird #2 Protected from Mechanical Loading.
(d) Prepared Ulna from Bird #5 Subjected to Continuous Loading from Springs.
[Lanyon *et al.* 1984]

reversal, (2) gradual more sustained one loss, and (3) stabilization of bone loss. When the bone was remobilized during the first two stages, recovery was revealed in the trabecular bone showing a reversible bone atrophy showing the continuing bone adaptation process through density.

Studies of prosthetic implants also gave insight to mechanical bone adaptations with studies such as the one done by Van Reitbergen *et al.* (1993). It was determined that whether using a bonded or unbonded stem, similar long-term amounts of resorption still occurred at the proximal cortex. Bonded stems which act more stiff induced a steady resorption pattern as a new equilibrium is established while the less-rigid unbonded stems experienced a more dynamic resorption as the stress patterns in the proximal bone changes with bone adaptations. The long-term results, still being the same, illustrate the stress-shielding that takes place with these implant devices as they share some of the load normally taken by the bone. These reductions in bone stresses and mass reinforce the role of bone density in adaptive bone remodeling in bone atrophy.

Hypertrophy investigations through exercise studies also show cortical bone density adaptations with heightened loading. Increased cortical bone thickness and cross-sectional area allow the bones to carry more load and improve structural strength. The study of pigs by Woo *et al.* (1981) and turkeys by Lanyon *et al.* (1984) showed that increased cortical bone thickness is a direct result of increased mechanical loading. However, as to what the bone exactly senses: magnitudes of loading, rate of change, stimulus duration, stimulus frequency, etc., it seems unclear as there appears to be no consensus among investigators. It is certain, though, that cortical bone thickness adaptations are induced with magnified loads allowing bone to absorb more energy before failure.

2.5.2. *Trabecular Orientation*

Trabecular orientation is also a consideration in the bone optimization process. Models such as Cowin's fabric tensor and Fhyrie and Carter's objective function (to be described in the following section) attempt to determine the alignment of the trabeculae struts with changing load and whether their orientations are in line with principal stress

trajectories as hypothesized by Wolff's Law. General patterns of trabecular orientations and distributions of apparent density are similar for the same of bones of different individuals. The magnitudes of the apparent density at specific locations within the bones, however, can be quite different as can be their apparent densities of bone at the same site in different bones. Researchers tend to agree that variations in apparent density within specific bones and among bones of different subjects are influenced by the loading histories to which the bone is exposed.

The two basic generalized theories that have been proposed to account for trabecular architecture remodeling are that: (1) trabecular orientation is a function of principal stress direction (also known as the Trajectorial Theory), and (2) bone apparent density is a function of an effective stress measure. Some of the limited studies which have dealt with trabecular bone remodeling experimentally include Lanyon's (1974) investigation of sheep calcaneus where trabeculae were aligned along principal strain directions measured from the cortex. In addition, he hypothesized that this arrangement was effective in reducing shear strains. A damage accumulation hypothesis was also proposed to explain trabecular remodeling based on experimentally induced and clinically observed microfracture of trabeculae by Martin and Burr (1982), Pollard *et al.* (1984), and Radin *et al.* (1972). [Goldstein *et al.* 1991]

Goldstein *et al.* (1991) developed an experimental model utilizing an implantable hydraulic device incorporating five loading cylinders and platens in direct contact with an exposed plane of trabecular bone. This model is capable of inducing controlled stress fields while it is applied to the femur of skeletally mature mongrel dogs. These particular animals were chosen to represent the response of trabecular bone to a variety of alterations in the mechanical environment induced by the implant. When a fast rise time (70 *msec)* loading wave form or squarewave was applied, significant bone ingrowth characterized by dense, thick trabeculae and a mass of almost solid bone overlying the platens occurred. Ingrowth often extended across the majority of the platen and through the porous surface to the underlying substrate. The trabeculae appeared to be oriented vertically and radiating away from the loading surface as bone appeared to be both lamellar and woven with the possibility of undergoing continuing rapid remodeling. The

slow rise time (700 *msec*) loading waveform or rampwave specimens showed less ingrowth penetration and were characterized by thin, sparse trabeculae with large open spaces between them. Sections contained a single horizontally oriented trabeculae or plate-like structures immediately adjacent to the loading platen as the trabeculae were lamellar with smooth surfaces.

The results of this experiment indicate significant remodeling induced by the activated implant as an increase in trabecular orientation toward the loaded platens was observed, especially in the case of the squarewave animals. While the squarewave animals revealed a consistent profile of ingrowth, the rampwave animals had a more inconsistent profile. Goldstein *et al.* hypothesize that the extent and profiles of bony ingrowth may be dependent on the character of the stress transmitted at the bone implant interface once it surpasses some stimulus threshold. Below this threshold, the amount and profile of ingrowth may be affected more by the fracture-like physiological response of the tissue due to surgical trauma. With the squarewave experimental animals, correlations were found between the change in stress parameters and the change in morphology measures. The correlations between Von Mises stress and morphology (i.e. volume fraction, surface volume ratio, and connectivity) versus time are plotted and reveal an improvement with time as animals are tested for longer terms, thus suggesting that the bone is moving towards some equilibrium point. **[Figure 2.25]** The relationship between mechanical stress and morphologic adaptation support the existence of a specific remodeling strategy in response to significant implant interface stimulation. The experimental observations imply that the first response to mechanical stimulation is a decrease in bone deposition followed by a secondary reorganizational phase which is similar to the fracture healing process.

While trabecular bone alignment has been shown to correspond to principal stress directions and thus reduce the apparent density required to achieve a certain equilibrium stress, there still needs to be a continued development in modeling techniques based on microstructural analysis which account for localized response (such as near implant surfaces). Management of loading boundary conditions provided by the implant coupled with histologic features similar to those observed in other human and animal implant

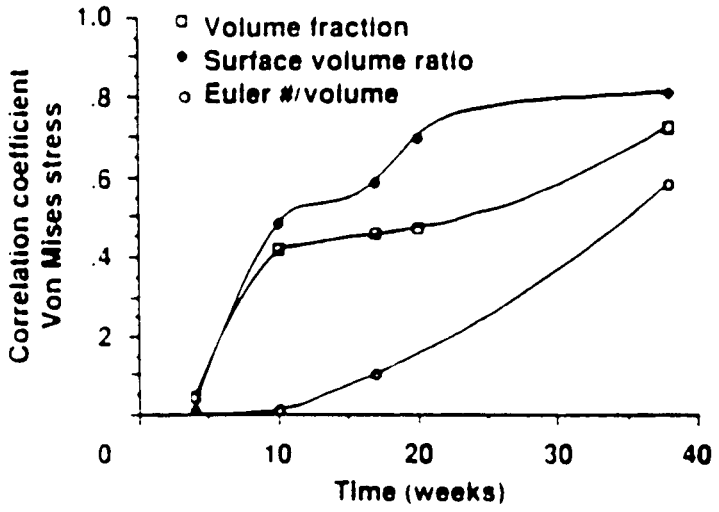

Figure 2.25: Correlation between Von Mises Stress and Morphology versus Time for Squarewave Loaded Animals. Correlations Coefficients between Changes in Von Mises Stress due to Implant and Changes in Trabecular Morphology are Plotted as a Function of Time. [Goldstein *et al.* 1991]

studies encourage the continued use of the models for evaluating trabecular bone adaptation under experimentally controlled mechanical conditions. The remodeling phenomenon of trabecular bone is not limited to this natural material alone, but rather many other materials designed by nature also possess similar adaptation processes which allow them to adjust to their changing environments. Further research in this field of bone mechanics will help develop an accurate trabecular bone remodeling model which will be able to predict its change in architecture orientation such that better designs in joint/stem prosthetics can be developed.

2.6. *Remodeling Theories*

2.6.1. *Trabecular Bone Models: The Fabric Tensor*

Trabecular bone remodeling is characterized as changes in size and orientation of the trabeculae. J. Wolff proposed that trabeculae alignment coincided with principal stress trajectories; changes in loading direction would result in altered trabecular alignment. S.C. Cowin gave a mathematical statement of Wolff's Law in terms of measurement alignment of the trabeculae by construction a fabric tensor (**H**) composed of measurements of the mean intercept length defined as $L(\theta)$. For a single phase structure, the mean intercept length is the average length between two grain boundaries, or trabeculae in this case, along a test line. **[Figure 2.26]** The mean intercept length tensor which gives a measure of bone microstructure was introduced by T. Harrigan and R.W. Mann (1984) based on work done by W.J. Whitehouse and E.D. Dyson (1974). The value of the intercept length is a function of the slope of the line (θ) along which the measurement is made. It is the average distance between two bone/marrow interfaces measured along a line.

Cowin used this theory to define the fabric tensor as the inverse square root of the mean intercept length tensor. While a superposition of parallel test lines over a planar slice of cancellous bone specimen is done, the number of intersections of test lines with the individual trabeculae is divided by the length of the test line giving the mean intercept

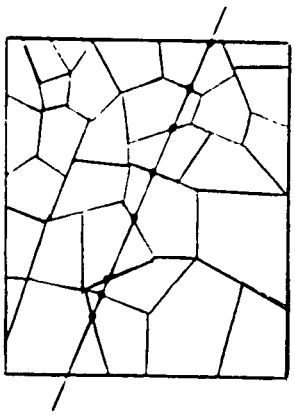

Figure 2.26: Stereological Lengths in One-Phase Structure - Illustration of Mean Intercept Length. [Turner 1992]

length. A rotation of the parallel lines is executed with respect to the bone specimen and the measurement is repeated such that the data fits the following equation:

$$\frac{1}{L(\theta)^2} = \frac{1}{H_{12}^{\ 2}} + \frac{1}{H_{11}^{\ 2}}\cos^2\theta + \frac{1}{H_{22}^{\ 2}}\sin^2\theta + \frac{2}{H_{12}}\left(\frac{1}{H_{11}} + \frac{1}{H_{22}}\right)\sin\theta\cos\theta$$

where θ is the angle of parallel test line orientation, $L(\theta)$ is the mean intercept length, and H_{11}, H_{22}, H_{12} are components of the fabric tensor in the test plane 1-2. The fabric tensor, **H**, is a second-rank, symmetric, positive definite tensor. Analysis reveals that the fabric tensor can be graphically represented by an ellipsoid in 3-D, or ellipses in 2-D **[Figure 2.27]** and is a good means of depicting the orientation of trabecular bone. Remodeling equilibrium is considered by Cowin to be when the principal axes of stress and strain and the fabric tensor all coincide, i.e.

$$\mathbf{T^*H^*} = \mathbf{H^*T^*} \quad , \quad \mathbf{E^*H^*} = \mathbf{H^*E^*}$$

with $\mathbf{T^*}$ is the stress tensor , $\mathbf{H^*}$ is the fabric tensor, and $\mathbf{E^*}$ is the strain tensor, all at remodeling equilibrium.

Trabecular bone is a nonhomogeneous, porous, anisotropic structure. Porosity and orientation of trabecular bone architecture vary with location over a wide range as do its elastic constants. With this relationship by Cowin, the determination of elastic constants is possible with the fabric tensor provided that certain elastic parameters are known. These parameters depend on the porosity of the bone, but are independent of the trabecular orientation. Thus they can be determined empirically from bone specimens. [Hart *et al.* 1989, Cowin 1986]

2.6.2. *Trabecular Bone Models: Fhyrie and Carter's Optimization Function*

Another approach to trabecular bone remodeling is proposed by D.P. Fhyrie and D.R. Carter (1986). They developed a unifying relationship between trabecular bone density, trabecular orientation, and stress with the premise that bone optimization is achieved when the structural mass is minimized for a given loading condition. Fhyrie and Carter define an objective function,

$$\tilde{Q}(\rho, \theta, \sigma)$$

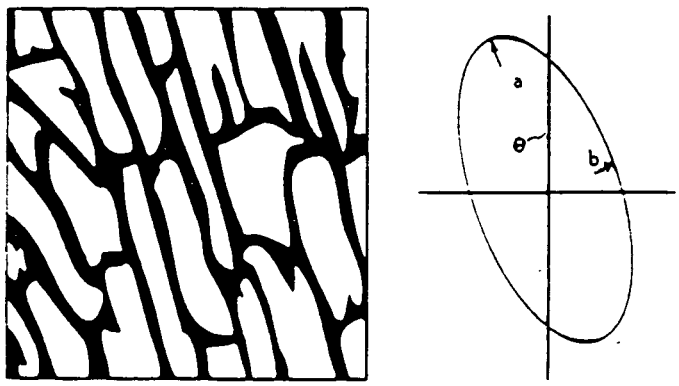

Figure 2.27: Representation of Actual Anisotropic Trabecular Bone Architecture; Fabric Ellipse Measured from Specimen Shown. [Turner 1992]

which measures the optimality of bone under a given load where ρ is the apparent density (bone mass per unit volume), θ is the orientation of the anisotropic material axes with respect to the principal axes, and σ is the static stress. Two suggestions are made for the objective function: strain energy density (which assumes bone optimizes its stiffness while using the least amount of material) and the failure stress function (which assumes bone optimizes its strength while minimizing material). The objective function can be used to find the optimal orientation of the material axes (θ^*) and the minimal sufficient apparent density (ρ_A) when

$$\rho_A = \rho_{min}, \qquad \text{such that}$$

$$\tilde{Q}(\rho,\theta^*,\sigma) = \min \tilde{Q}(\rho,\theta,\sigma) \leq Q_{max}.$$

Bone can become optimized for a given stress by finding the best orientation and the minimum bone apparent density such that the objective function is less than Q_{max}, where Q is defined as the physiologically normal value for the objective function. With the minimization of the apparent density, the objective function seeks to use the least amount of bone tissue while maximizing the bone's structural integrity (i.e. its stiffness or strength). As a result, by specializing these objective functions for orthotropic materials, correlations of trabecular architecture can be made, and the functions seem to be able to predict density and orientation consistent with Wolff's hypothesis. [Fhyrie *et al.* 1986]

2.6.3. *Optimization Model*

The relationship between mechanical stresses and bone morphology has been investigated with respect to the remodeling activity of bone, however, truly accurate models which are able to predict bone morphology, particularly trabecular bone architecture, have yet to be developed and confirmed experimentally. Carter *et al.* (1989) use the optimization principle described in the previous section to create such a model and implement a finite element bone remodeling technique to predict bone density distribution in the femoral head and neck for a loading condition representing the single-limb-stance phase of a gait. The loading history was simulated by defining the stress fields in a two-dimensional model which was exposed to various discrete loading cases. The total

stimulus was then calculated by superposition of each case as the apparent density and material properties of each element were changed and the stress solutions redetermined. In this approach, Carter *et al.* assumed that bone would remodel toward a state such that mechanical stimulus to the tissue is independent of its anatomical position and is governed by the cumulative influences of the many loading cycles and directions of the load.

In order to represent the loading history, single-loading direction and multiple-loading direction solutions were considered. **Figure 2.28** shows the single-load direction solutions which assume that each loading cycle is applied in the same direction. Multiple-loading direction solutions were calculated corresponding to the solutions with stress exponents, $M = 1.0$ and $M = 4.0$ for the relationship describing the local apparent density of trabecular bone:

$$\rho = K \left(\sum_{i=1}^{c} n_i \sigma_i^M \right)^{1/2M}$$

where c = the discrete loading condition, n = number of loading cycles, σ = scalar quantity continuum model peak effective stress, ρ = bone apparent density, and K = proportionality constant. M is an empirical weighing factor which accounts for the possible difference in relative importance of load magnitude and number of cycles in each physical activity. **Figures 2.29 - 2.33** illustrate the remodeling solutions for the five different loading conditions with the darkest region indicating an apparent density of less than 0.2 g/cm^3 and the lightest region showing an apparent density of 1.2 g/cm^3 or greater.

The remodeling solutions for the single-direction loads are illustrated in **Figures 2.29 - 2.31**. The first reaction force (2317 N directed 24° from vertical and a hip abductor force of 702 N, directed 28° from vertical) for these loads was determined through the force values generated from the authors' survey of literature while the remaining two loads represent extreme ranges of motion with reduced force levels. The first load case shows a progressive consolidation of bone density which begins to create a dense cortical diaphysis as well as a strong column of trabecular bone in line with the joint reaction in the femoral head. A peculiar abnormality predicted by the model for this case was the diaphysis atrophy of cortical bone about one-third down the shaft. The second load condition also predicted formation of cortical bone in the diaphysis, but different from the

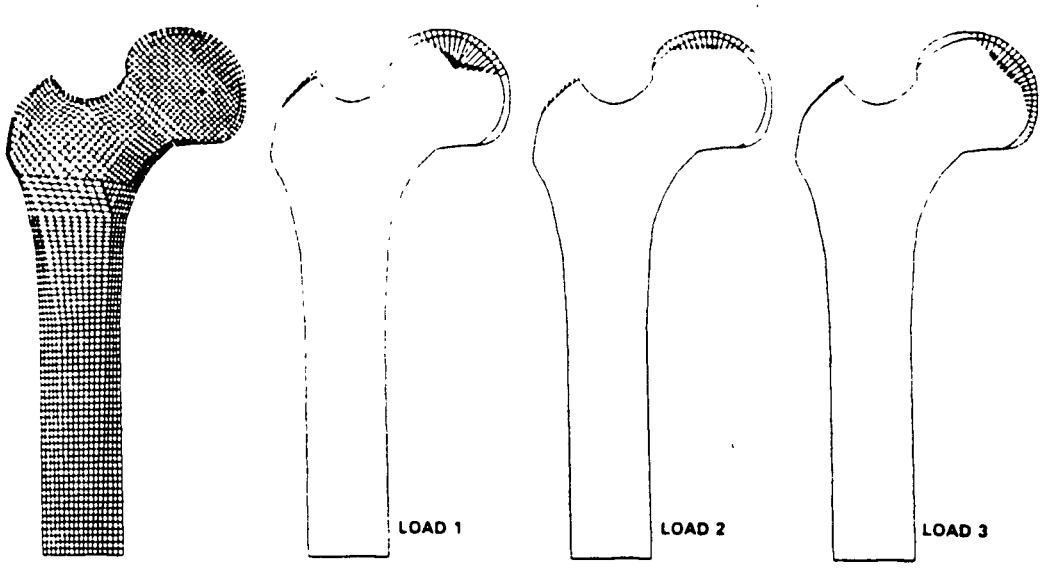

Figure 2.28: Finite Element Mesh and Three Loading Conditions Used for Single Load Analyses. [Carter *et al.* 1989]

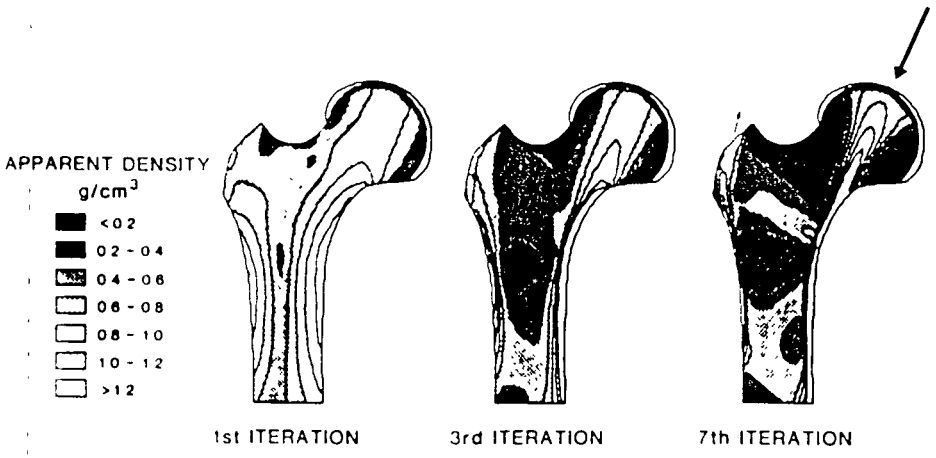

Figure 2.29: Remodeling Solution for Load Case 1. [Carter *et al.* 1989]

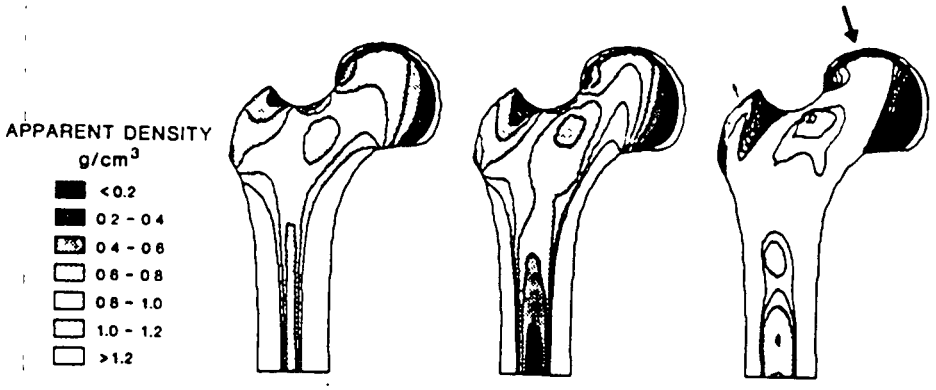

Figure 2.30: Remodeling Solution for Load Case 2. [Carter *et al.* 1989]

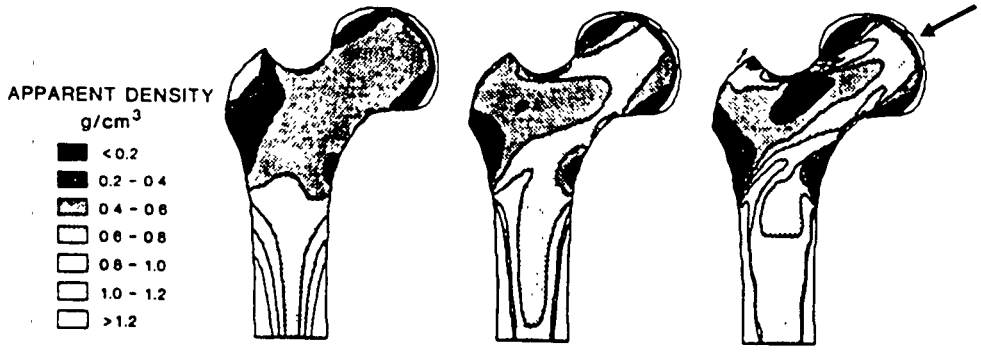

Figure 2.31: Remodeling Solution for Load Case 3. [Carter *et al.* 1989]

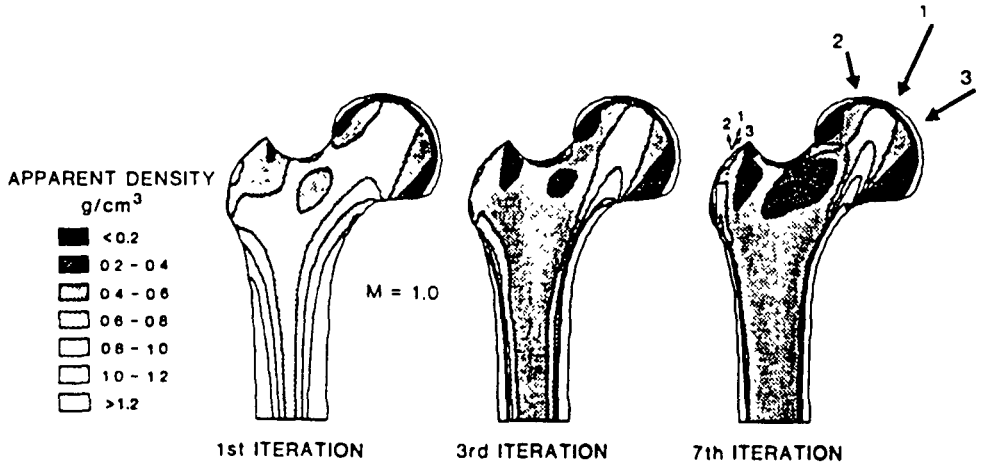

Figure 2.32: Remodeling Solution for Multiple-Load-Direction Stress, M = 1.0. [Carter *et al.* 1989]

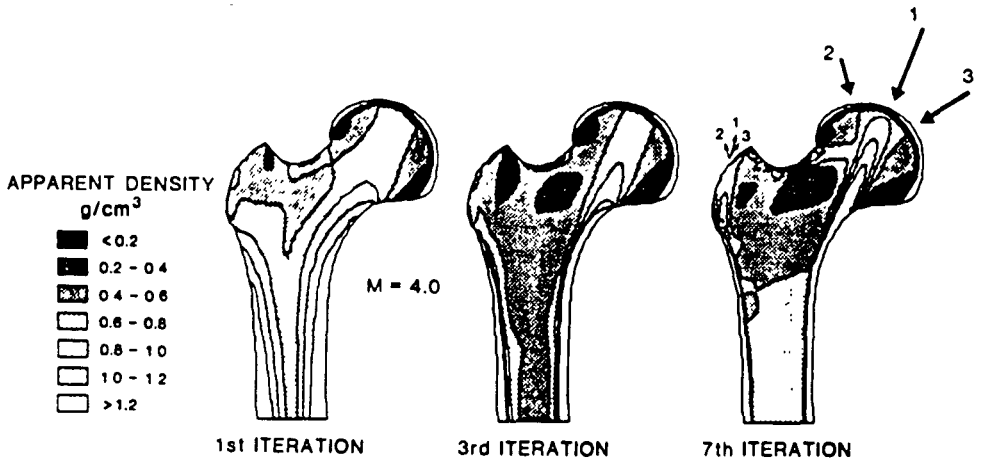

Figure 2.33: Remodeling Solution for Multiple-Load-Direction Stress, M = 4.0. [Carter *et al.* 1989]

first case, two areas of increased density was calculated in the femoral neck. One system which transferred compressive stresses extended from the joint contact area to the inferior neck region. Tensile stresses were transmitted from the superior neck of the femur into the head. The third single-direction load showed a progressive formation of the bone cortex as the medullary cavity became more defined. As in the second case, two systems of trabecular bone consolidation were also predicted. The two multiple-direction load analyses conducted calculated similar results to one another. **[Figures 2.32-2.33]** Both solutions showed a more diffuse distribution of proximal bone density compared to the first single-direction load case while the femoral head also exhibited a dense compressive trabecular column.

The bone density patterns displayed by the model predict progressive increase in bone density in some areas and decrease in others. The density calculations for the first three iterations appeared reasonable, but the distributions for the seventh iteration seemed invalid because the forecasted density and material property gradients were much greater than those observed in the proximal femur. Thus it appears that the method used in this model converges toward the condition in which most of the area will possess a density of 1.8 g/cm^3 or bone will resorb to a density of zero. However, the first few iterations did give the indication of the formation of normal bone architecture hinting that the basic approach of this model was correct, but modifications were necessary for subsequent analyses.

Polar plots of the equivalent normal stresses for selected trabecular bone elements after three iterations display trabecular bone orientation. For the first loading case, principal stress vectors were calculated for a homogeneous model, and these appeared to mimic trabecular orientations. However, the calculated principal stresses changed after each iteration of remodeling, and the magnitude and direction of these vectors altered by the third iteration. **[Figure 2.34]** A similar polar plot was also done for the multiple-load direction, and the authors conclude that the equivalent normal stresses correlate to local bone density and anisotropy for the third iteration. **[Figure 2.35]**

Some of the influences for modifications for this model that should be considered are the assumed fundamental relation of the apparent density equation stated above and

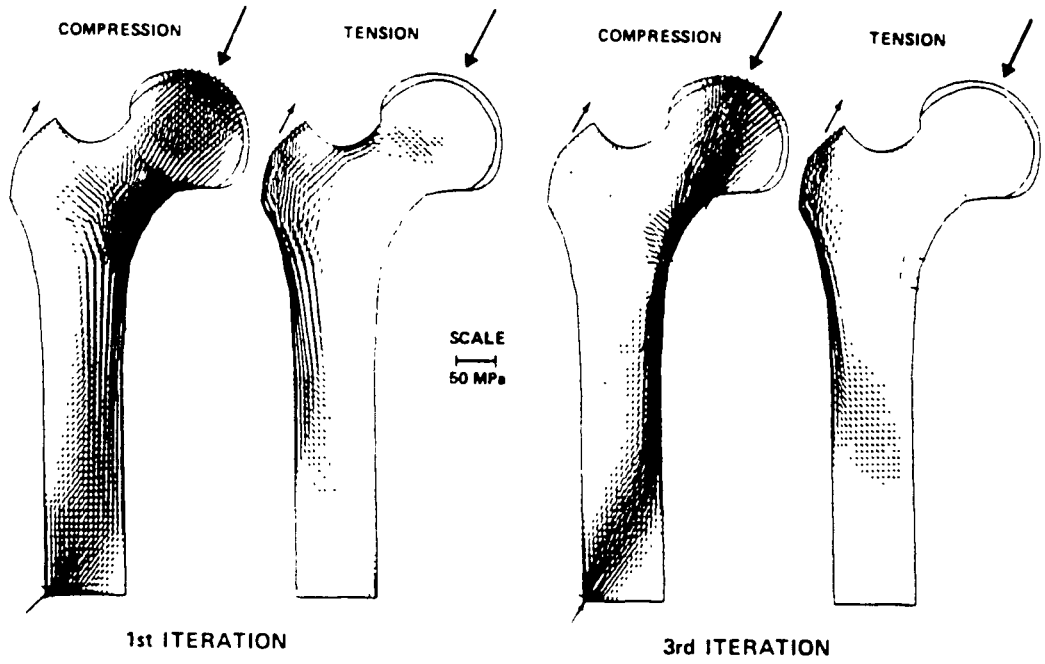

(a)

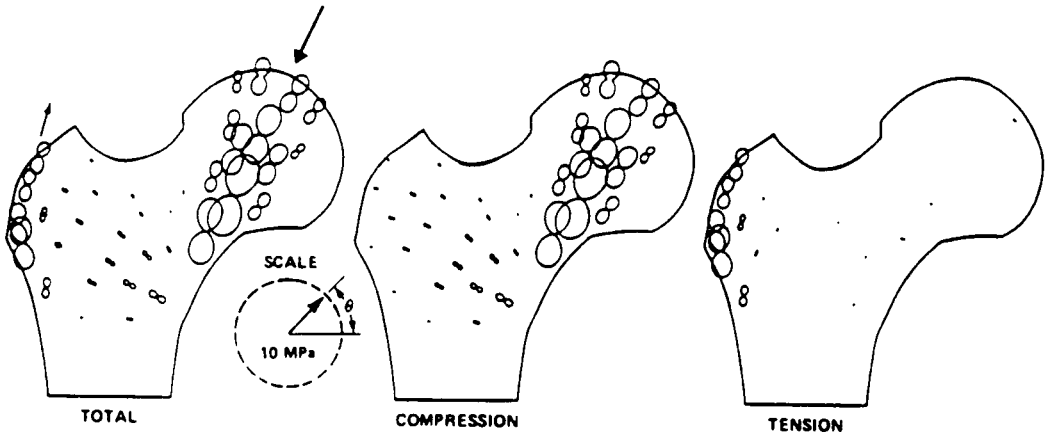

(b)

Figure 2.34: (a) Principal Stresses Calculated for Loading Case 1; (b) Polar Plots of Equivalent Normal Stress of Selected Elements for 3rd Iteration in Load Case 1. [Carter *et al.* 1989]

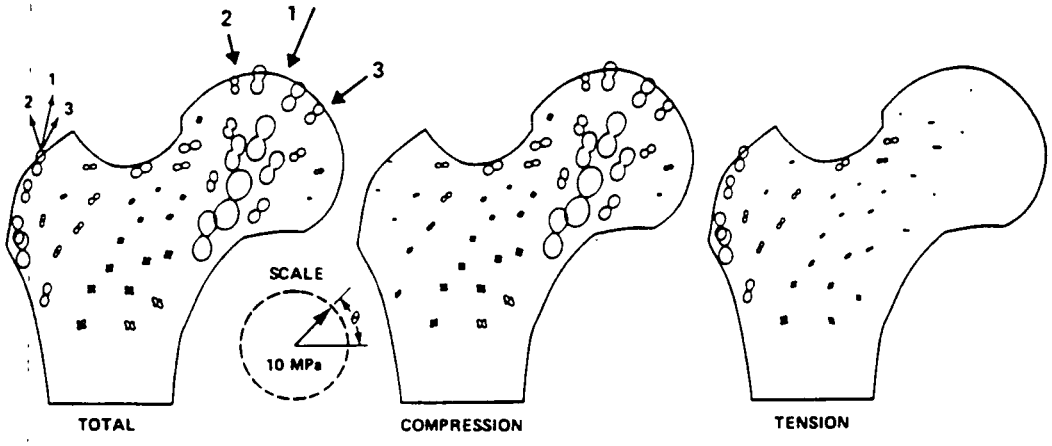

Figure 2.35: Polar Plots of Equivalent Normal Stress of Selected Elements for Multiple-Load-Direction (M = 4.0) Solution for 3rd Iteration. [Carter *et al.* 1989]

the assumed loading conditions. The authors relate the elastic modulus to cube of the apparent density of the bone with,

$$E = 3790\rho^3.$$

There is evidence that the trabecular bone modulus is more closely proportional to the square of the apparent density, rather than the cube. With the change in this relation, the authors found that the remodeling solutions showed less severe bone consolidation, and there also appeared to be less of a difference between the predicted density relationships of the third and seventh iterations. The assumed loading conditions also seemed to affect the variations in bone density. Greater variations in loading conditions tend to lead to more subtle changes in bone density as bone will be required in more dispersed regions. These two modifications are some of the basic adjustments contemplated by Carter *et al.* for altering this model but in no way limit the many other potential considerations involving the central remodeling theory behind this analysis.

In this particular study, the multiple-load theory was implemented so as to predict the density and orientation distributions in bone. The authors believe that the internal structure and morphology of long bones appear to be governed by the loading history of the bone. The multiple-load scenario was still a significant over-simplification of the true loading history to which a bone is exposed as normal physical activities involve changes in contact area in joints, joint and muscle force magnitudes, and direction of force in each cycle. However, it still proved to capture the essence of bone morphology within the femur and were more accurate than in the single-load cases. With the incorporation of more loading conditions each having a different number of loading cycles, a more accurate daily average loading history of a person may be simulated and improve the correlation with bone architecture. [Carter *et al.* 1989]

The basic procedure shown in this particular study can be applied to the general study of the relationship between loading history and bone morphology. Eventually the response to stress history changes due to alterations in physical activity that cause bone atrophy and hypertrophy can be predicted such that functional bone adaptations can be anticipated as the models developed will prove indispensable in the application of orthopaedic implants and appliances.

2.7. *Conclusion*

From the experiments of bone atrophy and hypertrophy that have been examined in this chapter, one can see that there is a relationship between mechanical stress with the change in morphology of bone. Cortical and trabecular bone adapt to increases or decreases in loading through tissue deposition and resorption. Studies by Uhthoff *et al.* (1978) and Jaworski *et al.* (1980) show that long-term immobilization of limbs of dogs cause reductions in cortical bone density and thickness and increases in medullary canal. The patterns of this bone loss has been characterized by a rapid bone loss followed by reversal, then a more gradual and sustained loss before bone stabilization. Van Reitbergen *et al.* (1993) looked at the effects of prosthetic press-fitted stems' postoperative bone morphology, and they also found sufficient amounts of bone resorption due to the prosthetic devices' redistribution of forces on the bone.

Bone hypertrophy was also evident in experiments by Woo *et al.* (1981) on pigs subject to exercise loading and Lanyon *et al.* (1984) on mechanically loaded turkey ulnae. Both cases show increased cortical thickness indicating adaptation of bone tissue to increased stress loading. As bone alters its morphology to accommodate loading variations, it appears that change in bone density is a significant variable in maintaining a functional strain. This underlines the concept that natural materials remodel their structure in order to optimize their performance for a given range of stress or strain with an inherent safety factor to prevent failure.

References

Alioa, J.F., S.H. Cohen, J.A. Ostuni, R. Cane, and K. Ellis. 1978. Prevention of Involutional Bone Loss by Exercise. *Ann. Intern. Med.*, v. 89, p. 356.

Allison, N. and B. Brooks. 1921. An Experimental Study of the Changes in Bone Which Result from Nonuse. *Surg. Gynecol. Obstet.*, v. 33, p. 250.

Andersen, Douglas M., Jefferson Keith, Patricia D. Novak, Michelle A. Elliot. 1994. Dorland's Illustrated Medical Dictionary, ed. 28, W.B. Saunders Company, Philadelphia.

Bertram, John E.A. and Sharon M. Swartz. 1991. The Law of Bone Transformation: A Case of Crying Wolff? *Biol. Review*, vol. 66, pp. 245-273.

Bouvier, Marianne. 1989. The Biology and Composition of Bone. In Bone Mechanics, ed. Stephen C. Cowin, CRC Press, Inc., Boca Ratan, Florida.

Burr, David B., R. Bruce Martin, Mitchell B. Schaffler, and Eric L. Radin. 1985. Bone Remodeling in Response to In Vivo Fatigue Microdamage. *Journal of Biomechanics*, v. 18, no. 3, pp. 189-200.

Carter, D.R., T.E. Orr, and D.P. Fyhrie. 1989. Relationships Between Loading History and Femoral Cancellous Bone Architecture. *Journal of Biomechanics*, v. 22, no. 3, pp. 231-244.

Cheal, Edward J. 1986. Trabecular Bone Remodeling Around Implants. Ph.D. Thesis. Massachusetts Institute of Technology, Cambridge, Massachusetts.

Cowin, S.C. 1986. Wolff's Law of Trabecular Architecture at Remodeling Equilibrium. *Journal of Biomechanical Engineering*, v. 108, pp. 83-88.

Cowin, S.C. 1989. The Mechanical Properties of Cortical Bone Tissue. In Bone Mechanics, ed. Stephen C. Cowin, CRC Press, Inc., Boca Ratan, Florida.

Currey, John. 1984. The Mechanical Adaptations of Bones, Princeton University Press, Princeton, New Jersey.

Dalin, N. and K.E. Olsson. 1974. Bone Mineral Content and Physical Activity. *Acta Orthop. Scand.*, v. 45, p. 170.

Fhyrie, D.P. and D.R. Carter. 1986. A Unifying Principle Relating Stress to Trabecular Bone Morphology. *Journal of Orthopaedic Research*, vol. 4, pp. 304-317.

Fung, Y.C. 1981. Biomechanics: Mechanical Properties of Living Tissues, Springer-Verlag, New York.

Gieser, M. and J. Treuta. 1958. Muscle Rarefication and Bone Formulation. *Journal of Bone and Joint Surgery*, v. 40, p. 282.

Goldstein, Steven A., Larry S. Matthews, Janet L. Kuhn, Scott J. Hollister. 1991. Trabecular Bone Remodeling: An Experimental Model. *Journal of Biomechanics*, v. 24, supp. 1, pp. 135-150.

Goodship, A.E., L.E. Lanyon, and H. McFie. 1979. Functional Adaptation of Bone to Increased Stress. *The Journal of Bone and Joint Surgery*, v. 61A, pp. 539-546.

Harrigan, T.P. and J.J. Hamilton. 1994. Bone Remodeling and Structural Optimization. *Journal of Biomechanics*, vol. 27, no. 1, pp. 323-328.

Harrigan, T. and R.W. Mann. 1984. Characterization of Microstructural Aniostropy in Orthotropic Materials Using a Second Rank Tensor. *Journal of Material Science*, v. 19, pp. 761-767.

Hart, Richard T. and Dwight T. Davy. 1989. Theories of Bone Modeling and Remodeling. In Bone Mechanics, ed. Stephen C. Cowin, CRC Press, Inc., Boca Ratan, Florida.

Hayes, W.C. and B. Snyder. 1981. Toward a Quantitative Formulation of Wolff's Law in Trabecular Bone. In Mechanical Properties of Bone, ed. Stephen C. Cowin, ASME, New York.

Jaworski, Z.F.G., Maria Liskova-Kiar, and Hans K. Uhthoff. 1980. Effect of Long-Term Immobilization of the Pattern of Bone Loss in Older Dogs. *The Journal of Bone and Joint Surgery*, v. 62B, pp. 104-110.

Jones, H.H., J.D. Priest, W.C. Hayes, C.C. Tichnor, and D. Nagel. 1977. Humeral Hypertrophy in Response to Exercise. *Journal of Bone and Joint Surgery*, v. 59A, pp. 204.

Kazarian, L.E. and H.E. Von Gierke. 1969. Bone Loss as a Result of Immobilization and Chelation - Preliminary Results in Maccaca mulatta. In *Clin. Orthop. Rel. Res.*, n. 65, pp. 67.

Keaveny, Tony M., Edward F. Wachtel, Catherine M. Ford, and Wilson C. Hayes. 1994. Differences Between the Tensile and Compressive Strengths of Bovine Tibial Trabecular Bone Depend on Modulus. *Journal of Biomechanics*, v. 27, no. 9, pp. 1137-1146.

Krolner, B., B. Toft, S.P. Nielsen, and E. Tondevold. 1983. Physical Exercise as Prophylaxis against Involutional Vertebral Bone Loss: A Controlled Trial. *Clin. Sci.* v. 64, p. 541.

Lanyon, L.E. 1974. Experimental Support for the Trajectorial Theory of Bone Structure. *Journal of Bone and Joint Surgery*, v. 56B, pp. 160-166.

Lanyon, L.E., P.T. Magee, and D.G. Baggott. 1979. The Relationship of Functional Stress and Strain to the Process of Bone Remodeling: An Experimental Study on the Sheep Radius. *Journal of Biomechanics*, v. 12, pp. 593-600.

Lanyon, L.E. and C.T. Rubin. 1984. Static versus Dynamic Loads as an Influence on Bone Remodeling. *Journal of Biomechanics*, v. 17, no. 12, pp. 897-905.

Martin, R. Bruce and David R. Burr. 1982. A Hypothetical Mechanism for the Stimulation of Osteonal Remodeling by Fatigue Damage. *Journal of Biomechanics*, v. 15, pp. 137-139.

Martin, R. Bruce and David R. Burr. 1989. Structure, Function and Adaptation of Compact Bone, Raven Press, New York.

Meade, John B. 1989. The Adaptation of Bone to Mechanical Stress: Experimentation and Current Concepts. In Bone Mechanics, ed. S.C. Cowin, CRC Press, Inc., Boca Ratan, Florida.

Pollard, A.W., S.A. Feik, and Storey. 1984. Remodeling of Bone and Bones: Effects of Translation and Strain of Transplants. *Br. J. Exp. Pathol.*, v. 65. pp. 655-670.

Radin, E.L., J.W. Pugh, R.S. Steinberg, H.G. Parker, and R.M. Roe. 1972. Trabecular Microfractures in Response to Stress: The Possible Mechanism of Wolff's Law. International Congress Series #291. *Orthop. Surg. and Trauma.*, pp. 59-65.

Roesler, H. 1981. Some Historical Remarks on the Theory of Cancellous Bone Structure (Wolff's Law). In Mechanical Properties of Bone, ed. Stephen C. Cowin, ASME, New York.

Roszek, B., H. Weinans, P. Van Loon, and R. Huiskes. 1993. In Vivo Measurements of the Loading Conditions on the Tibia of the Goat. *Acta Anatomica*, v. 146, pp. 188-192.

Turner, Charles H. 1992. On Wolff's Law of Trabecular Architecture. *Journal of Biomechanics*, v. 25, no. 1, pp. 1-9.

Uhthoff, Hans K. and Z.F.G. Jaworski. 1978. Bone Loss in Response to Long-Term Immobilization. *The Journal of Bone and Joint Surgery*, v. 60B, pp. 420-429.

Van Reitbergen, B., R. Huiskes, H. Weinans, D.R. Sumner, T.M. Turner, and J.O. Galante. 1993. The Mechanism of Bone Remodeling and Resorption Around Press-Fittted THA Stems. *Journal of Biomechanics*, v. 26, no. 4/5, pp. 369-382.

Whitehouse, W.J. and E.D. Dyson. 1973. Scanning Electron Microscope Studies of Trabecular Bone in the Proximal End of the Human Femur. *Journal of Anatomy*, v. 118, pp. 417-444

Woo, Savio L.Y., Steve C. Kuei, David Amiel, Mark A. Gomez, Wilson C. Hayes, Francis C. White, and Wayne H. Akeson. 1981. The Effect of Prolonged Physical Training on the Properties of Long Bone: A Study of Wolff's Law. *The Journal of Bone and Joint Surgery*, v. 63A, pp. 780-786.

Chapter 3: Wood

3.1. *Introduction*

For living trees, wood performs the role of *support* to help the tree remain erect as it extends in height, the role of *conduction* so that water can be transported from the ground to the upper portions of the tree, and the role of *storage* for food until it is required by the tree. As the tree grows, form and function are related, allowing the plant to modify its morphology to adapt to given situations. Trees are capable of reacting to their physical environment and adapting their form during growth; patterns within the plant structure reveal the complex process of the feedback between growth and form. Adaptive growth in trees involves the elaborate shaping of individual tree designs which are formed to accommodate the external load conditions. There are four main mechanisms which control tree shape:

- *Epinasty* - dominance of the leading shoot;
- *Negative Geotropism* - tendency of branches to grow in parallel and opposite to gravity;
- *Positive Geotropsim* - tendency of roots to grow in direction of gravity;
- *Phototropism* - tendency of shoots to grow toward best light reception.

The main biological aim of the tree is to receive maximum light reception by means of a large crown. When subject to stress or strain induced by mechanical loading, such as wind in the case of trees, the wood adapts its form to accommodate this change in loading. The wind is able to influence tree growth and development such that the tree will develop a homogeneous distribution of stresses acting on its surface. The emphasis of this chapter will be on the remodeling response of wood as its change in morphology attempts to maintain a constant state of surface stress. [Mattheck 1990, Ashby *et al.* 1980]

3.2. *Wood Composition and Structure*

The tree trunk functions to support the crown which is responsible for food and seed production. The trunk stores carbohydrates and conducts mineral solutions which

are absorbed by the roots and carried it upwards toward the crown. This process is usually restricted to the outer trunk region. Wood is a hard fibrous substance which is basically vascular tissue consisting of vessels and tracheids with wood fibers and parenchyma cells; it composes the majority of the stems and branches of trees beneath the bark. Woody plants are vascular, possessing conducting tissues that consist of both xylem (wood) and phloem (bark). Wood cell growth takes place in the cambium, the layer between the wood and bark; this layer annually forms new wood and bark that is inserted between the older wood and bark.

3.2.1. *Cell Wall Composition*

Wood and bark are made of individual cells that together determine their morphology. Cell walls make up nearly 95% of the mass of the woody plant with its main chemical components being cellulose, hemicellulose, lignin, and extractives. **[Table 3.1]** *Cellulose* is the chief cell wall component comprising 45-50% of the cell walls. This skeletal polysaccharide is a linear polymer composed of β-D, 1-4 linked anhydroglucose units. Covalent bonding within and between glucose units results in a straight and stiff molecule with high tensile strength. Hydrogen bonds induce the lateral bonding of cellulose molecules into linear bundles, and the large number of these hydrogen bonds provides crystalline regions (60 *nm* in length) in the cell wall. Carbohydrate polymers know as *hemicelluloses* are associated with the cellulose in the cell wall. However these sugar units differ from cellulose in that they are smaller polymers, branched, usually contain more than one sugar-type within the molecule, and do not form crystalline regions. The third major wood cell component is *lignin*, making up 20-30% of the cell walls. It is quite different from cellulose and hemicellulose because of its complex, cross-linked, three-dimensional units. Lignin acts as a cement between wood fibers providing stiffening of the fibers while it also serves as a barrier to enzymatic degradation of the cell wall. *Extractives* include a number of different chemical types such as fatty acids, aromatic compounds, volatile oils, and terpenes and related compounds. They are typically found in varying amounts in the heartwood zone. [Lewin *et al.* 1991]

Table 3.1: Chemical Composition of Wood. [Lewin *et al.* 1991]

Chemical	% Composition	Polymeric Nature	Role
Cellulose	45-50	Linear Molecular Crystalline	Framework
Hemicellulose	20-25	Branched Molecular Amorphous	Matrix
Lignin	20-30	3-D Molecule	Matrix
Extractives	0-10	Polymeric	Encrusting

3.2.2. *Wood Microstructure*

The vast majority (90-95%) of cells in wood are aligned with the vertical axis while the remaining portions are aligned in the radial plane (the ray cells). **Figure 3.1**, showing both a macroscopic and microscopic view of wood, illustrates the long, hollow, prismatic cells of roughly hexagonal cross-section that make up wood. The radial and tangential directions illustrate the long and slender shape of the cells. The structure also has tubular sap channels which run up the axis of the tree carrying fluids from the roots to the crown. The smaller cells which extend radially outward from the center of the trunk to the bark compose the rays. Neither the sap channels nor the rays carry much mechanical load.

Softwoods, also known as gymnosperms, contain elongated cells called tracheids that have dual roles of conduction and support. These plants are also called evergreens due to their retention of leaves. The longitudinal tracheids, strand tracheids, longitudinal parenchyma[1], and epithelial cells comprise the vertical system of cells. The horizontal system consists primarily of ray parenchyma and a small portion of ray tracheids and epithelial cells found in certain species of trees. Softwoods maintain two interpenetrating systems: a longitudinal system composed of non-living tracheids and a transverse system of rays composed of living ray parenchyma cells. Living parenchyma cells are considerably smaller than the longitudinal tracheids and perform the role of food storage as their thin cell walls contain pits with unperforated membranes.

Hardwoods are more complex than softwoods because they contain more cell types and show considerable variation in size, shape, and arrangement of individual cell types. These types of trees are also called angiosperms or deciduous trees and are known

[1] Parenchyma are food-storing cells which are short with relatively thin walls.

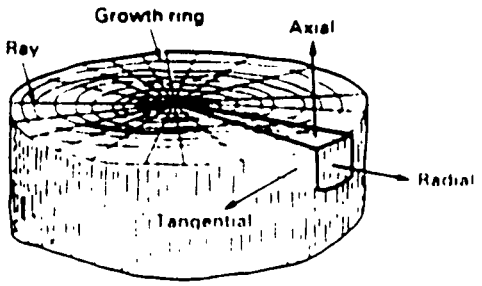

(a)

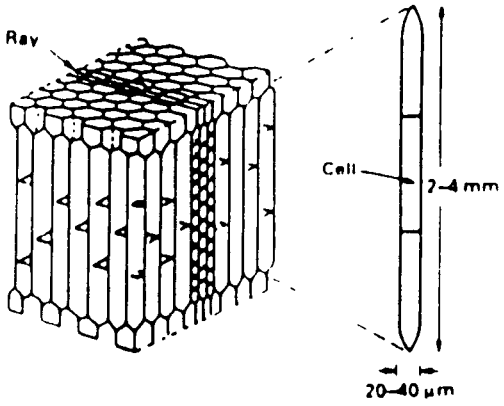

(b)

Figure 3.1: (a) Macrostructure of wood; (b) Microstructure of wood. [Ashby *et al.* 1980]

for their annual leaf shedding. In hardwoods vessels are responsible for the conduction of water. The fibers and tracheids, making up 60% of wood volume, support the tree while the structure of hardwood is characterized by the presence of vessel elements, tracheids, fibers, longitudinal parenchyma, and ray parenchyma. Both the longitudinal and ray parenchyma, which comprise approximately 40% of wood volume, function to provide food storage. More cell types and greater variation of wood volume give hardwoods a more complex structure with variable wood properties compared to softwoods. [Illston *et al.* 1979, Ashby *et al.* 1980, Lewin *et al.* 1991]

Table 3.2: Wood Cell Types. [Lewin *et al.* 1991]

SOFTWOOD			
LONGITUDINAL		**TRANSVERSE**	
Support, Conduction, or Both	**Storage**	**Support, Conduction, or Both**	**Storage**
- Longitudinal Tracheid - Strand Tracheid	- Longitudinal Parenchyma - Epithelial	- Ray Tracheids	- Ray Parenchyma - Epithelial

HARDWOOD			
LONGITUDINAL		**TRANSVERSE**	
Support, Conduction, or Both	**Storage**	**Support, Conduction, or Both**	**Storage**
- Vessel Elements - Fibers - Tracheids	- Parenchyma	None	- Ray Parenchyma

3.2.3. *Wood Formation*

The increase in diameter and extension of length in tree stems and branches are due to the production of new cells by tissues called *meristems* which consist of cells that retain the ability to divide and produce new cells throughout their life. After each cell division, one cell differentiates into another mature cell while the other remains meristematic. Height increase in the stem and length increase in branches are specified as part of the tree's primary growth for they are the outcome of cell production by apical meristems located at the tip of the main stem, branch, or root.

The lateral meristem, or vascular *cambium*, is located between the wood and bark completely encircling the tree stem and is responsible for increasing the stem diameter.

Wood cells are produced by division of the cambium, which is the zone of living cells that lie between the bark and wood portion of the trunk and branches. The beginning of growth takes place in the spring, and cells in a single layer subdivide radially to form the cambial zone with a width of about ten cells. The formation within each dividing cell of a new vertical wall develops into the primary wall. During the growing season, the cells undergo further subdivision; some cells remain cambial cells while others develop into bark or change into wood. To accommodate the increasing diameter of the tree, the cambial zone must also increase circumferentially which is achieved by periodic tangential cambial cell division. Cells produced radially from the cambium experience a series of changes which extend for about three weeks. This is known as the differentiation process as changes in the cell shape are paralleled with the formation of the secondary wall. Wood consists of two systems of cells; cells oriented longitudinally to the main tree stem are produced by cambial cells and are designated as fusiform initials while cells oriented transversely which are produced by ray initials.

Cell development in wood follows five different phases: (1) cell division, (2) cell enlargement, (3) cell wall thickening, (4) lignification, and (5) death. Cell division occurs when the cambial initial first divides and forms two cells. If the cell adjacent to the bark remains meristematic, the inner cell will develop into a mature wood cell as it undergoes the remaining four stages of development. However, if the innermost cell remains meristematic, the outer cell will differentiate into a bark cell. Thus, wood cell production moves the cambium further away from the center of the tree. The developing cell grows during the second stage of cell enlargement. Two differing processes take place in this phase when comparing softwoods to hardwoods. Softwood cells increase their diameter only in the radial direction; in contrast, transverse enlargement of vessels occurs both in the radial and tangential direction for hardwoods. In these trees, tangential growth pushes cells aside and interrupts the radial alignment of cells. **[Figure 3.2 - 3.3]** During the enlargement phase, a thin, plastic cell wall known as the primary wall encases the protoplasm. The cell wall thickness increases during the thickening phase and is extended by a secondary wall. The amount of cell wall thickening is dependent on the time of the year that the cells are formed and/or on the function of the cell, but once the wall

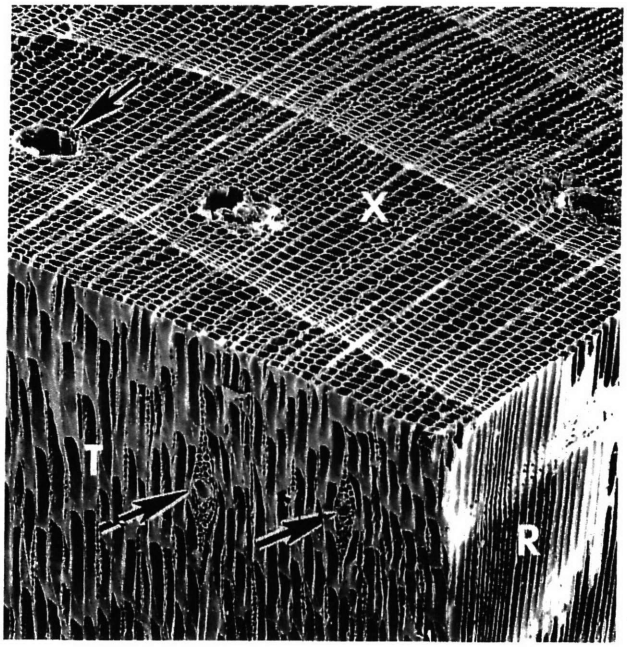

Figure 3.2: Cross-sectional View of Softwood Growth Rings. (*X*) Indicates a Longitudinal Resin Canal while Fusiform Rays (*arrows*) are Embedded in the Tangential Plane (*T*). (*R*) indicates radial plane. [Lewin *et al.* 1991]

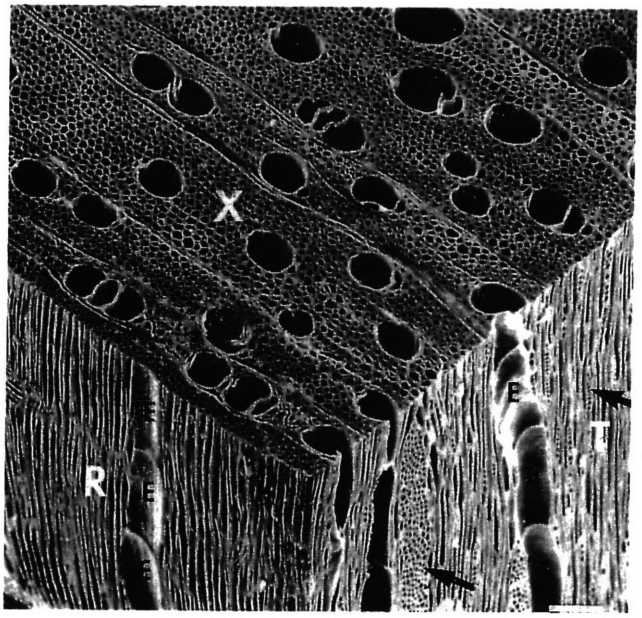

Figure 3.3: Hardwood with Fairly Uniform Vessel Diameters Across Section of Growth Ring. Formation of Vessels from Individual Vessel Elements (*E*) in radial (*R*) and tangential (*T*) directions. Arrows Indicate Presence of One-Cell Wide and Multi-Cell-Wide Rays. [Lewin *et al.* 1991]

thickening process occurs, no further growth of the cell is possible. Lignification in cell development involves the creation of lignin between the newly formed cells within their cell walls. Early lignification is rapid in areas between cells, designated middle lamella, and the primary wall while secondary lignification is more gradual and initiated when the middle lamella lignin concentration is about half of the maximum. The last stage of wood cell development is cell death which occurs immediately after lignification. For wood cells that perform storage functions, this step is postponed for an unspecified amount of time. After this death suspension period, cell termination occurs. [Illston *et al.* 1979, Ashby *et al.* 1980, Lewin *et al.* 1991]

3.2.4. *Gross Morphology of Wood*

The increasing trunk diameter of a tree matches the increasing crown diameter. On a macroscopic level, the *sapwood* composes the outer trunk region beneath the bark while *heartwood* is located in the center portion of the trunk as its cells no longer conduct nutrients to the crown of the tree. **[Figure 3.4]** The sapwood width varies with species and age, but it is typically less than a third of the total tree radius. Sapwood is the most recently formed wood and performs the role of support, conduction, and food storage. After a period of time, the food-storing cells die and a secretion of oxidized phenols and sometimes pigments (in woods with dark-colored heartwood) occurs. These secreted materials are the extractives, and in some species, the extractives are toxic to decay organisms and help the heartwood resist decay. The area where all of the cells are physiologically dead is known as the heartwood, and it functions only as support for the tree. As new wood is formed between the existing wood and the bark, the sapwood which is adjacent to the heartwood is converted to heartwood. Sapwood contains the only living cells in mature wood, and thus the majority of the cells that compose the wood portion of a living tree are dead. As the food-storage cells die and more heartwood is formed, the amount of living cells in the stem continues to decrease.

As the crown of the tree develops upward and outward, the radial growth of the trunk also corresponds in size with enlargement of existing branches and production of new ones. The main cells or tracheids of the wood run axially up and down the tree,

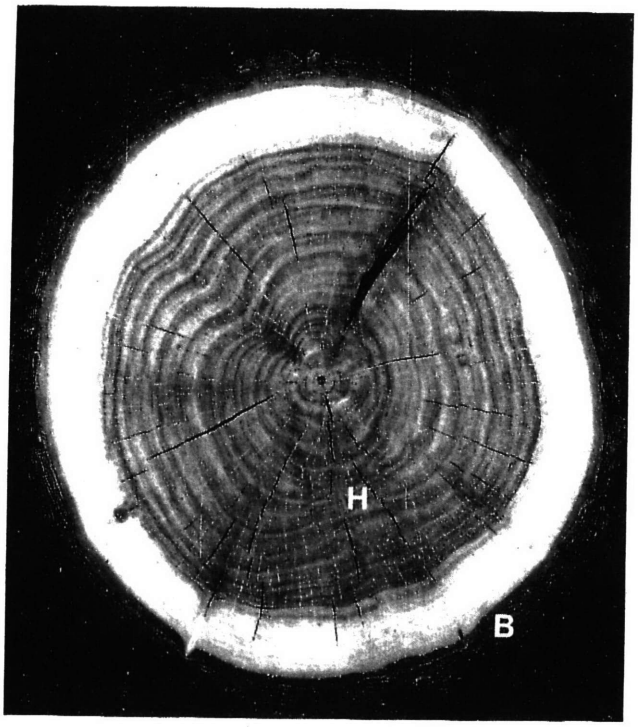

Figure 3.4: View of Tree Stem Showing Bark (*B*), Sapwood (*S*), and Heartwood (*H*). [Lewin *et al.* 1991]

which is the direction of greatest strength. With each growing season, trees add a new layer of wood between the existing wood and the bark throughout the tree from the branches to the roots. These new layers are termed *growth rings* as can be seen in **Figure 3.5**. Wood that is produced early or late in the growing season is differentiated by color such that the *earlywood* or springwood is lighter in color while the *latewood* or summerwood, produced last, is darker. This color difference is due to the variation in the structure of cells between the two: earlywood being less dense than latewood. While most wood cells have their long axis oriented parallel to the long axis of the tree stem, some cells have their long axis perpendicular to it. The transversely oriented cells are the wood *rays*. Rays appear as light-colored lines varying in width as they stretch across the growth rings. For softwood species, the rays are typically one cell width, but in hardwoods, they vary from one cell to many. **[Figure 3.6]**

3.2.5. *Reaction Wood*

A series of factors may cause defects in wood structure, and this may consequently lower its strength. When trees become inclined to a vertical axis due to wind or growing on a sloping ground, growth-promoting hormones are disturbed and distributed. The result is a formation of an abnormal tissue type. The regulation of the growth habit of a tree is controlled by reaction wood as its main purpose is to respond to the abnormal orientations of the tree and allow secondary movement of the stem. For softwoods, the reaction tissue with higher than normal lignin content grows on the compression side of the trunk. This compression wood is more brittle than normal wood and it pushes a bent or curved tree up into the correct geotropic position by axial compressive wood expansion. Compression wood xylem is characterized by tracheids with thickened and lignified secondary walls. The cells of this form of reaction wood contain a (1-3)-β-D-glucan, laricinan, and their circular nature creates air spaces in the middle lamella between tracheids. **[Figure 3.7]** In hardwoods, reaction wood forms on the tension side of the trunk and is characterized by higher than normal cellulose content. It is formed on the upper side facing away from the soil as the tree is pulled into position. **[Figure 3.8]** Tension wood's rubbery fiber characteristics make it more difficult for sawing and

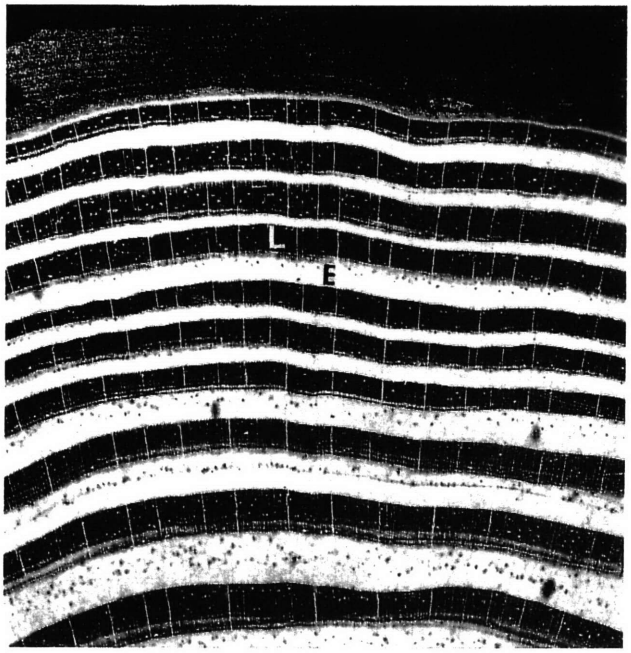

Figure 3.5: View of Softwood Stem Showing Growth Rings. Earlywood (*E*) is the Light Area While the Dark Area is Latewood (*L*). [Lewin *et al.* 1991]

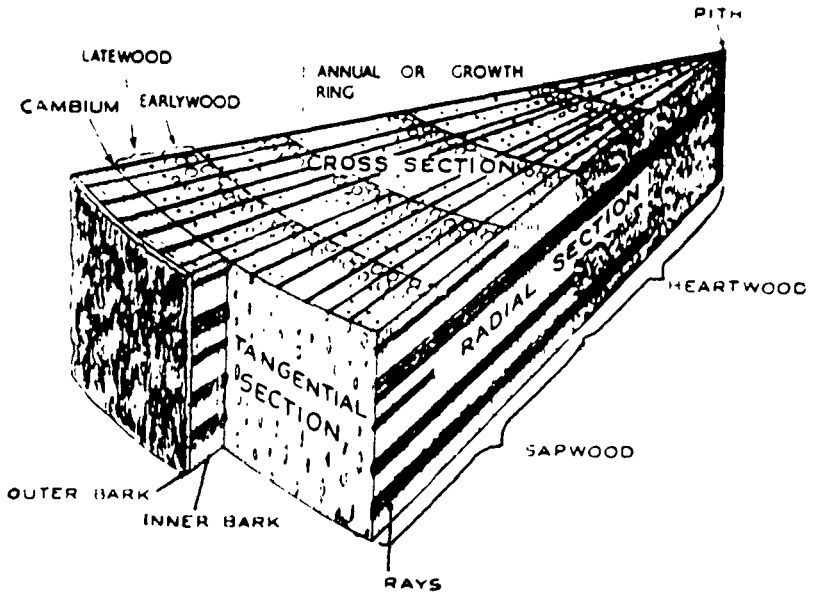

Figure 3.6: Diagram of Wedge-Shaped Segment Cut From Hardwood Tree Showing Principal Features. [Illston *et al.* 1979]

machining. It is characterized by an increased number of thick-walled, gelatinous fibers with smaller and fewer vessels.

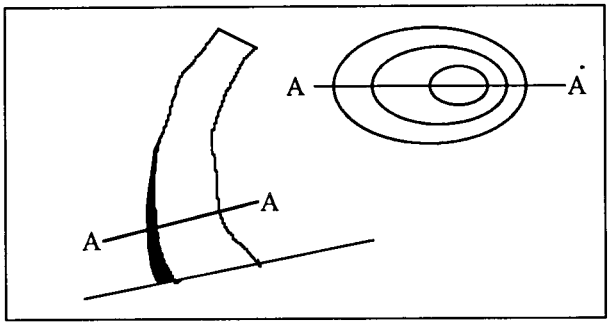

Figure 3.7: Compression Wood.

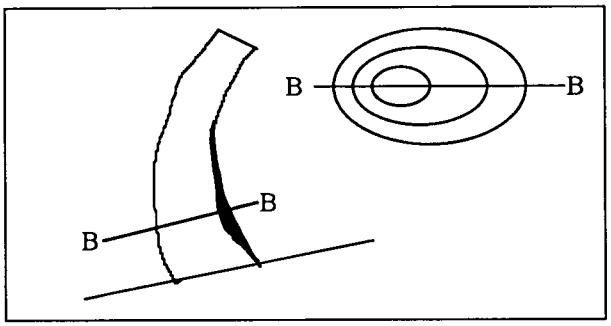

Figure 3.8: Tension Wood.

With reaction wood, the tree is able to adapt to the mechanical loading that it experiences through wind and growth to attain an overall optimized structure. The adaptive growth activity's primary objective is to achieve the best possible restoration of constant stress and even distribution of mechanical stress while it modifies the ideal tree design by adapting to a new situation. [Mattheck 1989]

3.3. *Wood Adaptation*

The effect of wind induced mechanical stress on stems of trees have been described in terms of stress and strain. From such mechanical relationships, the stress and strains that are experienced by trees can be evaluated to determine exactly how a tree responds to increased or decreased mechanical loading. The external stress acting on an organism can

induce secondary stresses and strains within the system; in this case, wood. These induced strains can be elastic such that chemical or physical alterations are reversible. An example of this can be seen in the swaying of a tree subject to wind which returns to its original position. Plastic strain involves the permanent displacement of a tree from its original orientation. Such strains can be considered harmful to the tree, but they have developed a form of recovery known as reaction wood.

Where regions of the tree may experience a higher strain level caused by a loading stress, this area will be strengthened by adaptive growth to reduce the surface strain. There are certain climactic conditions which incur acute wind stress that may exceed the biomechanical limits of the tree. Conditions like severe frontal systems or cyclonic storms cause failure such as canopy level branch failure, foliage loss, stem displacement, and sometimes complete failure of the whole tree by wind throw. Interestingly, the properties of the wood itself help to determine the type of failure which will occur. Trees with a high wood density and increased taper tend to become uprooted by intense wind stress. However, trees such as those found in tropical rain forests which possess a lower wood density and low stem taper will snap when they fail.

As a tree grows through a canopy boundary layer, the growth process that occurs is affected by biomechanical acclimation to the specific wind conditions within the foliage and the changes in self weight. During the complex growth, a tree attempts to maintain the criteria for stability and efficiency as it "competes" with other "better designed" trees in a field or forest. Wilson and Archer (1979) examine trees as cantilever beams subject to bending from both static loads of self weight and dynamic loads primarily induced by wind. As the tree grows, bending stresses increase with forces, and thus stiffness increases to reduce excessive bending or breakage. Weight is also increased with the addition of branches, leaves, and wood. The effective force of the wind can also become greater due to the crown's increasing size acting like a sail of a boat. Growth increases the moment arm length because of elongation and leaf production of the branches and stem. As a result, the center of gravity and point of action of the wind forces move. Further examination of the authors' findings will be discussed more thoroughly below.

3.3.1. *Physiological Response*

Trees respond to mechanical stress physiologically and developmentally. The physiological reactions of trees involve the leaves and growth of woody tissue. As wind stress acts on a tree, there are direct movement of foliage and secondary effects with change the local atmospheric conditions near the leaves within the canopy. With the mechanical motion of leaves, it has been found that net photosynthesis and transpiration decrease which can be due to a biochemical stimulation to the leaves (like that induced experimentally by rubbing) or clustering. Studies by Telewski and Jaffe (1986a) show that mechanical stress such as shaking can inhibit stem and needle elongation on firs (*Abies fraseri*). Other forms of stress, including wind-blown particulates, can also create indirect mechanical strain. Chemical stresses such as salt spray in coastal regions as well as pollutants can create problems on the surfaces of the leaves.

As wind poses compressive and tensile forces on the tree, dynamic flexural loading results. It follows that static compressive and tensile forces will also be induced within the stem of the tree. Both forms of forces affect woody tissue and its development. Wind sway initiates dynamic loading, but the position of a stem is not displaced for a long enough period of time to induce any gravitropic response. However both plastic and elastic strain can be initiated through tissue fatigue or failure, and bending, respectively. Static loads caused by a constant wind flow displaces a stem for a prolonged period thus spurring a gravitropic response. This load usually permanently displaces the stem.

A series of physiological responses takes place with the application of mechanical stress. One of the most prevalent is the production of the growth regulator, ethylene, as trees undergo flexure. Some of the observations of the effect of ethylene on the tree on a microscopic level include cambial division on tracheid formation, increased tracheid radial cell wall thickness, and increased proportions of wood density, resin canals, and ray parenchyma cells. The gravitropic response induced by static loads involve the growth of reaction wood which will be discussed below.

3.3.2. *Developmental Response*

Environmental agents including snow, landslides, erosion, earthquakes, and soil creep can also cause tree displacement. A tree's response to this leaning is the development of reaction wood. Vertical stems grow in the direction opposing gravity while lateral branches maintain an equilibrium position at an angle in relation to gravity. Compression wood in the coniferous species develops on the lower side of tilted stems and the underside of branches. In the angiosperm species, tension wood develops on the upper side of tilted stems and branches.

Consider the dynamic flexure of trees which are subject to sway in wind from low to high speeds. Compressive and tensile forces in the wood tissues will develop. An oscillating effect is created as the tree tends to overshoot its original orientation, but this oscillation will eventually damp out and return the tree to its initial position without the application of any further external force. The effects of these flexure stresses cause thigmomorphogenic growth which produces more compact growth, greater step taper (change in diameter with length), shorter branches, and smaller leaves. The details of this form of adaptive morphologic response in plants will be explained in greater detail in *Chapter 4 (Plant Stems)*. Ultimately, the changes that the tree experiences when subject to wind loading help reduce speed specific drag in the crown, maintain a geometric similarity between stem diameter and height growth, and produce a safety margin against mechanical failure.

Looking at the microscopic level, coniferous trees which develop compression wood and form an asymmetric stem radius have an increased number of shorter tracheids in the direction of flexure (the leeward side of the stem) compared to non-stressed trees. Changes in grain angle within the wood have also been observed. In the same study on firs (*Abies fraseri*), there is a reported increase in grain angle on the windward side of trees on a ridge and in laboratory experiments where flexure stress was induced. [Telewski *et al.* 1986a]

Morphological and anatomical changes influence the biomechanical properties of the wood. Response to flexure produces an increased second moment of area (I) because of increased radial growth due to reaction wood. However, there also tends to be a

reduction in elastic modulus (E) shown by flexure experiments in the firs of Telewski *et al.* (1986a) As a result, the flexural stiffness (EI) of the plant becomes altered as the predominant influence of I (which raises as the stem radius to the fourth power) increases. This suggests greater flexural stiffness.

3.4. *Constant Stress Hypothesis*

In 1979, Wilson and Archer first introduce the *constant stress hypothesis* (also known as the *constant strain hypothesis*) suggesting that there exists a relation between the measured stem diameter (D) and the related height (h) such that there is a constant mechanical stress along the whole length of the tree stem. When the theory looks at individual trees idealizing them with a long trunk and small crowns, wind force can be modeled by a single force acting laterally at the tree top causing a linear bending moment distribution downward along the stem. As a result, the requirement of constant surface stress leads to an empirical relationship of:

$$h \propto D^3.$$

Wilson *et al.* describe tree stems as cubic paraboloids of revolution; when an ideal beam of such form is bent, maximum strains along the outside of the beam remain constant along the entire length of the beam. This has been proposed as the D^3 *law*, and stems designed with this law possess no weak area where it was most likely to break when subject to sway in wind. The basis of this mechanical relationship begins with looking at a circular beam with diameter D, length h, and a transverse load P acting on it. Stress (σ) is proportional to the moment (M) and the distance from the centroid to the point of interest in the cross-section (y) while inversely proportional to the moment of inertia (I) such that:

$$\sigma \propto \frac{My}{I}.$$

Since we are looking at the surface stress, y is equal to the radius (r) which is proportional to D. So it follows that:

$$\sigma \propto \frac{PhD}{D^4}$$

where $M \alpha P * h$ and $I \alpha D^4$. With a constant stress, this relationship shows that

$$h \propto D^3.$$

One major problem with the D^3 law is the assumption that the beam is held rigidly at the base. In reality, a large tree in high wind may move up and down relative to the ground, making the tree anchored in an elastic foundation. Because of this, the beam may tend to exhibit more of a *D^2 law*. Regardless of stems following the D^3 law or the D^2 law, the more significant conclusion is that trees will grow to maintain the shape which keeps maximum strains along the stem constant. The biological implication of this is that new wood is added to areas with highest maximum strain in order to reduce this strain.

Claus Mattheck (1989) takes this theory one step further suggesting that if this theory holds true and trees grow thicker at points of higher stress until there exists a homogeneous stress state over the entire stem, the hypothesis should also be valid for branch/stem joints and root/stem joints where notch stresses (areas of stress concentration along the wood contour) should be avoided. If there is a notch along the tree stem such that the localized notch stresses are higher than those stresses distant from the notch, the tree will tend to heal these wounds which cause the highest stress-peak the fastest. In cases where a rigid body may come into contact with a tree, trunk contact stresses are created, and the tree attempts to reduce localized stress peaks through a process of adaptive growth. [Mattheck 1989, Wilson *et al.* 1979]

3.5. *Morphological Changes - Shape Optimization*

Mattheck provides numerous analyses of various trees in the field which conform to the theory of constant stress and illustrates their achievement of constant surface Von Mises stress through finite element analysis. He first defines shape optimization as the form where there is sufficient strength for all relevant loading cases while maintaining a minimum weight. Thus, good mechanical designs are characterized by a homogeneous stress distribution of the surface with the requirement of a constant Von Mises stress at the surface of a mechanically optimized structure.

3.5.1. *Branch Stem Joint*

Using finite element calculation with a simplified plane-strain mode, Mattheck evaluated the shape of a branch stem. **[Figure 3.9]** The upper-side of the branch tends to be most at risk to the danger of failure when subject to bending with the point load (F) applied at the outer end of the branch. The main tensile stresses along the contour in the range of the joint are normalized by dividing by σ_{appl} and plotted against S_o, the distance along the contour from $S_o = 0.0$ to $S_o = 1.0$. These stresses in the joint are due to a load acting in the downward bending motion of the branch. From the analysis, the branch stem joint shows excellent shape optimization for bending loads because notch stress peaks are avoided. The stress distribution shown is not significantly affected by the bending of the stem and exhibits a nearly constant normalized stress pattern without notch stresses. This same type of optimization also appears in other natural materials such as deer antlers. **[Figure 3.10]** The same type of analysis is done with the application of a load at the tip of the antler spike such that tensile stresses form along the joint contour. The plot of the normalized stresses shows good shape optimization with respect to bending loads as the stress distribution is nearly uniform from $S_o = 0.0$ *to* 0.2, and then it drops as S_o reaches 1.0. Thus, antler and the branch/stem joint appear designed in such a way to avoid localized stress peaks as well as grow into a state of constant surface stress.

3.5.2. *Tree Wounds and Overgrowth*

Mattheck applies the constant stress hypothesis to explain how trees grow to preserve their optimum design. If necessary, trees will restore a state of constant surface stress my permanent adaptation to the external loads to which they are exposed. Stress-controlled healing and self-repair in trees is evident in wounds caused by mechanical impact. A wound can essentially be a branch hole or impact point such that the local peak stresses (*notch stresses*) on the tree surface lead to a diversion of force flow; the tree surface becomes discontinuous. Wounds or notches tend to heal most quickly where the stress peaks are highest such as at the wound contour points that deviate from the ideal constant surface stress condition. Failure is most likely to occur in the regions of high notch stresses, therefore, such "weak" spots in tree design are "repaired" in the quickest

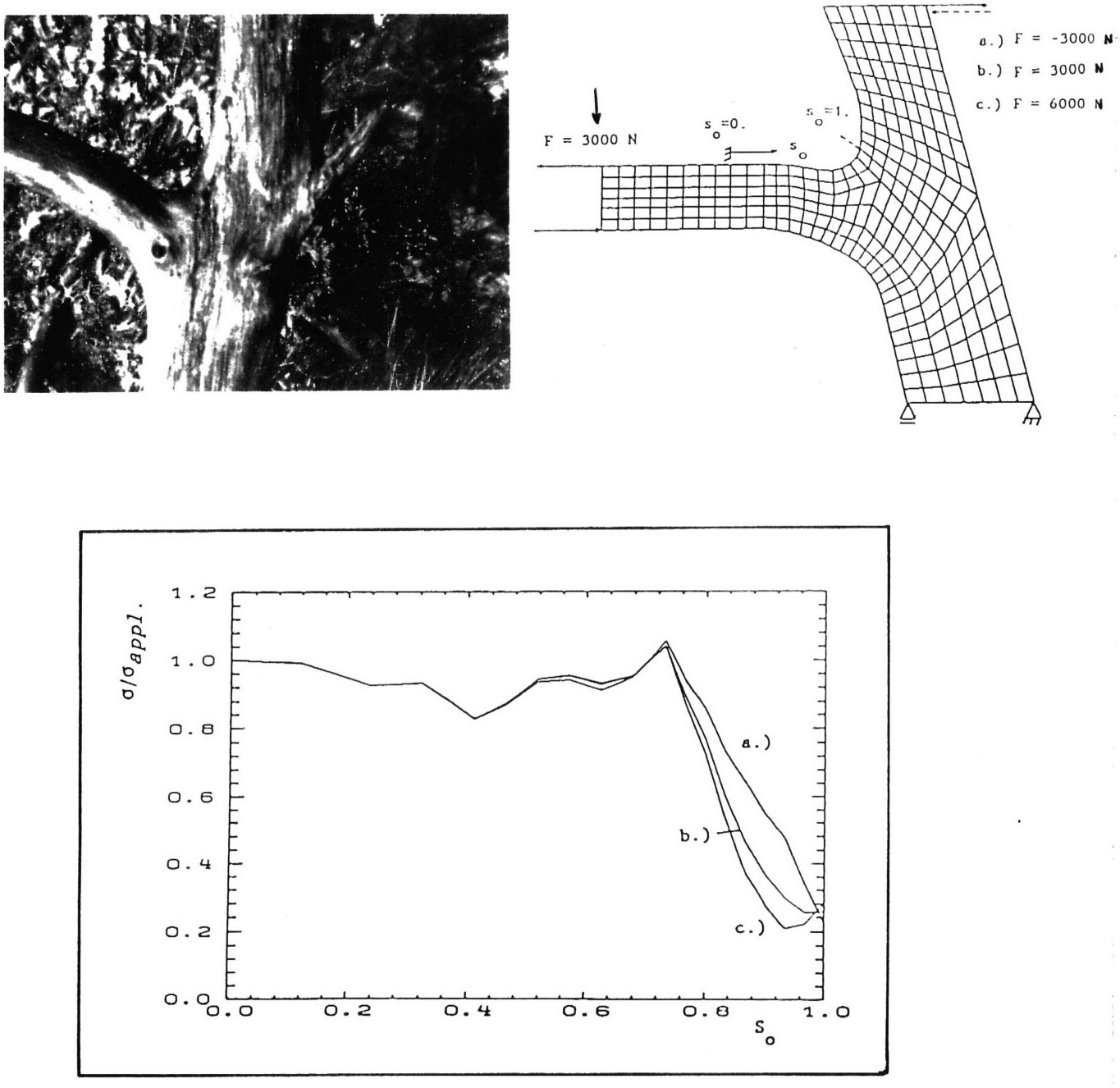

Figure 3.9: Finite Element Analysis of Branch Stem Joint. Normalized Stress Plotted Against S_o, the Distance Along the Upper Joint Contour. [Mattheck 1989]

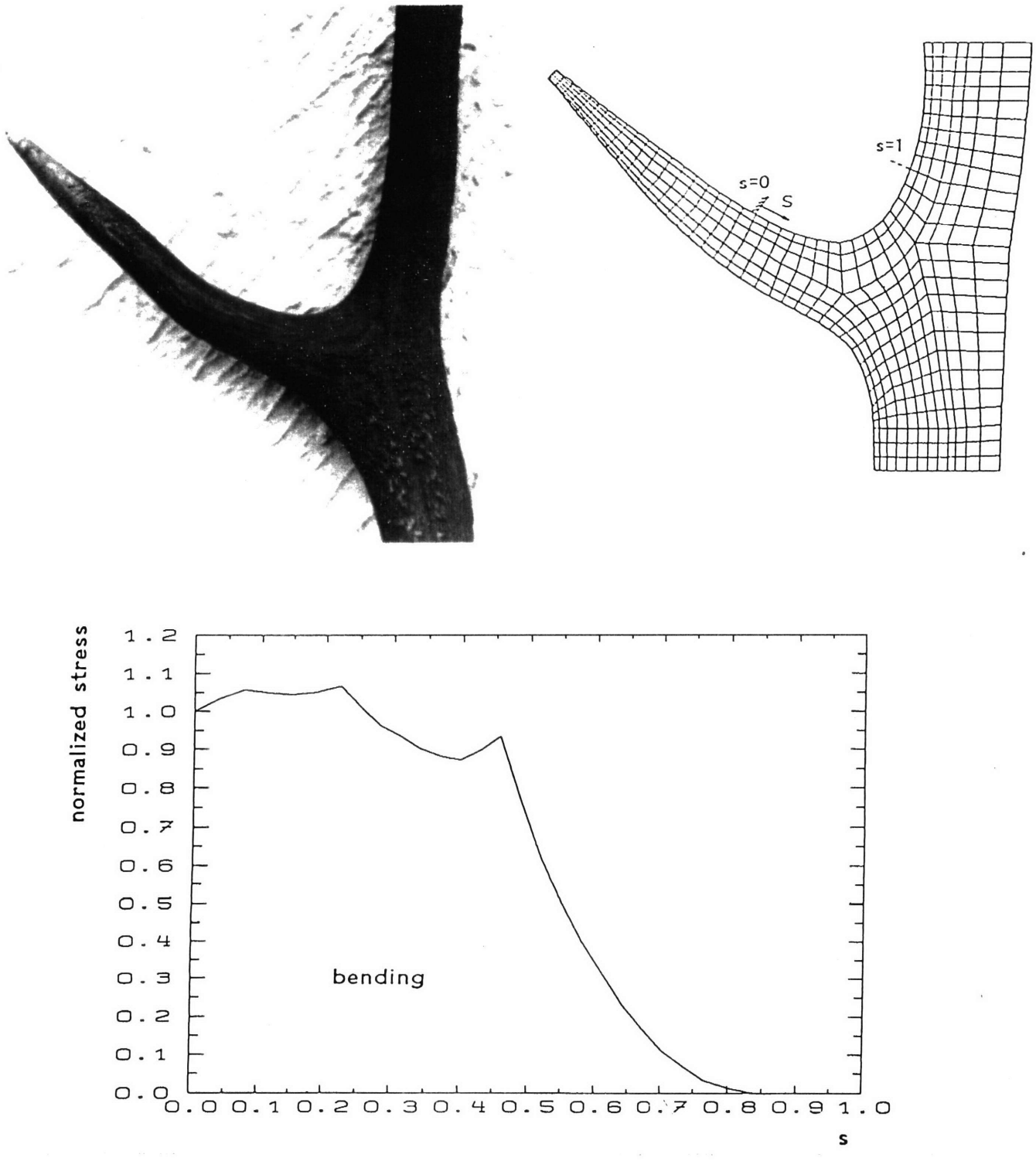

Figure 3.10: Finite Element Analysis of Deer Antler Joint Showing Shape Optimization with Respect to Bending Loads. Normalized Stress Plotted Against *S*, the Distance Along the Upper Joint Contour. [Mattheck 1989]

way, through the deposition of reaction wood to reduce these stresses. **Figure 3.11** shows a London plane tree (*Platanus acerifolia*) with branch holes healed at a particular angle with respect to the vertical stem because of force flow. These force flow trajectories are angled in the same was as main stress trajectories implying that wound healing involves restoration of constant surface stresses.

Ideal stress states can also be disturbed with the application of mechanical contact loads, such as if a foreign body (i.e. stone, dead branch from another tree) keeps pressing against the surface of the stem. Trees react by adaptive growth in order to reduce localized stress peaks by increasing the contacting area thereby reducing the contact stresses. Overgrowth is form of this stress-reducing adaptive response. A tree may grow around a foreign object, for instance a tree enveloping a stone, until it becomes completely integrated with the tree. Mattheck completes a finite element analysis of a tree which was in contact with a heavy stone **[Figure 3.12]** and finds a reduction of the maximum contact stress evident by the increase of contact area due to adaptive growth as the stress σ changes from *139 N/mm*^{2} to *63 N/mm*^{2}. The main stress trajectories which are superimposed on the photograph also coincide with the axial direction of the growth rings to avoid shear between them. [Mattheck 1989, 1991]

3.6. *Re-examination of Uniform Stress Hypothesis*

There have been various opinions regarding the validity of the constant stress hypothesis. It has been observed that because of the stem taper below the crown, many trees approximate a cubic paraboloid profile of height versus diameter. This stem shape gives an approximately uniform surface stress. Mattheck presumes that the theory of constant stress applies over the entire structure of the tree. Studies have shown that the stress distribution along stems also depend on wind velocity gradients with the canopy (West *et al.*, 1989) and that stems have some regions of maximum stress closest to the ground in stems with the greatest taper (Milne and Blackburn, 1989). This regions is where stem breakage often occurs in strong winds. [Morgan *et al.* 1994]

Figure 3.11: Long Axis of Partially Healed Wounds Coinciding with Main Stress Trajectories. [Mattheck 1989]

Figure 3.12a: Stone Contacts Tree Inducing High Localized Contact Stresses Reduced by Overgrowth. [Mattheck 1989]

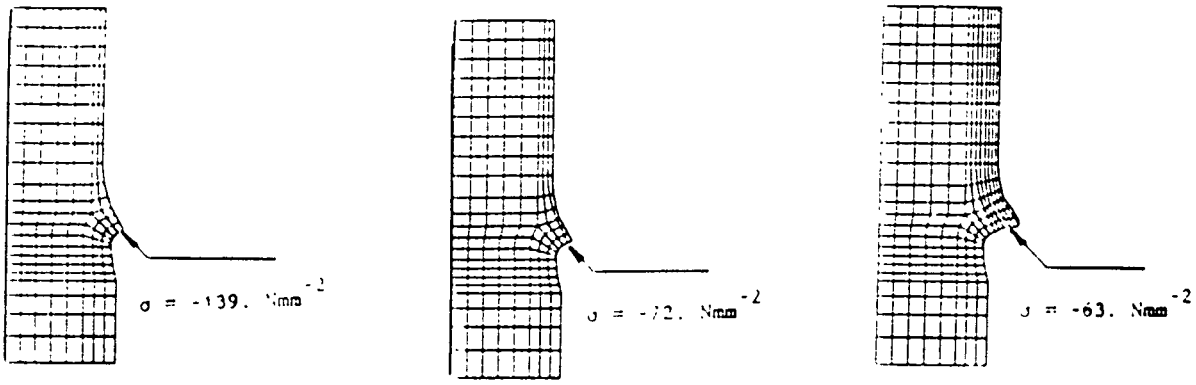

Figure 3.12b: Finite Element Analysis of *Figure 3.12a* Showing Reduction of Maximum Contact Stresses by Increase of Contact Area. [Mattheck 1989]

In an attempt to review the uniform stress hypothesis, Morgan and Cannell (1994) study the growth of branches using a transfer matrix method of structural analysis to examine evidence of uniform stress along tree stems. Using a set of matrix equations relating conditions (shear force V, bending moment M, angle θ, and deflection) of each of the subdivided section ends to a load, the distribution of forces can be determined given the length, diameter, and Young's modulus of the material. **[Figure 3.13]** In the studies of branches, iterative procedures were used by the authors to calculate the diameters to support self weights with given deflections, angles, stem taper, and Young's moduli. From this they were able to develop diameter-length profiles of trees. Morgan *et al.* claim that the profile of the stem diameter with height is a poor test of uniform stress hypothesis because the bending stress is inversely related to the cube of the stem diameter. Consequently, small differences in measured diameters associated with trunk irregularities give larger differences in calculated stress. As a result, the authors offer a slightly modified uniform stress theory in that the distribution of stress along the stem depends on the wind force. Stress may be uniformly distributed in a steady wind speed near the average wind speed, however it will not be uniformly distributed at high or low wind speeds. They hypothesize that if tree stems thicken in regions where there exists high bending and axial stress, the stem shapes observed will be a time-averaged response to the various forces throughout the tree life.

Taking the measured force distribution on crowns done by other studies, Morgan *et al.* calculated the height-diameter profile of the tree stem which gave the uniform stress distribution. These calculations were then compared to the measured height-diameter profile to determine if the results were the same. **Figure 3.14** shows the heights and diameters of ten sitka spruce trees (*Picea sitchensis*) normalized to a breast height diameter of 1.5 *m*. The actual trees averaged a height of 15 *m*, a breast height diameter of 0.165 *m*, a fresh weight of 162 *kg*, a fresh branch weight of 50 *kg*, and drag force of 1587 *N* at 20 *m/s*. When using the transfer matrix method, the authors assumed that the crown was distributed over the top half of the tree, the vertical distribution of forces was triangular approximating a nearly normal leaf area distribution, and an average wind speed of 5 *m/s* based on the conditions of the region. The figure shows a good agreement with

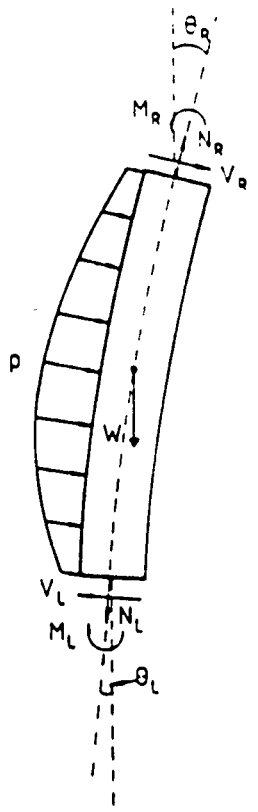

Figure 3.13: Section of Deflected Stem for Transfer Matrix Analysis Showing Forces Acting: V = Shear Force, N = Axial Force, M = Bending Moment, W = Weight, p = Distributed Force, θ = Angle. [Morgan *et al.* 1994]

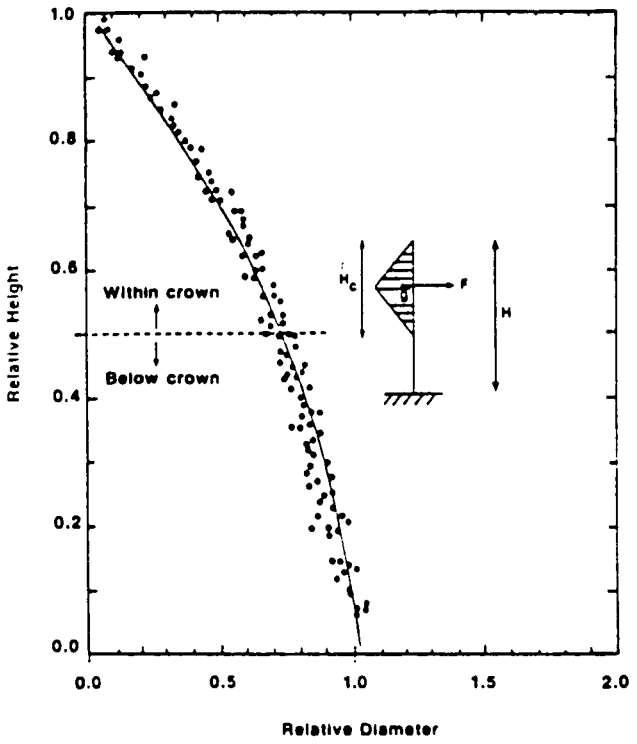

Figure 3.14: Measured Values of 10 Sitka Spruce (*Picea Sitchensis*) Trees Normalized to Diameter at Breast Height = 1.0. Measured values indicated by points and calculated profile indicated by solid line. Calculations made using transfer matrix method for uniform stress along stem with wind distribution shown in the inset with wind speed of 5 *m/s*. [Morgan *et al.* 1994]

the measured height-diameter profile (indicated by the points) and the uniform stress profile (indicated by the solid line).

Analyses of a 20-year-old eucalyptus (*Eucalyptus regnans*) and 22-year-old sitka spruce (*Picea sitchensis*) trees were done according to the horizontal force distributions indicated in **Figure 3.15**. Both trees showed the calculated height-diameter relation similar to the measured values with only a deviation in the region of butt swell of the tree (the portion of the stem where it meets with the ground).

When considering height-diameter profiles at different wind speeds, the transfer matrix was also used to evaluate a change in average wind speed over a range of 2.5-10.0 *m/s* (the average wind speed over a lifetime of many forests at different spacings). A profile of the spruce was done based on the same assumptions as **Figure 3.14** and the results are shown in **Figure 3.16**. The graph shows that the height-diameter profile was not significantly affected by the change in wind speed. The uniform stress profile at high wind sped (20 *m/s*) shows a greater stem taper while the profiles of uniform stress at speeds 2.5-10 *m/s*, represented by a thick line, are notable similar. From this diagram, it would appear that differing crown dimensions and vertical force distribution would have a more significant impact on stem taper than average wind velocities.

In summary, tree stem shapes optimize to a form that equalizes the average bending and axial stresses depending on the tree crown and average wind speed during the life of the tree. Observations showed that tree stems did develop shapes in response to average conditions, but they also display varying stress distributions in extreme conditions for stem regions like the butt swell. This explains some of the apparent evidence for non-uniform stress distribution. [Morgan *et al.* 1994]

3.7. *Other Forms of Adaptive Changes in Wood*

In addition to the optimization features in trees outlined by Mattheck in his uniform stress hypothesis, trees also experience other forms of adaptive changes in their shape when subject to load changes. Elfin tropical rain forests display dense growth of short, thick stemmed, gnarled trees with crowns tightly packed. These are usually found

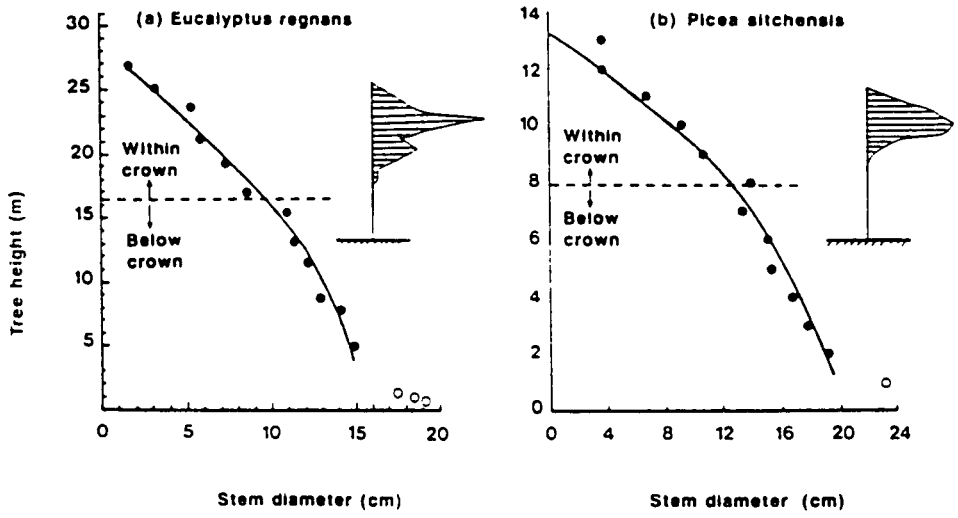

Figure 3.15: Height-Diameter Profiles (above butt swell) for (a) *Eucalyptus Regnans*, and (b) Sitka Spruce (*Picea Sitchensis*); Measured Values (points) and Calculated Profile (line). Lines derived using transfer matrix method for uniform stress up the stem and horizontal force distributions shown in the inset. Open points indicate diameters in region of butt swell. [Morgan *et al.* 1994]

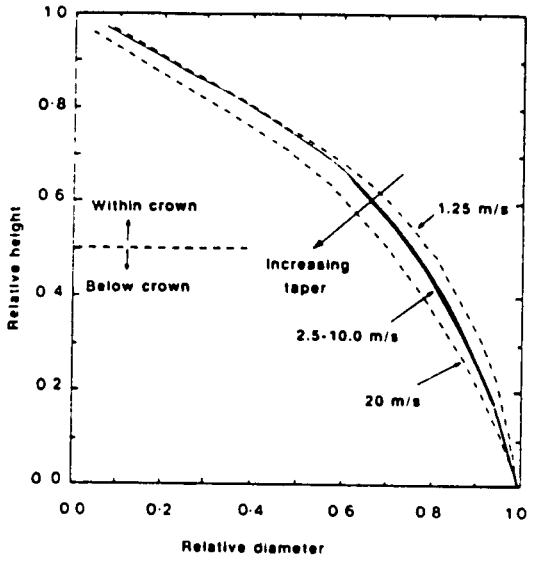

Figure 3.16: Calculated Height-Diameter for Sitka Spruce (*Picea Sitchensis*) with Different Constant Horizontal Wind Speeds and Uniform Stress Along Stem. [Morgan *et al.* 1994]

on the sea coast, exposed ridges, and gaps in forests. Sculpturing of the canopy of trees also occurs with wind producing a streamlined airfoil. This offers minimal resistance to the force loading of wind. A "plywood" effect can also be produced in the trunk with an induced grain helix angles to run in different directions which strengthens the trunk against rupture. [Jaffe *et al.* 1993] Such adaptive growth in trees helps prolong the life of the tree as it reacts to its changing physical environment.

3.8. *Conclusion*

Reviewing the theory and analyses of wood morphology, it is evident that wood is able to adapt to mechanically induced stress through the deposition of reaction wood, much like bone's remodeling process. The only difference between the two is that wood is unable to resorb like bone. The constant stress hypothesis gives us a means of evaluating the development of a tree as it is subjected to wind and gravity loads. Studies by Wilson *et al.* (1979) and Mattheck (1989) illustrate that wood wants to maintain a constant surface strain, and if subjected to increased loads or points of stress concentration in notches or joints, it will optimize its shape to keep that constant strain through growth. Morgan *et al.* (1994) also re-evaluated this theory proposing that tree stems form in such a manner that equalizes the average stresses it experiences during the entire life of the tree. Thus, it is obvious that form and function and closely related in the morphology of trees as they adapt to environmental conditions.

References

Ashby, Michael F. and David R.H. Jones. 1980. Engineering Materials II: An Introduction of their Properties and Applications, Pergamon Press, Oxford.

Illston, J.M., J.M. Dinwoodie, and A.A. Smith. 1979. Concrete, Timber and Metals: The Nature and Behavior of Structural Materials, Van Nostrand Reinhold Company, New York.

Jaffe, M. J. and S. Forbes. 1993. Thigmomorphogenesis: The Effect of Mechanical Perturbation of Plants. *Plant Growth Regulation*, v. 12, pp. 313-324.

Lewin, Menachem and Irving S. Goldstein, eds. 1991. Wood Structure and Composition. Marcel Dekker, Inc., New York.

Mattheck, Claus. 1989. Engineering Components Grow Like Trees.

Mattheck, Claus. 1990. Why They Grow, How They Grow: The Mechanics of Trees. *Arboricultural Journal*, v. 14, pp. 1-17.

Mattheck, Claus. 1991. Trees: The Mechanical Design. Springer-Verlag, Berlin.

Milne, R. and P. Blackburn. 1989. The Elasticity and Vertical Distribution of Stress Within Stems of Picea Sitchensis. *Tree Physiol.*, v. 5, pp. 195-205.

Morgan, John and Melvin G.R. Cannell. 1994. Shape of Tree Stems - A Re-Examination of the Uniform Stress Hypothesis. *Tree Physiology*, v. 14, p. 49-62.

Telewski, Frank W. and Mordecai J. Jaffe. 1986a. Thigmomorphogenesis: Field and Laboratory Studies of *Abies fraseri* in Response to Wind or Mechanical Perturbation. *Physiol. Plant*, v. 66, pp. 211-218.

Wangaard, F.F, editor. 1981. Wood: Its Structure and Properties. The Pennsylvania State University, University Park, Pennsylvania.

West, P.W., D.R. Jackett, and S.J. Sykes. 1989. Stresses in, and Shape of, Tree Stems in Forest Monoculture. *J. Theor. Biol.*, v. 140, pp. 327-343.

Wilson, Brayton F. and Robert R. Archer. 1979. Tree Design: Some Biological Solutions to Mechanical Problems. *BioScience*, v. 29, no. 5, pp. 293-298.

Chapter 4: Plant Stems

4.1. *Introduction*

As mentioned in the previous chapter on wood, plants use differing strategies to protect themselves against adverse environmental conditions. Unlike animals, which are mobile, plants are most often rooted in soil and are unable to move around in their surroundings to escape an unfavorable environment. As a result, they have been able to respond to climatic challenges and developmental changes by adapting to new conditions. The amphibious plant such as the water buttercup (*Ranunculus aquatilis)*, for example, can grow submerged in water and above a pond in the air. The two types of leaves it develops, the submerged leaves with little mesophyll tissue surrounding the veins and broad aerial leaves with well-developed mesophyll tissue, are so different, that they seem to belong to two different plants. Plants can also alter their development and use chemicals to protect themselves against predators and pathogens. They are able to respond to invading organisms developmentally by altering the structure of their cell wall and localize cell death around a particular site. Some plants also respond with biochemical changes leading to a synthesis of poisonous substances to kill invading bacteria or to repel preying animals. [Fosket 1994]

In a like manner, plants are subject to environmental stress as they experience flexure from wind. The mechanical perturbation they experience in these dynamic loading conditions alter their growth and development by either exhibiting or lacking secondary growth. This phenomenon known as *thigmomorphogenesis* involves motion-induced inhibition of growth. Some of the common mechanical stress vectors of nature not only include wind, as mentioned previously, but also involve bending due to rain, hail, and animal movements. Agricultural production can further add physical agitation to plants by pruning, pinching, tying, trimming, and guying. At the same time, urban high rise areas create similar air turbulence and downdrafts that can modify tree and shrub growth to be similar to plants which dwell on mountain slopes and seacoasts. Looking at various thigmomorphogenic studies, it will become apparent how sensitive plant growth can be to

brief episodes of mechanical stress and how its adaptive process protects and prolongs its life. This chapter will look at the adaptive changes of plant stems and some of the chemical responses that influence thigmomorphogenesis. In addition, plant stem remodeling will be examined with changes in the mechanical properties of the stems which optimize their functionality in survival.

4.2. *Plant Structure and Composition*

Before looking into some of the biochemical influences of thigmomorphogenesis, it may be useful to review the structure and composition of the plant. The plant body is notably elongated and polarized with its axes orientated at right angles to the surface of the earth. **Figure 4.1** shows the general form and principle parts of a typical plant illustrating the importance of gravity in determining and maintaining the plant's form. There are two systems of the plant: the root system which is typically underground and the shoot located above the ground. The root system can be highly branched but does not have any other lateral organs attached to it. The shoot, however, may contain a various number of other organs linked to it, such as leaves, flowers, thorns, tendrils and fruits. The main axis of the shoot, or the stem, consists of alternating nodes, which are the points where the leaves are attached, and internodes which are the regions inbetween nodes. Leaves, flowers, and the sort are commonly joined to the stem at the nodes in some form of regular pattern. In some cases, like for angiosperms (flowering plants), the petiole, or stalk, connects each leaf to the stem at the node such as in the water lily where the long and flexible petioles connect the leaves to an underground stem that grows horizontally in the mud at the bottom of a pond.

4.2.1. *Vascular System*

Land plants are subject to extremes in temperature and the risk of desiccation. In order to provide water and minerals to their cells, many plants have vascular tissue that conduct water and nutrients throughout the plant. Because of this vascular tissue, plants develop specialized organs and processes like photosynthesis that take place in the leaves

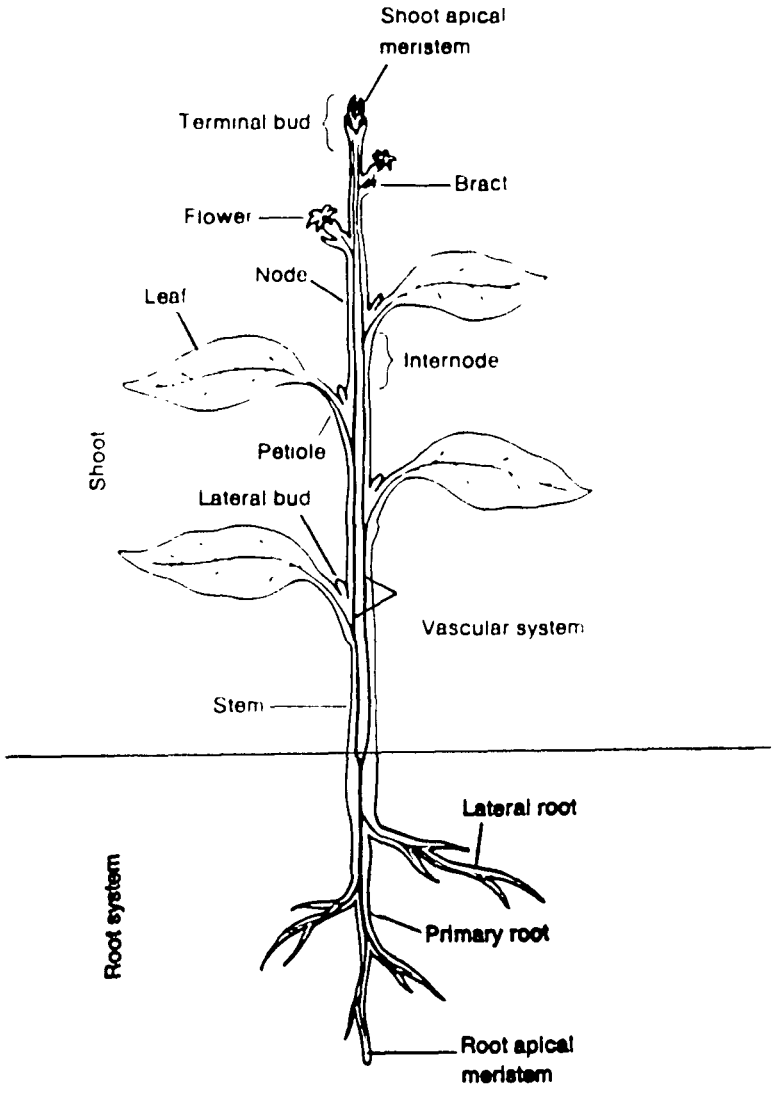

Figure 4.1: Diagram of Vascular Plant. [Fosket 1994]

and can supply food for the metabolism of cells in the stem and roots. At the same time, the roots are also developed for adsorbing water and minerals as well as anchoring the plant.

There are two elements which comprise vascular tissue: xylem and phloem. *Xylem* supplies a stream of water and dissolved minerals from the roots to the leaves and other tissues and organs of the plant. This particular tissue consists of four different types of cells: parenchyma cells, fibers, tracheids, and vessels. **[Figure 4.2]** The *parenchyma cell* is any type of mature, non-dividing cell with a primary cell wall, large vacuole, and non-specialized function. In the xylem, these cells are atypical because they often do not have thickened cell walls, but remain living at maturity and do not participate in water transport. Xylem *fibers* are elongated and sometimes pointed cells with thick secondary cell walls. Both the parenchyma cells and fibers basically function to provide mechanical support for the plant system.

Tracheary elements, which include the vessels and tracheids, are the conductive cells of the xylem. The *vessel* is a linear file of cells, each of which is a vessel element. The vessel element differentiation involves the synthesis and deposition of a secondary cell wall that reinforces the primary cell wall consisting of cellulose, non-cellulosic polysaccharides, and unique proteins as it is formed during cell growth. The secondary cell wall is formed after growth is complete, and it is comprised of essentially the same elements as the primary wall, but lacks protein and contains lignin. The secondary wall can be laid in an annular, spiral, or intertwined pattern so that some portions of the wall may not receive any reinforcement.

Tracheids differ from vessels in form as each tracheid is a single cell which is much longer than a single vessel element. Tracheids also undergo secondary wall deposition, but the wall is usually more evenly thickened except in areas of connection between tracheids where water passes. These connecting openings are much smaller than those of connecting vessel elements, and thus more water is able to move through the xylem containing vessels compared to and equal amount of xylem containing only tracheids. Gymnosperms (seed plants), for example, have vascular tissue which contain only

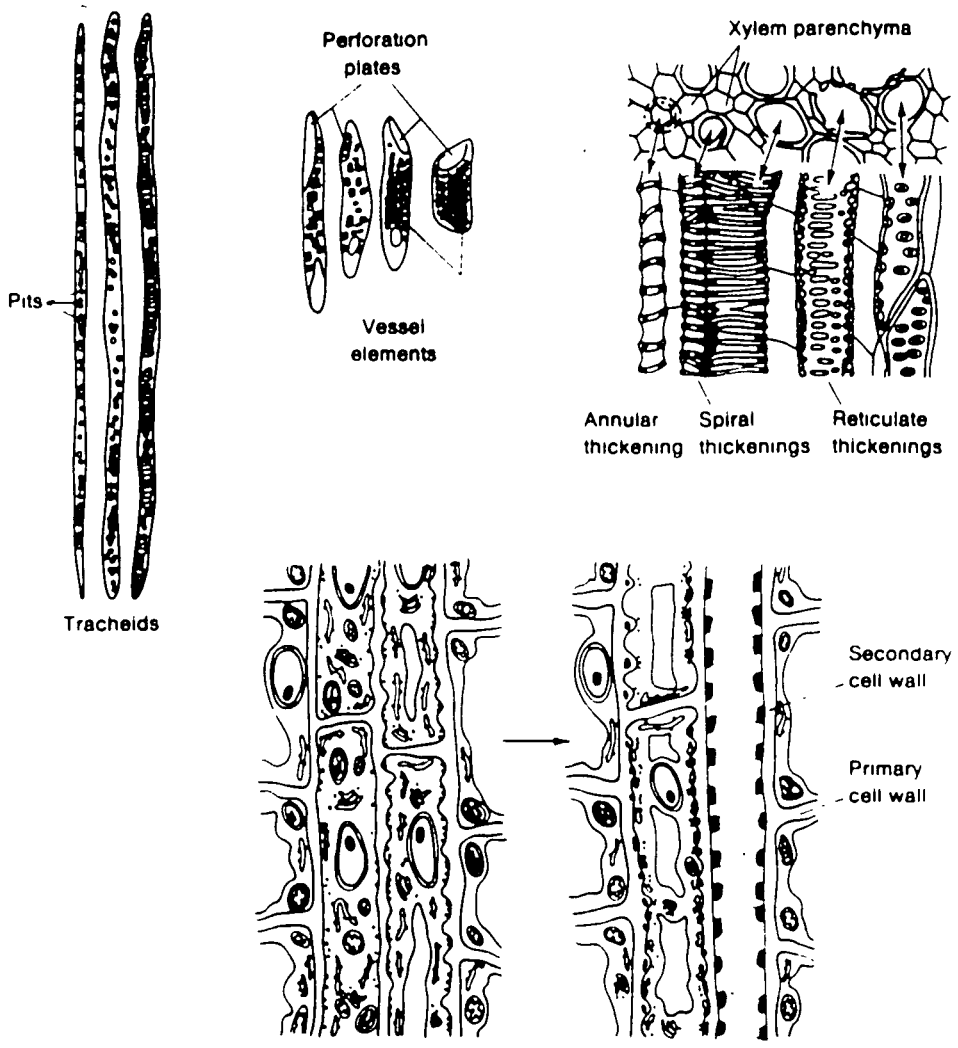

Figure 4.2: Tracheary Elements and Other Xylem Cell Types. [Fosket 1994]

tracheids, and as a result, they are less efficient in transporting water to their leaves compared to angiosperms whose vascular tissue comprises of tracheids and vessels.

The *phloem* in vascular tissue conducts food materials synthesized during photosynthesis. It also contains four basic cell types: parenchyma cells, fibers, sieve elements, and companion cells. **[Figure 4.3]** The parenchyma cells and fibers in phloem are similar to that in the xylem. *Sieve elements* form a linear file of cells and together compose sieve tubes. Sieve elements undergo some secondary wall deposition, but do not become lignified like tracheary elements. During the formation of the sieve plate, a file of cells differentiate and construct specialized end walls called sieve plates. Sieve elements and their *companion cells* share a common origin as they are derived from the same cell division. One becomes a companion cell whose function is still largely unknown while the other forms a sieve element.

4.2.2. *Meristems*

Meristems are regions of constant embryogenesis which create the plant body by producing cells that eventually form the roots stems, leaves, and flowers of the mature plant. **[Figure 4.4]** Activity within the meristem is regulated by environmental and physiological signals such that when conditions are unfavorable to growth, the meristem is not active, but still maintains its potential for growth. Small cells in the meristem called *initials* divide indefinitely and do not differentiate. The manner in which the cells divide in the meristem determine the position of leaves and the organization of the tissues within the organs. Embryogenesis establishes the basic plant axis. Most of plant development occurs postembryonically as none of the organs of the mature plant are formed during embryogenesis (with the exception of the first leaves and cotyledons in some plants). The plant body is constructed of meristems which begin their activity after the completion of embryogenesis and when seed germination has begun.

Two primary meristems are formed during embryonic development, the shoot and root apical meristems, and compose the plant body; they are responsible for producing secondary tissues such as wood and bark in trees. These additional secondary meristems develop from mature cells later on in the plant development. Herbaceous plants may lack

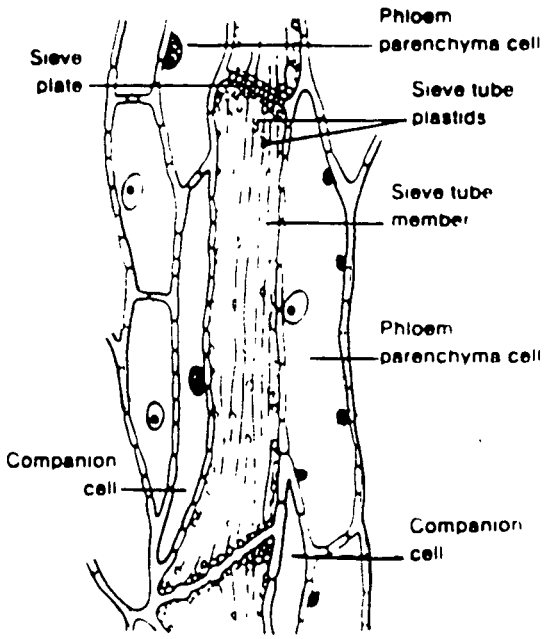

Figure 4.3: Phloem Cell Type. [Fosket 1994]

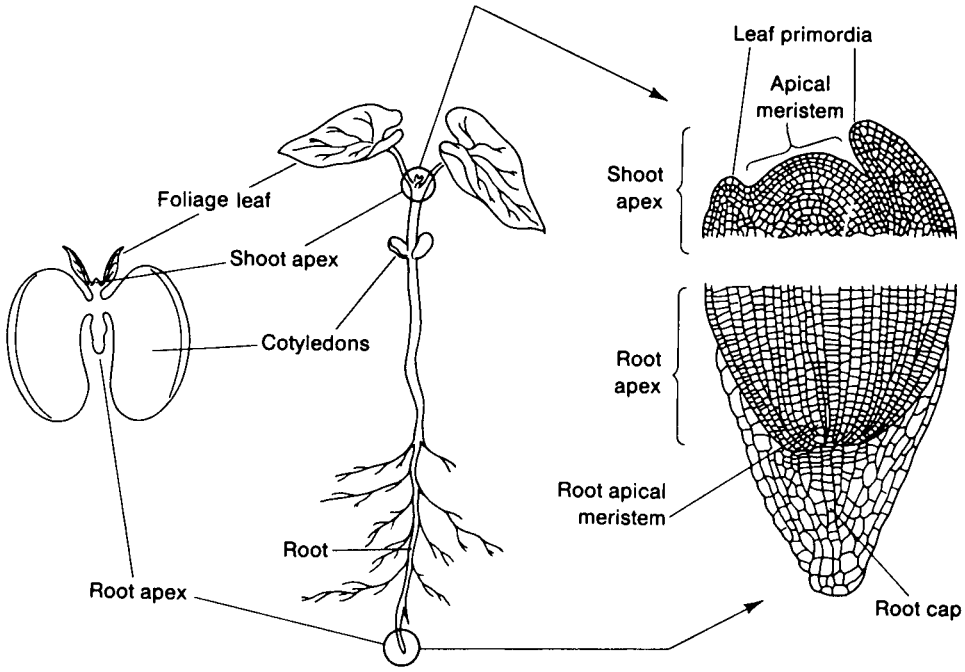

Figure 4.4: Primary Meristems Formed During Embryogenesis. Diagram Shows Origin and Position of Apical Meristems in Bean Seedling. [Fosket 1994]

secondary meristems or may be poorly developed. In contrast, woody plants have very well developed secondary meristems.

The *apical meristem of the shoot* is located at its extreme tip. The cell divisions within this meristem lead to the development of mounds of cells which grow and differentiate into leaves known as leaf primordia. Below the apical meristem, the cell divisions that occur differentiate into the tissues of the stem. The vegetative development process is very repetitive and produces the same leaf, bud, and stem tissue structures over and over again. Growth tends to be active in the spring and early summer while becoming more dormant in the late summer and autumn, and resuming its growth again in the spring.

The *root apical meristem* is covered by a tissue known as the root cap which protects the meristem through the soil. The root apical meristem is different from the shoot in that it does not produce any lateral organs. Instead, it generates cells that form the root cap and the primary tissues of the root axis. Adventitious meristems that appear in mature regions of the primary root later on form later roots.

4.2.3. *Roots and Stems*

The roots of a plant are specialized organs which function to absorb and transport water and minerals while anchoring the plant. They increase in length at their tips as new cells are added to the root stem by the meristem. These cells then elongate and differentiate to undertake particular tasks within the root. There are different zones in the root (the root cap, the meristem, the region of elongation, and the region of differentiation) where development takes places. Growth occurs in the region of elongation where protoderm, ground meristem, and procambium tissue can be found. Protoderm can be distinguished as the epidermis while the procambium becomes the vascular tissue and the ground meristem differentiates as the cortical tissue. Many of the epidermal cells of the root develop root hairs which are thin-walled outgrowths that remain part of the epidermal cell. The root hairs help increase the surface area of the root exposed to the soil and make uptake of water and minerals more rapid. Minerals and water are taken up into the tracheary elements for transport to the shoot system.

Primary stem growth and tissue differentiation occurs at several centimeters of the shoot tip. Development of the shoot apical meristem form protoderm, ground meristem and procambium tissues, just as in the root. These three tissues then further differentiate into epidermal, ground, and vascular tissues, respectively. Each vascular bundle contains both xylem and phloem aligned on the same radius. **[Figure 4.5]**

4.2.4. *Vascular Cambium and Secondary Growth*

Secondary meristems formed in the stem and roots after primary plant body tissues have differentiated develop into vascular cambium and cork cambium. The vascular cambium aids in increasing the diameter of the stem and roots and is responsible for forming woody tissue in trees. Some of the bark in trees is produced by the cork cambium. The primary xylem and phloem differentiate from procambial tissue in these vascular bundles. For dicot stems, the vascular cambium initially differentiates from procambial tissue in vascular bundles. Cell division by the cambium produces cells that become secondary xylem and phloem. As these tissues accumulate, they increase the circumference of the stem and form wood and bark. For temperate zone plants, cambial activity is seasonal and the wood and bark can be seen to be laid in distinct annual rings.

Looking at these tissues in more detail, the *vascular cambium* layer is a layer of dividing cells that differentiate into either xylem elements or phloem elements. These dividing cells consist of long, narrow, *fusiform initials* from which tracheary elements are derived, and *ray initials* from which ray parenchyma are formed. The fusiform initials and ray initials look very similar as both are small, flattened cells with thin walls. However, the ray initials when viewed in tangential section seem relatively short while the fusiform initials appear long and narrow. Tracheary elements differentiate from fusiform initial derivatives while derivatives of ray initials differentiate as ray parenchyma. These ray parenchyma make possible the transport of water from the xylem to the cambium and tissues of phloem in addition to the transport of photosynthate from the phloem into the cambium to the living cells of the xylem.

The *cork cambium* forms a large portion of the bark of woody plants. It first arises within the cortex as a layer of concentric dividing cells forming a cylinder. The

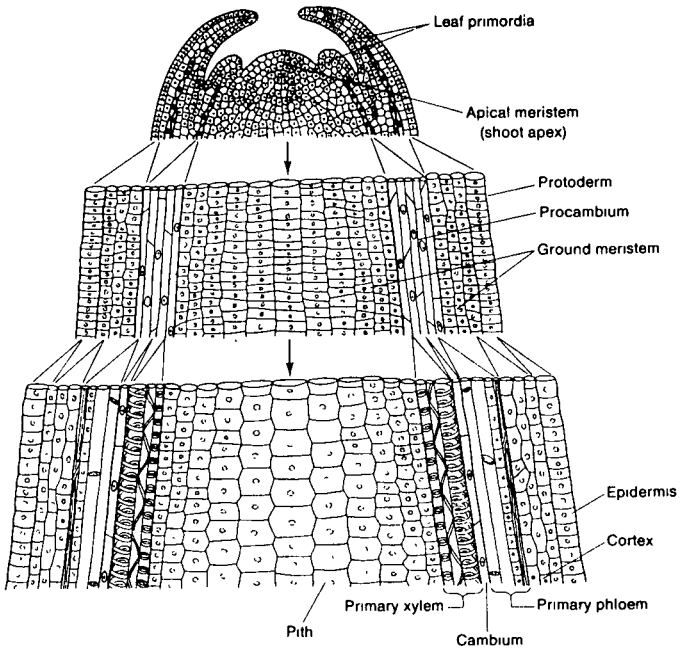

(a)

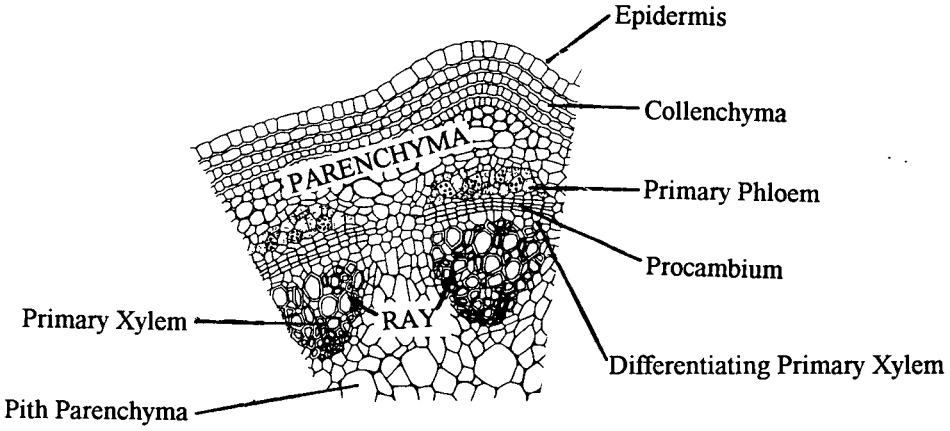

(b)

Figure 4.5: Stem Structure. (a) Shoot Apical Meristem Structure; (b) Stem Arranged in a Ring in Dicot Stems. [Fosket 1994]

derivatives of this cell layer form cork, also called phellem, toward the outside of the stem while the inner portion of the stem differentiates into phelloderm. Suberin which is deposited in the cell walls of the phellem protect the stem from water loss and mechanical damage. As the tree increases in girth, the outer layers of the bark are sloughed off, and additional cork cambia arise within the secondary phloem as the plant develops.

4.2.5. *Leaves*

An angiosperm leaf is a thin, flat structure approximately a few cells thick. Photosynthesis occurs in the chloroplasts which are abundant in the mesophyll cells of the leaf. The two main processes encompassing photosynthesis include the fixation of carbon from atmospheric carbon dioxide (CO_2) and the reduction of carbon using the energy obtained from light. An intermediate reacts enzymatically with CO_2 to form an organic acid in carbon fixation. Two different mechanisms, known as C3 and C4 pathways, fix carbon for photosynthetic reduction. In C3 plants, fixation of carbon dioxide, carbon reduction, and synthesis of sugars occur in chloroplasts of the same mesophyll cell. For C4 plants, initial fixation of atmospheric carbon dioxide occurs in the mesophyll cells, but it is used to make organic acids that are transported into bundle sheath cells. In both C3 and C4 plants, the mesophyll tissue is surrounded by a layer of epidermal cells that lack chloroplasts. **[Figure 4.6]** The mesophyll tissue also secretes a waxy material which coats the leaf's outer surface and helps prevent desiccation. Since photosynthesis requires the exchange of atmospheric carbon dioxide between the air and inner portions of the leaf, small openings called *stomata* enable this to occur. Stomata can be open or closed by the action of guard cells which are specialized epidermal cells that contain chloroplasts and special wall thickening. Vascular bundles make up the leaf veins and form an interconnected network through the plant. Reticulate venation describes the veins occurring in a netted pattern while parallel venation characterizes the large veins running side by side with small lateral interconnections. Leaf venation patterns are carefully controlled and help characterize plant identification. [Fosket 1994]

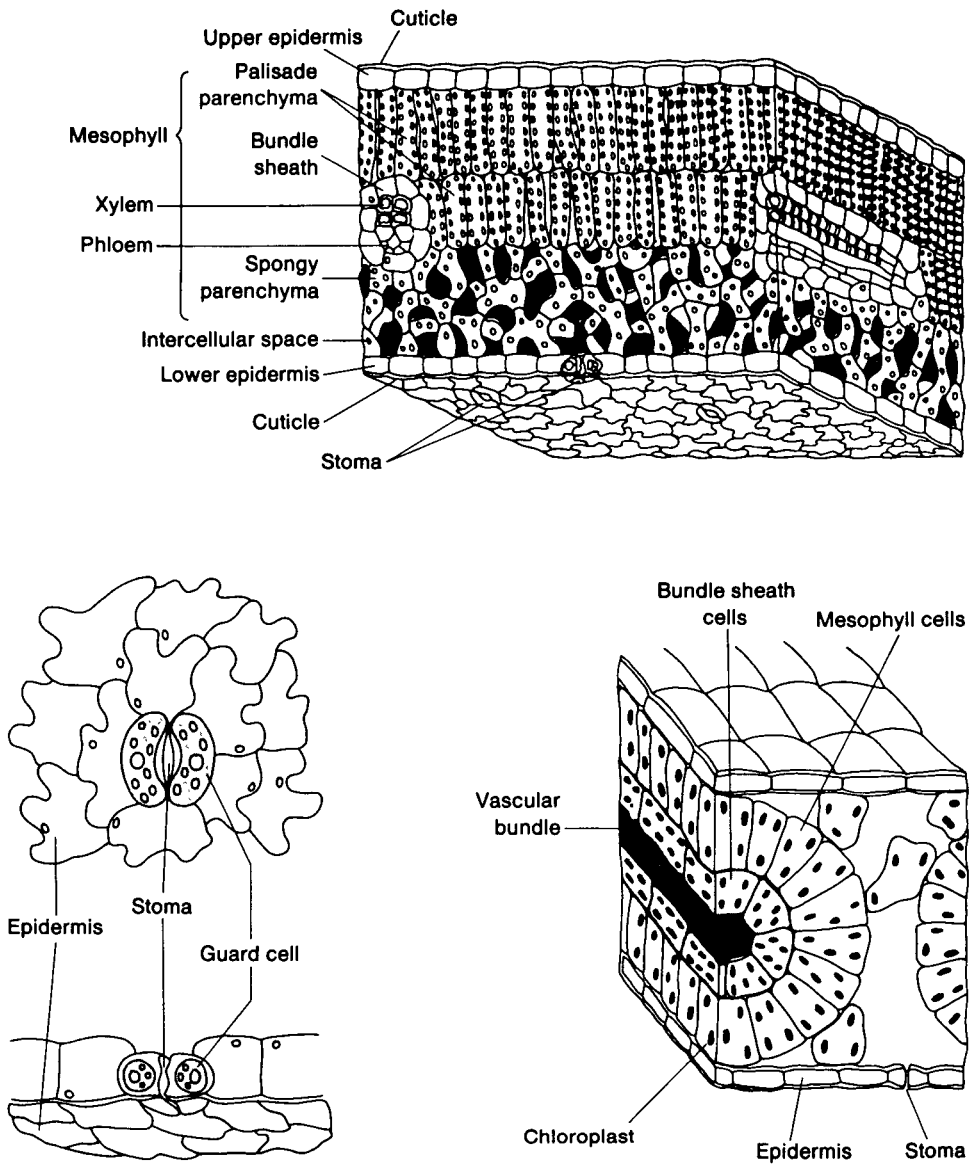

Figure 4.6: **(A) Diagram of Leaf Structure for C3 Plant;**
(B) Surface View of Leaf Epidermis Showing Guard Cell Structure and Position Around Stomata;
(C) Diagram of Leaf Structure for C4 Plant. [Fosket 1994]

4.3. *Remodeling Theories: The Chemical Response to Thigmomorphogenesis*

Studies of field- and greenhouse- grown plants show the effect of thigmomorphogenesis which is defined by Mordecai Jaffe (1973) as the physiological and morphogenic response of plants to mechanical stimulus. Plants whose stems were mechanically perturbated by rubbing or bending eventually showed growth changes which included inhibition of stem elongation and increased radial growth in the direction of the stimulus. For example, trees that are supported by guy wires to prevent swaying in the wind tend to grow taller and less in trunk diameter compared to unguyed trees which are free to bend under the wind load. This form of thigmomorphogenic response to such a mechanical stress is common in a wide variety of vascular plants.

The mechanisms that contribute to thigmomorphogenic response can be attributed to two chemicals, ethylene and auxin. While most of the studies of mechanical effects on plant growth have involved morphological and anatomical changes, physiological responses have also been investigated to determine if any growth-influencing hormone may affect the response of plants to mechanical perturbation.

4.3.1. *Ethylene*

In 1972, Neel and Harris were the first to suggest that a hormone was involved in thigmomorphogenesis based of the 1966 findings of Goeschl *et al.* who found mechanically perturbed pea plants produced ethylene and also reported that ethylene stimulated swelling and inhibited stem elongation. Five years after Goeschl *et al.*'s study, Neel then tested pine (*Pinus radiata*) and sweet gum (*Liquidambar styraciflua*) finding that ethylene also induced thigmomorphogenesis in both of these plants.

Ethylene (C_2H_4) is known as the "stress hormone" with respect to mechanical stress growth regulation. Reactions of ethylene and mechanical stress typically produce inhibited stem elongation, stem swelling, and loss of gravitropic sensitivity and leaf epinasty. Experiments by Biro and Jaffe in 1984 show that mechanically stressed plants release ethylene at an elevated rate one hour after perturbation. The enzyme, 1-aminocyclopropate-1-carboxylic acid (ACC) which catalyzes production of the immediate

precursor of ethylene, also displays increased activity 30 minutes after a plant is stressed. It has also been revealed that cobalt and lithium, which are known to be ethylene synthesis inhibitors, prevent certain plant responses to mechanical stress. At the same time, experiments on branches of pine plants (Brown *et al.*, 1973; Barker, 1979; Telewski *et al.*, 1983) resulted in increased radial growth in branches. [Mitchell 1996]

Telewski and Jaffe (1986c) conducted an experiment to determine the role of ethylene in response to mechanical perturbation. Ethylene production was monitored for 48 hours in two half-sibs of greenhouse-grown loblolly pine (*Pinus taeda*) and given flexing mechanical perturbation. Field-grown firs (*Abies fraser*) were also exposed to wind-mediated mechanical perturbation and monitored for 22 hours. As a result, both plants produced peak quantities of ethylene 18 hours after mechanical perturbation while displaying increased radial growth. **[Figure 4.7 - 4.8]**

4.3.2. *Auxin*

The extent of the growth hormone auxin's involvement in thigmomorphogenesis entails supraoptimal auxin which mimics mechanical stress effects. Auxin stimulates ACC[1] oxidase and the subsequent production of ethylene. Such an example can be seen in the thigmic stress of dark-grown pea seedlings (*Pisum sativum*) which resulted in a elongation reduction of subsequently cut pea stem sections floated in auxin solution. [Mitchell 1996] Polar auxin transport is also inhibited by mechanical stress or ethylene. It is likely that auxin which originates from within the plant cannot move below the point of mechanical stress application in an unhardened pea stem. As a result, auxin accumulated above the point of thigmic stress and depletes below. Irritation of stem tissue by rubbing can also activate membrane-associated peroxidases which destroy natural auxin. Depending on the point of stress application, elongating cells in the growth zone become inhibited because the growth hormone auxin becomes depleted or above optimal within those cells. Ethylene is known to be a polar auxin transport antagonist, and its role in growth

[1] 1-aminocyclopropate-1-carboxylic acid (ACC) is an enzyme which catalyzes production of the immediate precursor of ethylene.

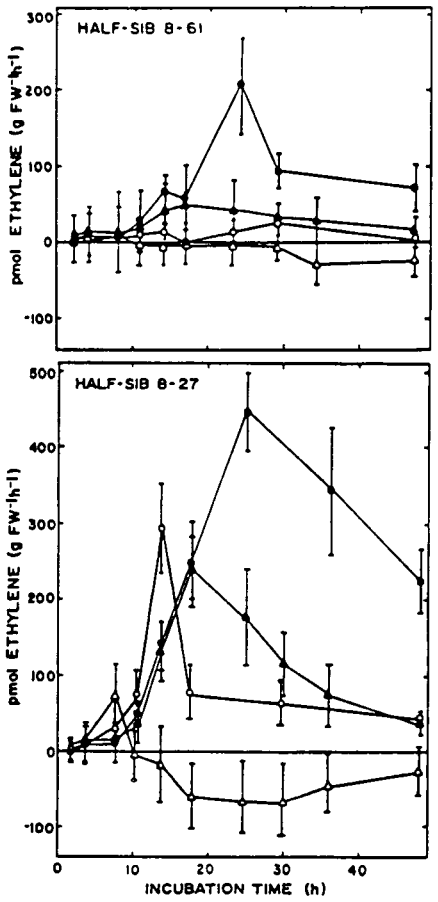

Figure 4.7: **Time Courses of Mechanically-Perturbed and Wound-Induced Ethylene Production of 2 Half-Sibs of Loblolly Pine (*Pinus Taeda*).**
● = Wound Ethylene Production in Non-Preconditioned Seedling;
▲ = Wound Ethylene Production in Preconditioned Seedling;
○ = Mechanically-Perturbed Ethylene Production in Non-Preconditioned Seedling;
Δ = Mechanically-Perturbed Ethylene Production in Preconditioned Seedling.
[Telewski *et al.* 1986c]

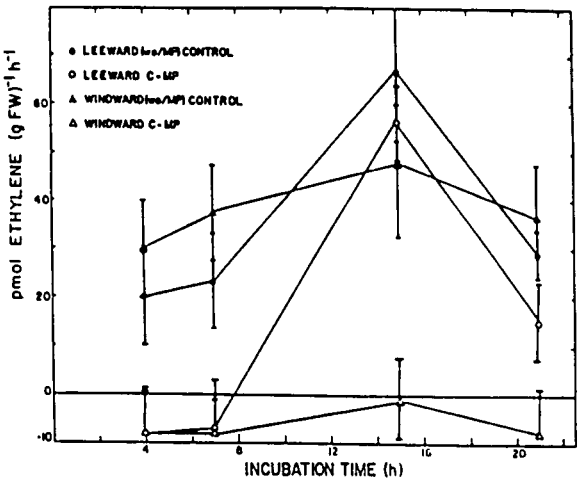

Figure 4.8: **Time Course of Wound- and Mechanically-Perturbed -Induced Ethylene Production in firs (*Abies fraseri*) Growing on Leeward and Windward Sites of Roan Mountain, NC.**
● = Wound Ethylene Production in Leeward Trees;
▲ = Wound Ethylene Production in Windward Trees;
○ = Mechanically-Perturbed Ethylene Production in Leeward Trees;
Δ = Mechanically-Perturbed Ethylene Production in Windward Trees.
[Telewski *et al.* 1986c]

inhibition due to mechanical perturbation may also be partially linked to the control of auxin levels. [Mitchell 1996, Erner *et al.* 1982]

Research by Erner and Jaffe (1982) looked at young kidney bean plants (*Phaseolus vulgaris*) which were either mechanically perturbed for 10 days or treated with ethephon[2]. In both cases, the plants accumulated large quantities of auxin-like substances and increased amounts of the native growth retardant abscisic acid (ABA). Higher amounts of auxin were detected in the perturbed and ethephon treated plants when compared to the controls while inhibition of auxin transport in the first internode section caused by mechanical perturbation or ethephon treatment was significant. This data confirms that ethylene does indeed reduce auxin transport. A possibility of auxin increase in bean plants is the result of ethylene production which blocked basipetal auxin transport. Auxin synthesis could have also occurred in bean plants due to mechanical perturbation at the perturbed area. Another plausible reason for auxin increase was the formation of new cells due to mechanical perturbation which synthesized auxin for activity.

Erner and Jaffe also found that when ABA was applied topically to plants, elongation was retarded and concluded that ABA was a probable participant in thigmomorphogenic growth retardation in addition to mechanically perturbed-induced auxin accumulation and production of ethylene. As a result of such findings, auxin and ethylene both prove to be important in thigmomorphogenesis.

4.4. *Experiments: Morphological Changes and Adaptations*

4.4.1. *Rubbed and Wind-Exposed Plants*

Several experiments have been conducted which attempt to record the morphological changes induced by mechanical perturbation. The common traits that run through all the perturbed plant specimens include elongation retardation and increased radial growth in the perturbed region. Jaffe and his colleagues tested various plants' development under mechanical stimulation. One study [Jaffe 1973] examined barley (*Hordeum vulgare*), byrony (*Bryonia dioica*), cucumber (*Cucumis sativus*), kidney bean

[2] Ethephon is an ethylene-releasing compound.

plants (*Phaseolus vulgaris*), mimosa (*Mimosa pudica*), and castor-oil plant (*Ricinus communis*) as their internodes were rubbed for 10 seconds, 1-2 times daily. In all of the plants, the simple, gentle rubbing of the stem produced a decrease in elongation. It was also found that the mechanical stimulus affected many other developmental properties of the plant such as retardation of flower bud production as well as inhibited growth of tendrils, leaves, and petioles. In general, the response to rubbing appeared immediate, but the recovery of normal growth by the plant occurred gradually over a period of several days after the removal of the stimulus. From this experiment, it can be deduced that thigmomorphogenic response represents the adaptation designed to protect plants from the stresses produced by high winds and moving animals by producting thicker stems, and in this respect, wind acts as a natural hardening agent.

Hunt and Jaffe (1980) studied kidney bean plants (*Phaseolus vulgaris*) both in the lab and in the field to determine the effects of wind loads on plants as they were sheltered or exposed to the wind for 10 days. They observed more internodal secondary xylem production in wind-exposed plants compared to the sheltered plants. **[Table 4.1]** The laboratory experiments also showed that as the wind velocity increased, thigmomorphogenesis increased in an approximate linear fashion. **[Figure 4.9]** At the same time, low temperatures which interacted with mechanical perturbation reduced the amount of thigmomorphogenesis found in the field due to wind and in the lab due to rubbing. Hunt *et al.* go on to conclude that thigmomorphogenesis due to the wind occurs naturally.

Table 4. 1: Mean numbers of secondary xylem produced in control and experimental (wind exposed) bean plants. *n* = number of plants per experiment. [Hunt *et al.* 1980]

Experiment No.	*n*	Control	*n*	Mechanically Perturbed
1	24	5.1±1.0	27	6.8±0.5
2	26	3.6±1.7	24	4.0±1.1
3	25	7.1±1.3	25	9.1±1.9

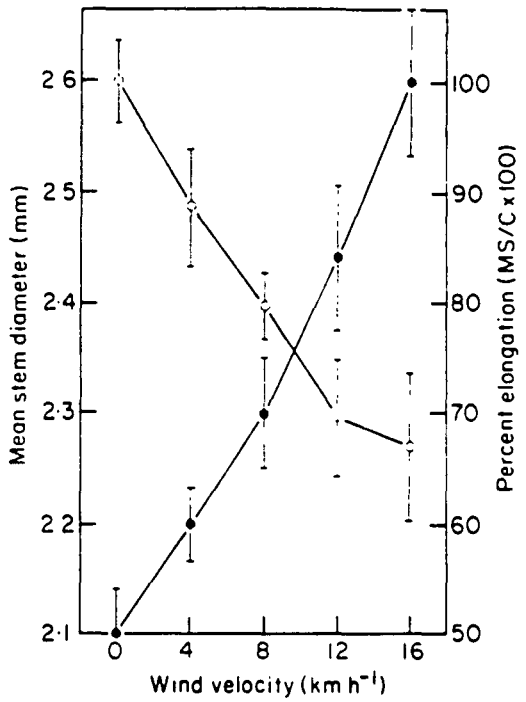

Figure 4.9: First Internode Diameter (●) and Percent Elongation (○) Compared With Control for Kidney Bean Plants (*Phaseolus vulgaris*). Percent Elongation $= \left(\frac{\text{Mechanically Stressed}}{\text{Control}} \times 100\% \right)$

[Hunt *et al.* 1980]

Biro *et al.* (1980) also examined microscopic changes in cell division and elongation of internodes of kidney bean plants. The plants were either mechanically perturbed or ethrel[3]-treated. Both experimental plants showed decrease in elongation and increased radial growth. **Figure 4.10** compares the time course elongation of the control plant and the mechanically stressed one, which shows a significant inhibition of elongation at the treated internode. Examining the longitudinal section of both the control and mechanically-perturbed plants, it appears that the stem length decrease could be attributed to reduced cell elongation of the outer tissues. **[Table 4.2]** An average increase was also observed in both the control and experimental plants with the mechanically stressed bean plant exhibiting a faster rate of radial increase. **[Figure 4.11]** The increase in diameter appears to be a function of both increased cell diameter and number. **[Table 4.3]** The increase in cortex size is primarily due to the radial cell enlargement while a larger portion of the stem diameter increase is due to the production of secondary xylem tissue. Thus, the accelerated cambial activity can be attributed to a rapid response to mechanical stress.

The effect of ethrel application was also examined, and the results are summarized in **Figure 4.12**. The graph shows that high concentrations of ethrel, which lead to production of high amounts of ethylene, have a significant effect on the length decrease and width increase of the stem compared to low concentrations. From both of these experiments, a general trend of shorter internode lengths accompanied by greater radial dimensions follows mechanical perturbation of plants.

Other experiments also show that thigmomorphogenesis reduced mechanically stimulated stems' flexibility while it increased its elasticity. Telewski and Jaffe (1986a) tested firs (*Abies fraseri*) under wind and mechanical perturbation and observed inhibited stem and needle elongation, reinforcement of branch bases around the stem, and increased radial growth in the direction of the stimulus. They suggest that the increase in radial growth caused by the wind or mechanical flexure was due to greater cell divisions of vascular cambium which lead to an increased tracheid number and the decrease in stem elongation was partly due to decreased tracheid length. This agrees with the previously

[3] Ethrel (2-chloroethyl phophonic acid)

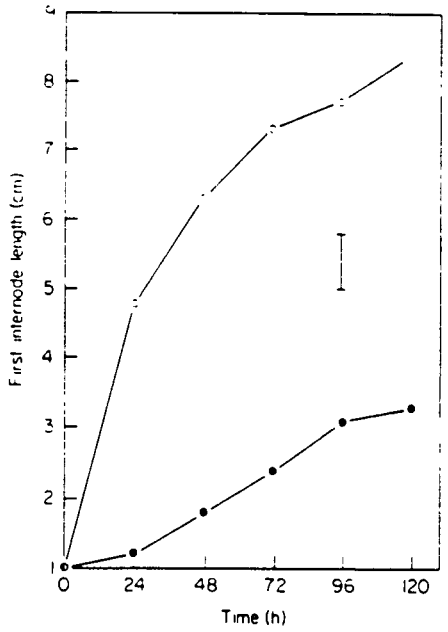

Figure 4.10: Time Course Elongation of Kidney Bean Plants' (*Phaseolus vulgaris*) First Internode. Control Plant (○), Mechanically Stressed Plants (●).

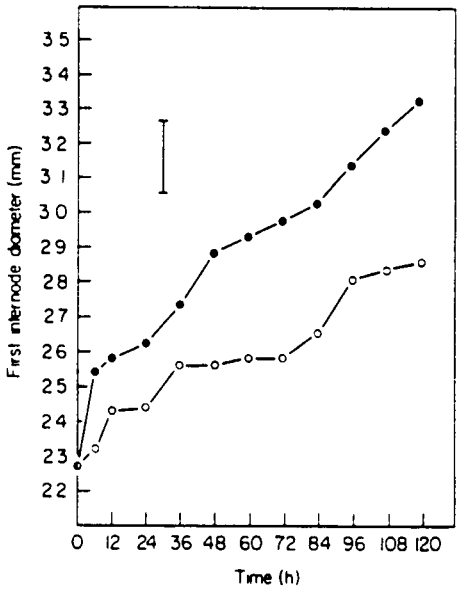

Figure 4.11: Time Course of Radial Enlargement of First Internode of Kidney Bean Plant (*Phaseolus vulgaris*) comparing Control Plants (○) and Mechanically Perturbed Plants (●). [Biro *et al.* 1980]

Table 4.2: Effect of mechanical perturbation on cell lengths as observed in longitudinal sections of the first internodes of bean plants. [Biro *et al.* 1980]

	LENGTH	
Cell Type	**Control (μm)**	**Mechanically Perturbed (μm)**
Epidermal*	110±10	47±6
Cortical*	102±4	86±10
Pith	189±12	202±17

*Outer cell tissues

Table 4.3: Comparison of cell numbers in control and mechanically perturbed bean internodes. [Biro *et al.* 1980]

	Number of cells along section radius		Radial thickness of tissue type (μm)	
Tissue	**Control**	**Rubbed**	**Control**	**Rubbed**
Pith	6.8±0.5	8.8±0.4	283.7±2.6	313.0±4.8
2° Xylem	5.1±0.3	8.3±0.3	70.8±1.4	88.6±1.7
2° Phloem	6.6±0.4	6.8±0.2	58.6±0.9	57.7±1.3
1° Phloem	3.0±0.2	3.2±0.2	23.2±0.6	12.9±0.8
Cortex	4.2±0.3	4.7±0.3	108.5±1.0	131.7±2.0

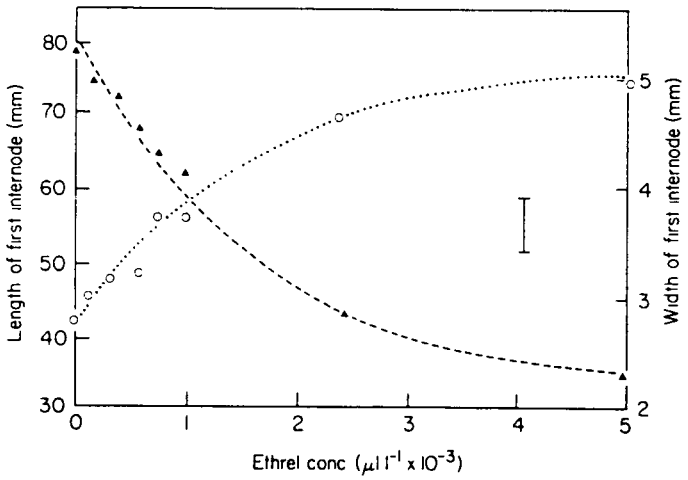

Figure 4.12: Effect of Various Concentrations of Ethrel to Surface of First Internode of Kidney Bean Plants (*Phaseolus vulgaris*) on Length (▲) and Width (O) as Observed 10 Days after Treatment. [Biro *et al.* 1980]

mentioned experiment by Hunt *et al.* (1980). Telewski and Jaffe (1986b) also conducted another experiment on greenhouse-grown pines (*Pinus taeda*) subjected to flexing at about 45° from the vertical 20 times a day and found decreased flexibility, increased elasticity, and increased plasticity of the stem.

4.4.2. *Elfin Forests*

Another intriguing example of mechanical adaptation in plants is seen in a particular vegetational formation, the elfin forest. These forests are characterized by dense growth of short trees which are sometimes gnarled in appearance; their crowns are also tightly packed into a single canopy layer. Elfin forests are most commonly found in tropical montane rain forests, particularly in areas such as small hills, exposed ridges, or gaps within the forest. Hypotheses have been made as to the main contributing determinant of the formation of these unusual forests, and it is commonly believed that wind plays a significant role in the elfin stature.

Robert O. Lawton (1982) tracked the growth of an elfin forest located along the crest of Cordillera de Tilaran situated in the northwest region of Costa Rica for 28 months in an attempt to provide an adaptive explanation of the development history of the elfin forest. With the notion to study the growth of elfin trees and correlate their growth trends with the local gradients of wind stress and forest stature, he hypothesized that wind-exposed trees should have thicker trunks relative to their height compared to trees of the same species growing in wind-protected locations, and branches exposed to wind should, in the same way, be thicker and growth-retarded.

Lawton found that there is indeed a physiognomic gradient that parallels the environmental gradient as winds are stronger on the ridgecrest and increase with altitude, and the trees growing along this crest have thicker trunks and stubbier branches for their height. Further analysis shows that these trees tend to invest more of their resources in increased strength (i.e. trunk and twig thickness) to withstand wind stress. The results also suggest that the observed physiognomic trends are a result of thigmomorphogenesis, the physiological and morphogenic response of plants to mechanical stimulus, rather than genetic differences (although genetic differentiation should not be completely ruled out as

a contributing factor) or physiologic strain since the ridgecrest trees produce the same amount of leaves per unit time as taller, more sheltered trees. From these observations of reduction in branch elongation, in appears that material is freed for use in other forms, such as stem strengthening, and as a result, additional wind stress on the stem is reduced. In addition, shorter branches tend to sway less in the wind thus reducing the natural frequency of vibration and the potential for collisions and fracture of twigs in windy environments. These forms of mechanical adaptations observed in elfin forests coincide with the thigmomorphic findings in the perturbed plant stems and illustrate the morphological changes that occur in plants to oblige external stresses.

4.5. *Optimization*

4.5.1. *Stem Hardening*

As plants are subjected to different forms of environmental stress such as flexure from wind, they alter their growth to accommodate the particular load. Experiments show that some of the induced responses of mechanical perturbation not only involve retarded elongation and stem thickening, but also stem hardening and increased flexibility. Jaffe *et al.* (1984) studied kidney bean plants (*Phaseolus vulgaris*) whose stems were rubbed periodically. They define the parameter elastic resilience as the capacity of the internode to absorb and release energy such that:

$$\text{Elastic Resilience (\%)} = \left(\frac{\text{Ref}}{\text{Def}}\right) \times 100$$

where *Ref* is the reflection (in meters) or the amount of return bending back toward the linear axis after the applied force load has been removed. *Def* is the deflection (in meters) or bending away from the linear axis of the stem under applied force load. These same parameters are used to describe plasticity (the ability of the stem to be deformed by an applied force load):

$$\text{Plasticity (\%)} = \left(\frac{\text{Def} - \text{Ref}}{\text{Def}}\right) \times 100 \quad .$$

The ability for the stem to resist bending under an applied force load is defined by flexural stiffness (*FS*):

$$FS = E \times I$$

where *E* is the elastic modulus and *I* is the second moment of area. The results of this experiment are summarized in **Table 4.4**. Hardening was caused by an increase in elastic resilience in the stem, decrease in elastic modulus, and increase in the second moment of area of the stem, rather than flexural stiffness which remained unchanged. The decrease in modulus of elasticity, which leads to an increase in flexibility, was large enough to overcome tendency toward stiffness due to an increase in second moment of area. In comparing the perturbed plants with the controls, flexibility and second moment of area were greater while the flexural stiffness remained the same. With this in mind, it can be concluded that when plants age and become more exposed to mechanical perturbation, mechanical differences increase suggesting that stems growing in windy environments become more capable of surviving in that area. It has also been found that stem hardening can also aid the plant in its resistance to frost injury. Jaffe and Forbes (1993) observed plant hardening to injury due to stresses other than mechanical while protecting it against

Table 4.4: Summary of the average mechanical parameters of control and mechanically perturbed bean first internodes. [Jaffe *et al.* 1984]

Parameter	Control	Mechanically Perturbed	Effect of MP (%)
Length (mm)	69+3	47+2	-32
Diameter (mm)	2.72+0.01	2.93+0.01	+8
Force (N) at which half the plants rupture RF_{50}	1.28+0.05	1.88+0.10	+47
Elastic Resilience, % (Ref/Def)x100	64+2	78+3	+22
Plasticity, % [(Def-Ref)/Def]x100	36+1	22+1	-39
Elastic Modulus, E (10^{-8} N/m)	1.8+0.1	1.3+0.1	-29
2nd Moment of Area (I)	2.7+0.1	3.8+0.1	+41
Flexural Stiffness (FS)	4.9+0.3	4.9+0.3	0

Ref = Reflection (amount of return bending) after applied force load has been removed; *Def* = Deflection (amount of bending away from axis) under applied force load.

frost. This response involved similar changes in membrane lipids caused by mechanical perturbation and other similar stimulus.

4.5.2. *Reduction of Wind Drag*

Windy environments have also shown to produce plants and trees with less drag. Telewski and Jaffe (1986b) show that changes in morphology and anatomy of mechanically stimulated plants have been interpreted as an adjustment of plant to withstand mechanically induced strain resulting in a stronger stem. **[Table 4.5]** Trees have been found to acclimate themselves to mechanical perturbation by producing a structure capable to withstand increased mechanical loading such as an increase in second

Table 4.5: Mechanical properties of the upper stem of 2-year-old mechanically perturbed and control full-sib loblolly pine (*Pinus taeda*) saplings. [Telewski *et al.* 1986b]

		Plant Identification			
Parameter	**Treatment**	*EBA-266*	*GOA-578*	*EBA-801*	*EBA-206*
Young's Modulus	C	92.5±7.5	47.4±8.1	72.1±8.0	75 3±6 8
E (MN/m^2)	MP	72.9±7.1	19.1±4.1	29.2±1.9	60 9±10 6
2nd Moment of cross-	C	2.8±0 3	5.0±1.1	3.5±0.6	3.9±0.8
sectional area, I ($x10^{-9}$ m^4)	MP	4.6±0.7	13.0±1.3	9.5±0.7	5.2±0.9
Flexural Stiffness	C	2.5±0.3	1.8±0.2	2.3±0.2	2.6±0.3
EI ($x10^4$ N/m^2)	MP	3.1±0.3	2.2±0.4	2.7±0.2	2 5±0.2
Rupture Force (N)	C	27.2±5.5	-	-	-
	MP	63.4±5.8	-	-	-

C = Control, MP = Mechanically Perturbed

moment of area and decrease in Young's modulus providing a more flexible structure. Another biomechanical property observed is plastic displacement as mechanically perturbed seedlings remain deformed to a greater extent than controls which are exposed to the same force. Seedlings which were preconditioned with stimulation stayed in wind-blown form taking several days to recover. The control seedlings, however, were able to recover within 24 hours after wind tunnel tests were complete. **[Table 4.6]** This finding suggests that the increase in plastic nature of stems and branches could be important in the development of wind-swept growth. As we have seen with the examination of the elfin

forest, this type of wind-swept growth influences the plant morphology to produce a more efficient structure that is able to reduce wind drag that may have been formerly experienced. At the same time changes in cell wall chemistry, structure, size, and number can alter the biomechanical properties of plants, and in particular the wood in trees. Changes in the biomechanical properties and cell number in tissues in stems are not the only important factors for plants to remain vertical in windy conditions, but the shorter stature of stems and needles help reduce the surface area available to resist wind resulting in less drag.

Table 4.6: Mechanical properties of 6-month-old stems of loblolly pine (*Pinus taeda*) half sibs. [Telewski *et al.* 1986b]

		Plant Identification	
Parameter	**Treatment**	*8-61*	*8-27*
Young's Modulus	C	51.2±9.3	50.9±10.3
E (MN/m^2)	MP	52.6±11.1	42.5±12.1
2nd Moment of cross-	C	1 3±0.5	1.3±0 3
sectional area, I ($x10^{-10}$ m^4)	MP	1.0±0.2	1.4±0.3
Flexural Stiffness	C	6.4±1.4	6.8±1.3
EI ($x10^{-3}$ N/m^2)	MP	5.2±1.0	6.0±1.2
Plastic Displacement	C	3.0±0.9	3.4±0.7
P (degrees)	MP	3.5±0.8	4.5±0.9

C = Control, MP = Mechanically Perturbed

Thigmomorphogenesis is found to be a widespread phenomenon in nature as it promotes important adaptive advantages in plants. Such adaptations as stem thickening and reduced elongation facilitate the survival of the plant in environmental stresses with increased flexibility. This process strengthens plants in their resistance to rupture and drag in strong winds while also protecting itself against other environmental stresses like frost damage and drought. As other factors such as temperature, and regional effects may play a role in thigmomorphogenesis, it is interesting to note that there exists a commonality in natural material remodeling as it is subjected to different mechanical environments. The previous chapters on bone and wood show that these living materials continue to survive because of their objective to maintain their structure against failure.

4.6. *Conclusion*

Thigmomorphogenesis is a means by which plants alter their structure when experiencing mechanical stress. Experiments by Jaffe (1973), Biro *et al.* (1980), and Telewski *et al.* (1986a, 1986b) have all showed that plant stems directly adapt to stresses through adaptive growth. Plant stems respond to mechanical perturbation such as wind or rubbing by producing thicker stems and decreasing elongation. This reaction serves to increase flexibility and prevent rupture by a reduction of Young's modulus and increase in moment of inertia. Wind-swept growth also aids in the reduction of wind-drag as plants and trees alter their shape to reduce the surface area resisting wind. In its attempt to achieve optimal performance in bending without rupture, plants have been able to remodel their structure to allow more flexibility and plastic displacement. This form of morphological adaptation serves as an important factor in trying to understand the mechanisms behind natural material optimization through growth.

References

Barker, J.E. 1979. Growth and Wood Properties of *Pinus Radiata* in Relation to Applied Ethylene. *N. Z. J. For. Sci.*, v. 9, pp. 15-19.

Biro, R.L., E.R. Hunt, Jr., Y. Erner, M.J. Jaffe. 1980. Thigmomorphogenesis: Changes in Cell Division and Elongation in the Internodes of Mechanically-Perturbed or Ethrel-Treated Bean Plants. *Ann. Bot.*, v. 45, pp. 655-664.

Biro, R. and M. Jaffe. 1984. Thigmomorphogenesis: Ethylene Evolution and its Role in the Changes Observed in Mechanically Perturbed Bean Plants. *Physiol. Plant*, v. 62, pp. 289-296.

Brown, K.M. and A.C. Leopold. 1973. Ethylene and the Regulation of Growth in Pine. *Can. J. For. Res.*, v. 3, pp. 143-145.

Erner, Yair and Mordecai J. Jaffe. 1982. Thigmomorphogenesis: The Involvement of Auxin and Abscisic Acid in Growth Retardation Due to Mechanical Perturbation. *Plant and Cell Physiology*, v. 23, n. 6, pp. 935-941.

Fosket, Donald E. 1994. Plant Growth and Development: A Molecular Approach, Academic Press, Inc., San Diego.

Goeschl, J., L. Rappaport, and H. Pratt. 1966. Ethylene as a Factor Regulating the Growth of Pea Epicotyls Subjected to Physical Stress. *Plant Physiol.*, v. 41, pp. 877-884.

Hunt, E.R. Jr. and M.J. Jaffe. 1980. Thigmomorphogenesis: The Interaction of Wind and Temperature in the Field on the Growth of *Phaseolus vulgaris* L. *Ann. Bot.*, v. 45, pp. 665-672.

Jaffe, Mordecai J. 1973. Thigmomorphogenesis: The Response of Plant Growth and Development to Mechanical Stimulation - with special reference to *Bryonia dioica*. *Planta*, v. 114, pp. 114-157.

Jaffe, M. J. and S. Forbes. 1993. Thigmomorphogenesis: The Effect of Mechanical Perturbation of Plants. *Plant Growth Regulation*, v. 12, pp. 313-324.

Jaffe, Mordecai J., Frank W. Telewski, and Paul W. Cooke. 1984. Thigmomorphogenesis: On the Mechanical Properties of Mechanically Perturbed Bean Plants. *Physiol. Plant*, v. 62, pp. 73-78.

Lawton, Robert O. 1982. Wind Stress and Elfin Stature in a Montane Rain Forest Tree: An Adaptive Explanation. *American Journal of Botany*, vol. 69, pp. 1224-1230.

Mitchell, Cary A. 1996. Recent Advances in Plant Response to Mechanical Stress: Theory and Application. *HortScience*, v. 31, no. 1, pp. 31-35.

Neel, P.L. and R.W. Harris. 1972. Tree Seedling Growth: Effects of Shaking. *Science*, v. 175, pp. 918-919.

Telewski, Frank W. and Mordecai J. Jaffe. 1986a. Thigmomorphogenesis: Field and Laboratory Studies of *Abies fraseri* in Response to Wind or Mechanical Perturbation. *Physiol. Plant*, v. 66, pp. 211-218.

Telewski, Frank W. and Mordecai J. Jaffe. 1986b. Thigmomorphogenesis: Anatomical, Morphological and Mechanical Analysis of Genetically Different Sibs of *Pinus taeda* in Response to Mechanical Perturbation. *Physiol. Plant*, v. 66, pp. 219-226.

Telewski, Frank W. and Mordecai J. Jaffe. 1986c. Thigmomorphogenesis: The Role of Ethylene in the Response of *Pinus taeda* and *Abies fraseri* to Mechanical Perturbation. *Physiol. Plant*, v. 66, pp. 227-233.

Chapter 5: Blood Vessels

5.1. *Introduction*

As already discussed, biological tissues have the ability to change morphology and mechanical properties in response to the their mechanical environment. A common example can be seen in the examination of the cardiovascular system. It has been observed that dimensional changes, such as blood vessel wall thickness, of hypertensive aortas and overloaded left ventricles occur in order to maintain the mechanical stress developed under in vivo conditions at almost the same level as normal organ and tissue. In turn, mechanical properties of the vessel might also become altered due to this form of functional adaptation.

One kind of mechanical stress that is applied to the blood vessel is the condition of hypertension. Most of the morbid events due to hypertension are related to some alteration of large arteries of the brain, heart, or kidney. Such alterations include ruptures, stenosis (the narrowing of an opening or cavity of a vessel), or thrombosis (the formation of a clot in any part of the vascular system). For the most part, the definition of hypertension remains arbitrary in a given population's distribution of blood pressure as persons with blood pressure above a certain limit are said to have hypertension. This limit is defined from two quantitative values: peak-systolic blood pressure and end-diastolic blood pressure, such that *systole* is explained as the contraction of the heart by which blood is forced onward and circulation kept up, and *diastole* is the rhythmical expansion or dilation of cavities of the heart. It is difficult to divide a population of values into discrete categories according to individual measurements; however, from a clinical viewpoint, a distinction has been developed between abnormal (hypertensive) and normal (normotensive) based blood pressures. Normotensive blood pressures (BP) are defined as having a systolic BP less than 140 *mmHg* and diastolic BP less than 90 *mmHg*. The varying degrees of hypertension are outlined in more detail in **Table 5.1**. While peak-systolic and end-diastolic pressures are used for defining limits of hypertensive BP, it is

also important to consider the general shape of the blood pressure curve in order to better define hypertension as a cardiovascular risk factor. [Safar 1996]

Table 5.1: International Classification of Hypertension According to Blood Pressure (BP) Level. [Safar 1996]

Classification	Systolic BP (mmHg)		Diastolic BP (mmHg)
Normotension	< 140	and	< 90
Mild Hypertension	140 - 180	and/or	90 - 105
Subgroup: Borderline Hypertension	140 - 160	and/or	90 - 95
Moderate & Severe Hypertension	> 180	and/or	> 105
Isolated Systolic Hypertension (ISH)	> 160	and	< 90
Subgroup: Borderline ISH	140 - 160	and	< 90

The dynamic consequences of the cardiovascular system can be deduced from the knowledge of its normal functioning state compared to changes caused by its environment. Living tissue has the ability to remodel itself when stress and strain acting on the tissue deviate from the norm. Remodeling of the tissues due to any types of changes in any organ is usually non-homogeneous because the stress distribution is usually non-homogeneous. Thus, by comprehending the morphological changes in biological tissues, such as those that compose the blood vessel, as well as the forms of stress that a vessel experiences, the remodeling that takes place can be better understood. Hypertension allows one to examine the adaptive changes in the blood vessel wall and determine the type of response that occurs with alterations in stress. The objective of this chapter seeks to look at the morphological changes in the blood vessel tissues and their mechanical properties with changing mechanical environment.

5.2. *Organization and Structure of the Vascular System*

The circulatory system serves as a conduit for distribution of arterial blood (blood from the heart) to the capillaries and the return of venous blood to the heart. It also functions to buffer the pulsatile input from the heart to a steady flow in the capillaries, to regulate the volume and the pressure of the blood in the arteries, and to maintain

circulation while the exchange of vascular and extravascular substances occurs in the capillary bed. The basic composition of the circulatory system consists of a closed system of "tubes" of varying diameters and physical characteristics. These are divided into three general categories: arterial, capillary, and venous components. The arteries and veins are considered a series of distributing and collecting tubes while the extensive system of thin-walled capillaries permit the exchange of substances between blood and tissues.

5.2.1. *Vascular Wall Cells*

Blood is confined to a closed circuit of vessels called *endothelium* which serves as a partition and a semipermeable barrier. *Endothelial cells (ECs)* form a layer that lines the entire vascular system. These cells have a polygonal, elongated morphology whose orientation is determined by blood flow-induced shear stress. Under normal circumstances, adult endothelium is a slowly renewing population. However, the potential growth is an intrinsic property of ECs in cases where there is inflammation and wound healing, or tumor growth and vascular repair. Endothelium can also respond to stimuli by undergoing specific alterations in function, structure, and metabolism. For instance, altered shear stresses in a blood vessel can change EC metabolism and thereby increasing replication.

Smooth muscle cells (SMCs) alter blood vessel function by contraction or relaxation as a response to physiologic changes, neural stimuli, and pharmacological interventions. SMCs are circularly or helically arrayed around arteries which contract in response to various stimuli by decreasing vessel diameter. They are also responsible for the structural integrity of the vessel wall while serving as the regulator of vasomotor tone. SMCs synthesize basement membrane material as well as other collagens, elastin, and mucopolysaccharides. Each SMC is surrounded by the basal lamina it secretes and some collagen. Vascular SMCs are often connected by gap junctions which are important in the coordination of adjacent cell functions.

5.2.2. *Wall Structure of Vascular System*

The vascular system maintains a common architectural pattern. The blood vessel wall is composed of three layers: the intima, media, and adventitia, and the basic structural constituents that comprise these are endothelium, muscular tissue, and connective tissue including elastic elements. The *intima* is the innermost layer of the blood vessel and contains endothelial cells, basal lamina, pericytes, subendothilial connective tissue, and the internal elastic lumina. The middle layer, known as the *media*, contains smooth muscle cells and a varied number of elastic sheets, bundles of collagenous fibrils and networks of elastic fibrils. The dividing line between the media and the adventitia (the outermost layer of the vessel) is a layer of elastin. The *adventitia* is mainly composed of collagen fibers and ground substances. It also contains some fibroblasts, macrophages, blood vessels (*vasa vasorum*), myelinated nerves, and nonmyelinated nerves. **[Figure 5.1]**

The blood vessel wall is supplied with blood flow except in the smallest vessels whose cells are within a short distance (i.e. 25 μm) from blood. The vessels perfusing larger blood vessel walls are called *vasa vasorum*. Arteries are less dependent on the vasal supply for their wholeness, however, veins quickly degenerate when the vasal supply is interrupted. The structure of blood vessels varies along the arterial tree as large arteries possess an increased number of lamellar layers with increasing wall thickness. When the relative wall thickness in smaller arteries increases, elastin is less prominent in the media. As distance of the small arteries increases from the aorta, eventually only the inner and outer elastic laminae can be distinguished clearly. In the peripheral vessels, muscle fibers also increase in amount and in helical pattern with a small pitch. These fibers are arranged in quasi-concentric layers with prominent muscle-to-muscle attachment. In the capillaries, the endothelium remains. **[Figure 5.2]**

5.2.3. *Arteries*

The arterial system has two basic functions: (1) act as a conduit by which an adequate amount of blood can be delivered to body tissues, and (2) act as a cushion such that the pulsations from ventricular ejection are dampened. As conduits, the arteries

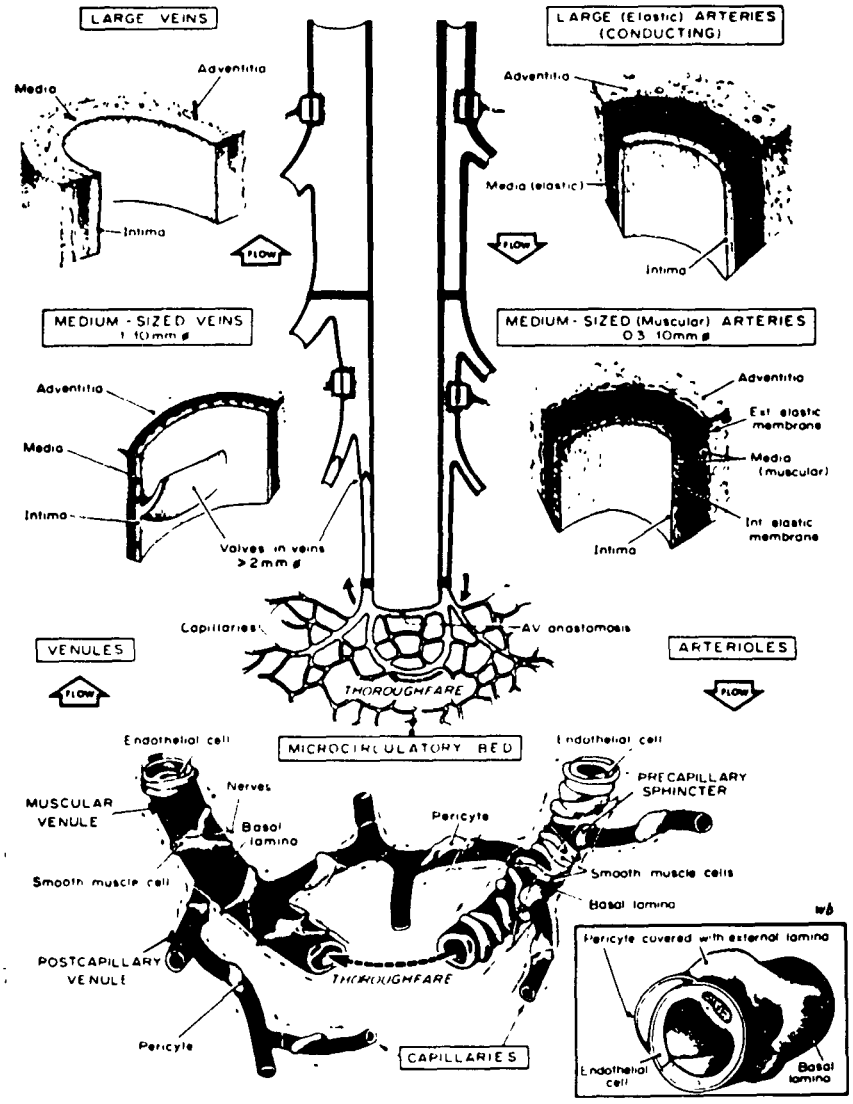

Figure 5.1: The Vascular System and Structure of Vascular Wall at Different Levels of Circulation. [Rhodin 1981]

provide a continuous, steady, constant flow of blood from the heart to the peripheral organs and tissues of the body. In order to maintain this flow, a steady pressure must overcome the energy losses resulting from the viscosity of the blood and friction, and thus, overcome vascular resistance. The resistance is the relationship between mean blood pressure and blood flow, where mean blood pressure is the area under the blood pressure curve divided by the time interval involved, and blood flow. **[Figure 5.3]** The efficiency of the arterial conduit function depends on constancy of mean blood pressure with an indistinct mean pressure gradient between the ascending aorta and peripheral arteries. As cushions, the arteries serve to smooth out pressure oscillations from intermittent ventricular ejection. Large arteries can instantaneously accommodate the volume of blood dismissed by storing part of the volume during systole and draining this volume during diastole. This cushioning allows a continuous flow to organs and tissues, and it is due to the viscoelastic properties of the arterial wall. Efficiency of the arteries as cushions also depends on the compliance and distensibility of arterial walls. Disturbances in the cushioning function can have destructive effects on the heart due to inadequate increase in systolic pressure and relative decrease in aortic diastolic pressure.

The arterial system can be divided into categories of elastic vessels, muscular arteries, and arterioles. The larger arteries or *elastic arteries*, such as the aorta and its branches, contain more collagen fibers and fewer smooth muscle cells in their walls compared to the muscular arteries while both possess a prominent tissue component. The elastic elements are stretched during systole to accommodate cardiac stroke volume and permit the energy given to the blood by contraction of the heart to be stored as potential energy in the elastic arterial wall. The intima of the elastic arteries includes endothelium and a thin layer of connective tissue while the media has abundant elastic tissue in the form of membranes which alternate with layers of SMCs and lesser amounts of collagen. The adventitia is considerably thinner than the media and contains mostly collagen fibers.

Muscular arteries are branches of the elastic arteries whose media are predominantly circularly- or spirally- arranged SMCs. The muscular arteries contain a well developed internal elastic lamina which separates the intima from the media. The adventitia has predominantly longitudinally arranged collagen fibers. **[Figure 5.4]**

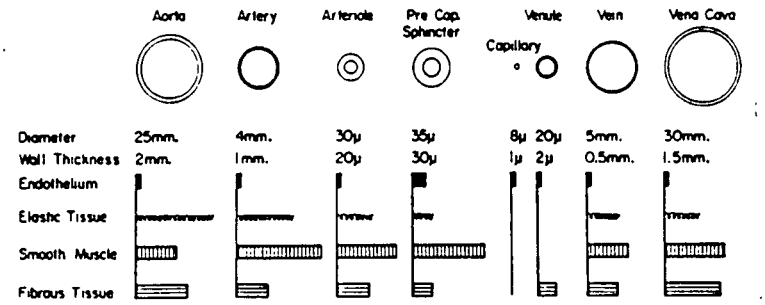

Figure 5.2: Internal Diameter, Wall Thickness, and Relative Amounts of Principal Components of Vessel Walls of Various Blood Vessels. [Schoen 1996]

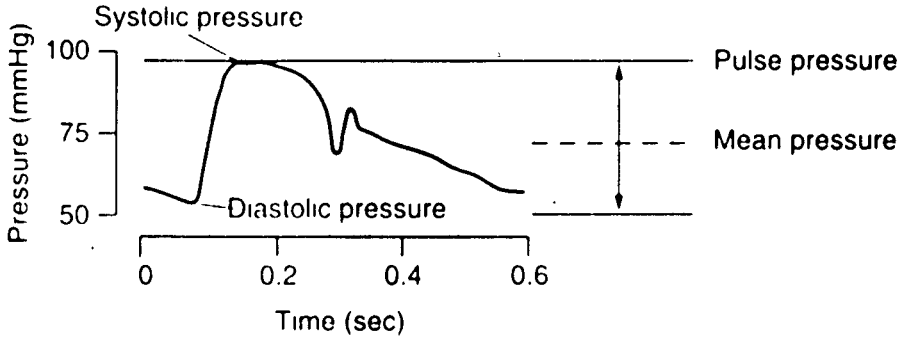

Figure 5.3: Blood Pressure Curve [Safar 1993]

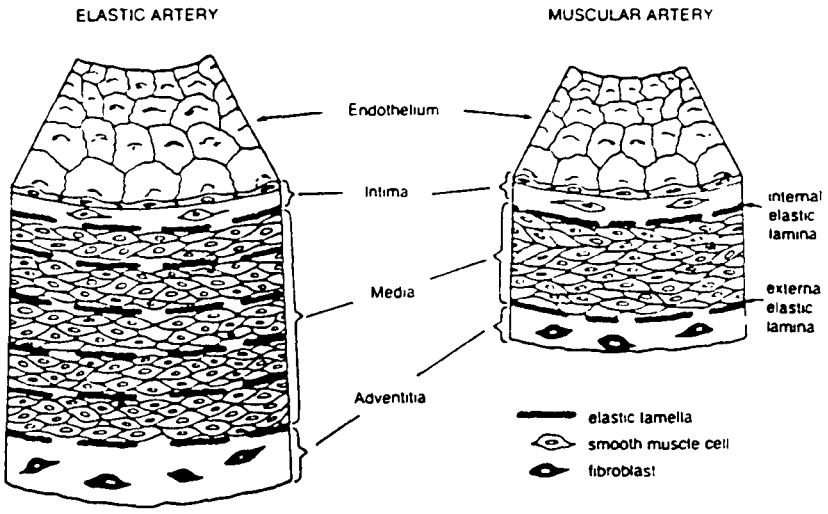

Figure 5.4: Structure of Elastic Artery and Muscular Artery. [Schoen 1996]

The *arterioles* (distal arteries) regulate blood flow into the capillary beds and are essentially small arteries with an average width less than 0.5 *mm*. These short vessels contain a layer of smooth muscle that is under a dual system of neural and chemical control. Large arterioles have at least two layers of SMCs while the smallest, called *precapillary sphincter areas*, have only one layer of SMCs or SMCs scattered widely apart in the vessel wall.

5.2.4. *Capillaries*

Capillaries are their associated structures constitute microcirculation as the majority of these structures are less than 100 μ in diameter. Thin-walled capillary vessels begin from slightly larger metarterioles which act as relatively direct, high resistance, pathways through the capillary bed between the arteriole and venule. The capillary vessels form a network of variable configuration and density before coalescing into a postcapillary venule. The microstructure of the capillary wall varies, and there is no typical organization, but in general these vessels are composed of a single layer of endothelial cells with a thin membrane to provide support. While some ECs form tight junctions at their margin with other cells, there usually is a cleft or intercellular space of about 50-60 Å wide between each cell which acts as a pathway for material to move in and out of the capillary lumen. At the same time, some capillaries have cells outside the EC layer known as pericytes. **[Figure 5.5]**

Capillary vessels are ideally designed to exchange fluids, dissolved gases, and small solute molecules. Their small size gives them the maximum diffusing surface for their total volume. Their narrow diameter also allows them to have higher internal pressure than larger veins and still maintain a thin wall due to the small amount of internal tension.

5.2.5. *Veins*

Blood drains from the capillaries into the venules whose vessels are formed by the combination of the through-channel metarterioles and capillary vessels. As the heart is approached, the number of veins decreases and the thickness and composition of the vein

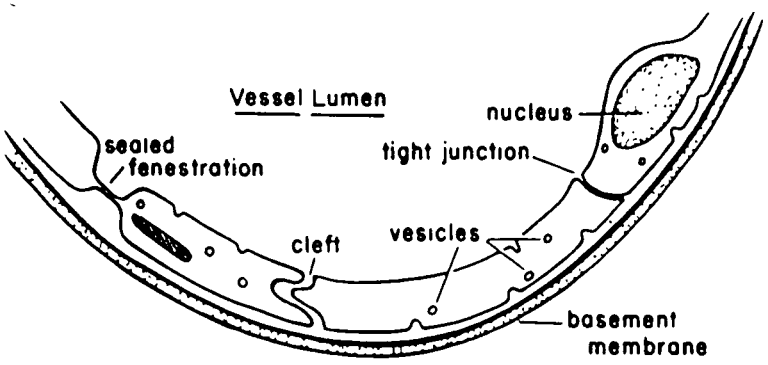

Figure 5.5: Diagram Showing Capillary Wall Structure With Endothelial Cells Making Tight Junctions of Clefts. [Little 1977]

wall changes. Since the total cross-sectional area of the venous channels is progressively reduced as one moves toward the heart, velocity of blood flow also increases. Like capillaries, small openings have also been found in the endothelial lining of the venule wall as the venules converge to form the veins of increasing diameter. Basic vein structure is similar to that of the arteries but with a lower relative wall thickness and with the media containing very little elastic tissue. **[Figure 5.6]** Larger veins possess an intimal surface with semi-lunar-shaped valves that are generally arranged in pairs. These are associated with a distinct local widening of the vessel. The adventitia of veins is relatively thick containing considerable amounts of collagen. In general, veins contain high amounts of collagen with an elastin-collagen ratio about 1:3. There are at least two or more veins that tend to interconnect freely for each artery of the same size. Thus the total cross-sectional area of the venous system is greater than that of the arteries. It is estimated that 75% of circulating blood volume at any one time is contained in the venous system while 20% is in the arterial vessels with the remaining in the capillaries.

Arteries and veins both possess an inner endothelial lining, middle muscular coat, and outer adventitial layer, however veins tend to have thinner walls and relatively fewer elastic fibers. As a result, veins are more structurally stiff compared to arteries. The collapsible nature of veins, nonetheless, still permits the increase of their internal volume several fold with small increases in pressure by a change in their cross-sectional profile from a flattened ellipse to a more circular shape.

5.2.6. *Relationship Between Wall Thickness and Vessel Lumen*

The ratio of vessel wall thickness to radius appears to have physiological significance as seen in **Table 5.2**. The arterioles possess a large ratio illustrating the prominent muscle layer in the vessel wall and small radius. Thus, contraction of the external layer of the circular muscles in the wall of the arteriole displaces the remaining muscle mass toward the vessel center. This causes the reduction of the lumen and changes in the resistance to blood flow produced by vasomotor activity of the arteriole. The large *w/r* ratio permits other thick-walled vessels to close completely as a result of minimal contraction of the circular muscular elements. In veins, which have thin walls and small

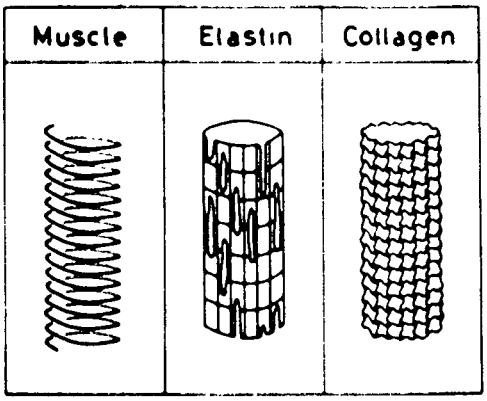

Figure 5.6: Diagram Showing Structure of Vein's Components. [Fung 1993]

Table 5.2: Approximate Characteristics of Different Components of Human Vascular System. [Little 1977]

Structure	Diameter (mm)	Wall Thickness (mm)	Length (cm)	Ratio of Wall Thickness to Radius, (w/r)	Wall Tension (dynes/cm)	Internal Pressure (mmHg)
Aorta	25.0	2.000	40.0	0.16	170,000	100
Medium Arteries	4.0	0.800	15.0	0.40	60,000	90
Arterioles	0.3	0.020	0.2	0.75	1,200	60
Capillaries	0.008	0.001	0.075	0.25	16	30
Venules	0.02	0.002	0.20	0.20	26	20
Medium Veins	5.0	0.500	15.0	0.20	400	15
Large Veins	15.0	0.800	20.0	0.10	9,750	10
Vena Cava	30.0	1.500	40.0	0.10	21,000	10

w/r ratio, contraction of the muscular coat does not have nearly the effect on blood flow as do the arterioles. **[Figure 5.7]**

Muscular tissue in vessel walls are arranged primarily with longitudinal orientation such that shortening produces a minimal effect on the vessel diameter during contraction. [Fung 1993, Little 1977, Safar 1996, Rhodin 1981, Schoen 1996]

5.3. *Experiments: Morphological Changes and Adaptations*

5.3.1. *Stresses in Arterial Wall*

Tissues are organized in a manner to ensure stability over a range of physical stresses to which they are subjected. As growth takes place, proliferative and biosynthetic responses are engaged to provide reinforcement to the tissue. The same occurs when the tissue is exposed to chronic deviations in stress. The objective of these responses is to maintain or restore the equilibrium mechanical conditions and preserve normal tissue architecture.

Glagov *et al.* (1992) reviewed the tissue reactions to mechanical stresses in relation to the arterial wall stability. By studying the interactions between mechanical stresses and tissue responses, they identified the primary stresses in the artery wall which were generated by blood pressure and blood flow and evaluated their influence of the vessels' architectural features.

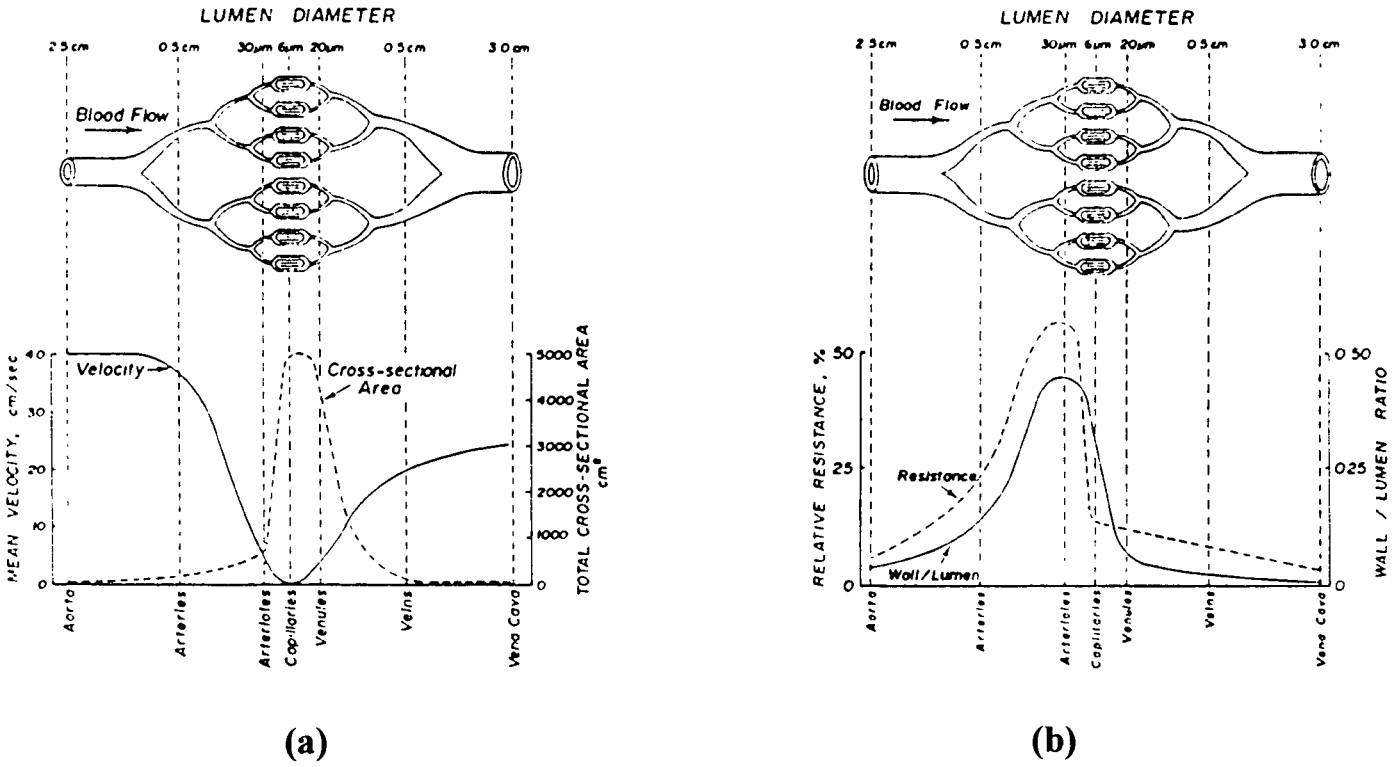

Figure 5.7: (a) Changes in Cross-Sectional Area, Velocity, (b) Wall to Lumen Ratio, and Relative Resistance to Blood Flow With Respect to Segments of Systemic Blood Vessels. [Schoen 1996]

The authors define *mural tensile stress* as "proportional to intraluminal distending pressure and effective radius." [Glagov *et al.* 1992] This stress results in axial, radial, and circumferential strains. The strains that are developed tangent to the blood vessel curvature are easily defined through modifications of the radius and wall thickness. Axial and radial strains are characterized less frequently since vessels tend to be relatively restrained by surrounding tissues, however a change in strain related to pressure pulses during the cardiac cycle is quite evident in the tangential direction perpendicular to wall curvature.

Wall shear stress acts axially in straight, cylindrical arteries and is determined largely by the flow velocity gradient near the wall. Under normal conditions, the mean wall shear stress tends to be relatively constant (15 $dynes/cm^2$) in most mammalian arteries and is independent of location or level in the arterial tree. Changes in the vessel radius follow increases or decreases in wall shear stress, and in order to maintain stability, remodeling must occur. Wall shear stress is directly related to volume flow and viscosity while it is inversely proportional to the radius cubed. Thus a small adjustment of the radius may compensate for a large change in volume flow. Wall tension is related to the distending pressure and radius, but its baseline values change with location in the arterial tree due to differences in the distribution of tensile stress. These tensile stress distributions are a function of the vessel's distance from the heart, local pressure-pulse wave characteristics, pulse rate, and presence of vasa vasorum within the media. Distinctive features of composition and structure in the vessel are associated with combinations of the aforementioned variables, and in spite of the obvious differences in radius relative to animal size, blood vessels tend to have similar structural features and similar ratios of diameter-to-wall thickness. For instance, both humans and cynomolgus monkey posses a diameter-to-wall thickness ratio of 25 while they differ in weight by a factor of 30. Evidence of this is also seen in aortas which are composed of uniform, same width, fibro-cellular layers as their ratio of tangential tension to number of layers is constant. At the same time, the main pulmonary artery, proximal coronary artery, and renal artery are also composed of layers different in architecture from the aorta and with less interstitial matrix, but their ratio of tension to number of layers is also constant for each similar species.

In their study of mechanical stresses in relation to arterial wall stability, Glagov *et al.* find that wall tension increases as blood pressure elevates. The adjustment of wall thickness and composition help restore equilibrium tensile stress and maintain normal transmural architectural features. The structure and thickness may be considerably modified to provide alternate means for the preservation of stability. There also exists a strong correspondence between tensile stress levels and vessel wall architecture and composition when there is a departure from the normal values of tensile stress during growth.

As arteries become subjected to increased volume flow, they enlarge in an attempt to restore the equilibrium wall shear stress. This increased radius results in an increase in mural tension. Restoration of this equilibrium stress is usually accomplished by hypertrophy and hyperplasia of the SMCs in the media as well as thickening of intima. During development, the diameter of the artery is intimately related to flow, and experiments show that reduced flow causes a reduced artery diameter; with increased flow, there is also an increased diameter. Swift and chronic modifications of the diameter with flow appear to be endothelium dependent as the reconstruction of the media and intima are speculated to be induced by the redistribution of local tension.

5.3.2. *Cellular Alignment*

Cellular alignment in vital tissue has also been found to form the most effective configuration to function. Studies have been done on the effect of cyclic strain on cellular orientation response and morphological change. Pulsatile induced stress has been found to be an influential factor of orientation in vivo for endothelial cells which compose the inner lining of the blood vessels and smooth muscle cells within the media. The cell's adaptive behavior may be a consequence to continually loaded stress. The pulsatile nature of flow in the arteries cause pressure waveforms acting on the vessel wall and periodically produce circumferential stretching. As a result, it is theorized that the helical orientation of smooth muscle cells, which are not usually exposed to blood flow, may be due to these periodic stretches.

Kanda and Matsuda (1993) take upon a biomechanical approach to the orientation response and morphological change of vascular cells which were subjected to periodic stretches. As they attempted to quantify cellular response of different cell types under fixed conditions, they found stress-loaded cells tended to align perpendicularly to the direction of stretch with time while more pronounced orientation was attained under conditions with higher amplitude and frequency of stretching. Endothelial cells (ECs), smooth muscle cells (SMCs), and fibroblasts (FCs) were extracted from bovine aorta and subjected to periodic stretch on extensible membranes as the effect of the mechanical stress on two-dimensional cellular orientation and morphology were analyzed. The operating variables included amplitudes that ranged from 5-20% of unstretched length of the films and frequencies ranging from 15-20 *rpm* for a total period of 24 hours. Orientation parameters and morphological parameters were quantified to evaluate the mechanically induced stress effects.

Before stress loading was initiated, the SMCs spread on the polyurethane films showed a polygonal shape with random orientation. After about three hours of stretching with a 5% amplitude and frequency of 60 *rpm*, the SMCs tended to align perpendicular to the direction of stretch. In comparison to the control cells, these nonstressed films remained in random orientation. **Figure 5.8** shows the histograms indicating the distribution of orientation angles of the bovine SMCs at different intervals of time, and after 12 hours of mechanical stressing, it is evident that most of the loaded SMCs were aligned 90° away from the stretch direction. Meantime the stationary, unstretched films continued to show random cell orientation. The average orientation angle was also determined for both the control and experimental films to define an average value of minimal deviations from the direction of stretch. The nonstressed SMCs had an average orientation angle equal to 45°, indicating random orientation. The stressed cells were becoming perpendicularly aligned with the stressed direction. **[Figure 5.9]**

When the amplitudes and frequencies were varied in the SMC stretching, marked increases of average orientation angles with respect to time were exhibited. **Figure 5.10** shows the effect of amplitudes of 5%, 10%, and 20% with a fixed frequency of 60 *rpm*. At 20%, there is a pronounced increase in the average orientation. When the amplitude of

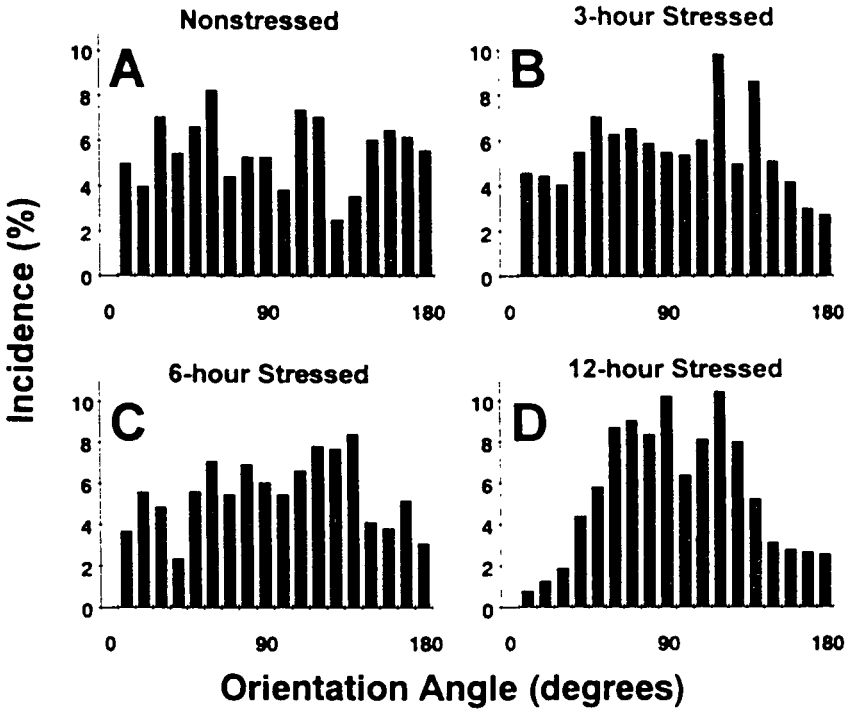

Figure 5.8: Histograms Showing Distribution of Orientation Angles of Bovine Aortic SMCs Undergoing Periodic Stretch With 5% Amplitude at 60 *rpm* at 4 Different Time Periods. [Kanda *et al.* 1993]

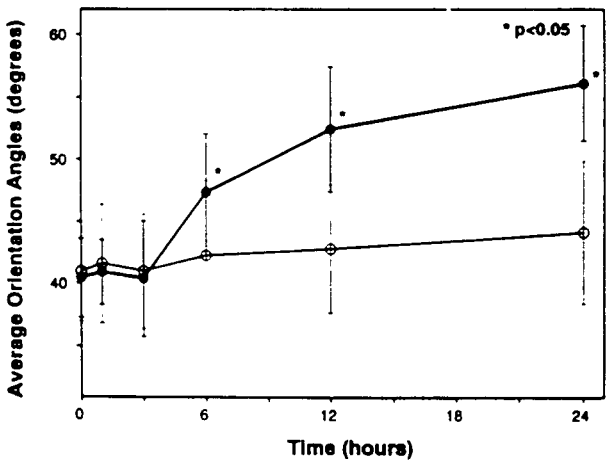

Figure 5.9: Time-Dependent Changes of Average Orientation Angle of Bovine Aortic SMCs. Nonstressed SMCs (○) in Range of 40-45°. Stressed SMCs (●) at 5% Amplitude, 60 *rpm*. [Kanda *et al.* 1993]

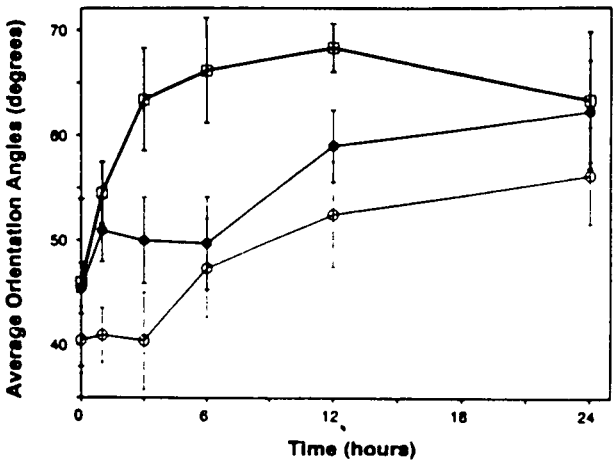

Figure 5.10: Time-Dependent Changes of Average Orientation Angles of Bovine Aortic SMCs at Amplitudes: 5% (○), 10% (●), and at 20% (□) at Frequency of 60 *rpm*. [Kanda *et al.* 1993]

5% was fixed and the frequencies varied at 15, 60, and 120 *rpm*, significant increases of average orientation were also displayed. **[Figure 5.11]**

Compared to the SMCs, the response of the ECs was less dramatic and obvious reaching a peak average orientation less than 50° while staring at an average orientation of approximately 44°. The FCs exhibited a similar response to the SMCs. **[Figure 5.12]** The histograms also indicate that the initiation of alignment perpendicular to stress direction occurred earlier in the FCs compared to the ECs and SMCs. The time-dependent changes of morphological parameters (cellular longitudinal length, peripheral length, spread area, and circular index) were also examined, but insignificant change was observed, and therefore it was concluded that the stress-loading did not play an influential role in morphological change.

When the arterial wall is subjected to pulsatile flow, it experiences two major vector elements: a hydrodynamic shear stress parallel to the longitudinal axis of the vessel and a periodic circumferential stretch. Arteries with high shear rate and low flow turbulence show their ECs in the intimal layer aligning themselves parallel to the flow direction. **Figure 5.13** supports this notion showing very little change in average orientation angle with respect to time for the ECs in comparison to the SMCs and FCs. Other studies have also shown that ECs cultured in flow-regulated chambers tend to align themselves with flow direction. Thus, it appears that flow shear stress is a primary mechanical factor responsible for EC orientation.

SMCs, which are not directly exposed to blood flow because of their residence in the arterial media, exhibit a spiral orientation. Their circumferential orientation appears to be attributed to the periodic stress of the arterial wall, as this experiment's results show that SMCs tend to align perpendicular to the stretch direction. Looking at the results of Kanda *et al.*, four factors seem to influence cellular orientation induced by periodic stretch: stress loading time, amplitude, frequency, and cellular species. Thus, understanding mechanically-induced orientation response of cells provides a basis for understanding the biomechanics of morphological adaptation of tissues.

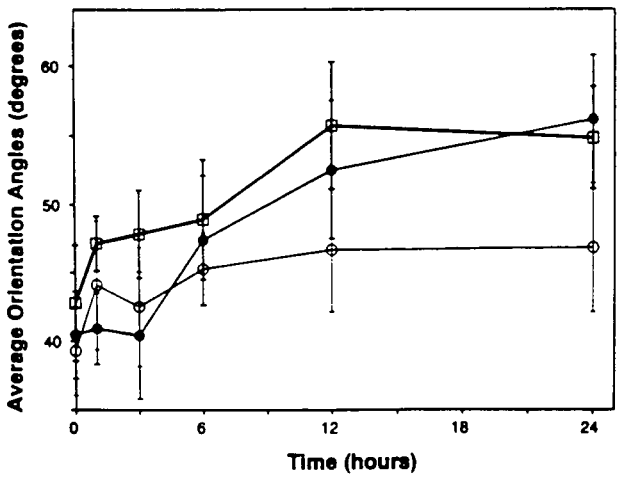

Figure 5.11: Effect of Stretching Frequencies (15 *rpm* = ○, 60 *rpm* = ●, 120 *rpm* = □) with a Fixed Amplitude of 5% Over Time for Bovine Aortic SMCs. [Kanda *et al.* 1993]

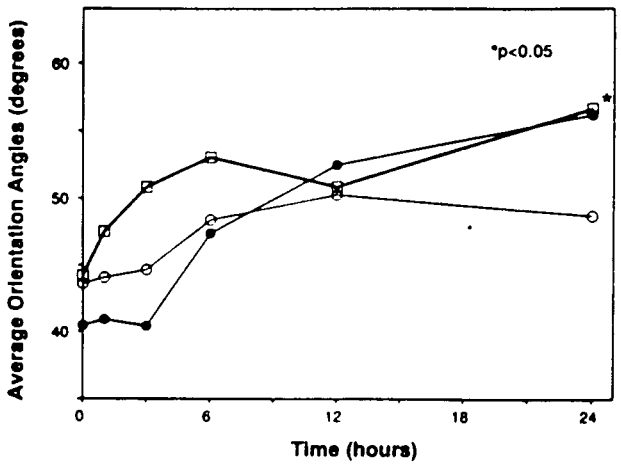

Figure 5.12: Comparison of Average Orientation Angles of Different Bovine Aortic ECs (○), SMCs (●), and FCs (□) With Respect to Time. [Kanda *et al.* 1993]

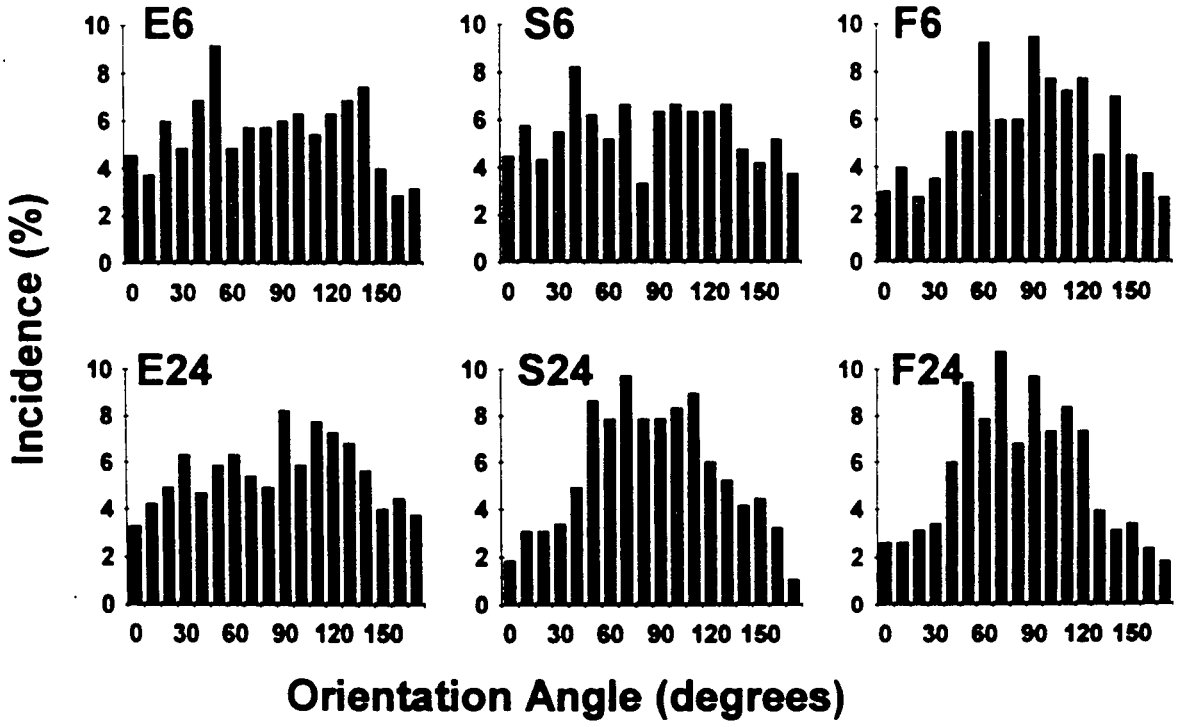

Figure 5.13: Histograms Indicating Distribution of Orientation Angles of Bovine Aortic ECs (E6, E24), SMCs (S6, S24), and FCs (F6, F24) at Amplitude 5%, 60 *rpm* for 6 Hours (E6, S6, F6) and 24 Hours (E24, S24, F24). [Kanda *et al.* 1993]

5.3.3. *Structural Changes in Large Arteries in Hypertension*

Mechanical properties of the arterial wall are influenced by the structural elements of the artery, namely the endothelium, adventitial, intima, and media. The two major contributors, however, of structural components to mechanical properties arises from the intima and media which consist mainly of smooth muscle, elastin, and collagen. Morphological studies have shown hypertensive vessels exhibit changes in dimensions and properties due to smooth muscle hypertrophy and hyperplasia (abnormal or unusual increase in cell tissue) as well as increased amounts of elastin and collagen. It is reported that the Young's modulus for noncontracting smooth muscle was very low with a value of approximately 6×10^4 *dynes/cm*^{2}, thus making it more extensible than the arterial wall. However, isolated elastin tissue possessed a modulus estimated at 3×10^6 *dynes/cm*^{2} while collagen had a reported value of approximately 10^9 *dynes/cm*^{2}. This shows that the volume fraction of elastin and collagen make the principal contribution to the passive mechanical properties of the arterial wall. The accumulation of elastin and collagen in vessels also occurs during aging to a relative degree, and as a result, some have suggested that hypertension is a form of accelerated aging. Macroscopically, the changes in the larger arteries show increases in aortic mass, size of lumina, and wall thickness while more marked changes occur in the subendothelial layer and media with increases in connective tissue. Upon the examination of the changes that take place within the blood vessels, the following sections will evaluate both macroscopic and microscopic effects of stress alterations. [Safar 1996]

5.3.4. *Hypertension Remodeling*

Hypertension has been known to cause morphological changes in blood vessels such as increased thickness and stiffness. These same types of adaptations are also noted in aging. Morphological studies that have been conducted show that such changes are due to smooth muscle hypertrophy and hyperplasia, and increased amounts of mural mucopolysaccarides, collagen, and elastin. Harvey Wolinsky (1971, 1972) compares the short-term (2.5 months) and long-term (16 months) effects of hypertension on the dimensions and chemical composition of the vessel wall. His results show that long-term

hypertension produces increasing amounts of elastin and collagen while elevated wall tension was associated with progressive increase in wall thickness.

Wolinsky induced hypertension in 7-week old rats weighing 135-145 *g* by clipping their renal artery. Hypertension was defined for this experiment as a systolic blood pressure greater than or equal to 150 *mmHg*. Animals were killed 2.5 months and 16 months after documented hypertension. For morphological studies, micrometric techniques were employed to measure wall thickness and medial laminae. The cross-sectional area of the media was calculated as:

$$\text{Medial Area} = \pi (r_1 + r_2)(r_1 - r_2),$$

where r_1 and r_2 are the radii of the two circles. Tangential tension was determined according to the law of Laplace such that:

$$\text{Tension } (dyne/cm) = \text{Blood Pressure } (dyne/cm^2) \times \text{Radius } (cm), \quad \text{and}$$

$$\text{Wall Stress } (dyne/cm^2) = \frac{\text{Tangential Tension}}{\text{Medial Thickness}}.$$

The aortic wall was examined to compare the morphological findings of these experiments and are summarized in **Table 5.3**. The vessel diameters of the hypertensive aorta were significantly greater than that of the control, as it had also been in the short-term case. Interestingly, the hypertensive vessels in both the short- and long-term cases were not significantly different, however the diameters of the normotensive vessels increased significantly due to aging. **Table 5.3** also shows the medial area of the aorta reporting differences between the control and experimental rats as this finding was consistent at both 2.5 and 16 months. Wall thickness also seemed to increase with age in the normotensive and hypertensive animals. The tension per lamellar unit was reported significantly greater in the hypertensive cases for the short- and long-term cases, but no changes were seen with increased duration of hypertension since the factors used for the calculation (diameter, blood pressure, and lamellar units) did not change. Wall stress, which is also related to tangential tension and diameter, increased in the hypertensive aortas at 2.5 months. With prolonged hypertension, the increase in wall thickness resulted in a wall stress that was not much different from the control vessel. At the same time, it

Table 5.3: Dimensions of and Calculated Stresses on Aortic Wall. [Wolinsky 1971, 1972]

Short-Term (2.5 mo.) Hypertension	Control	Hypertensive
Diameter (mm)	2.35 ± 0.07	2.89 ± 0.12
Wall Thickness (mm)	0.097 ± 0.005	0.124 ± 0.008
Lamellar Units	7.83 ± 0.12	7.90 ± 0.17
Tension/Lamellar Unit (dynes/cm x 10^3)	1.96 ± 0.12	4.53 ± 0.42
Wall Stress (dynes/cm^2 x 10^6)	1.60 ± 0.13	2.94 ± 0.40
Medial Area (mm^2)	0.747 ± 0.017	1.204 ± 0.076

Long-Term (16 mo.) Hypertension	Control	Hypertensive
Diameter (mm)	2.74 ± 0.05	3.08 ± 0.11
Wall Thickness (mm)	1.178 ± 0.027	1.743 ± 0.041
Lamellar Units	8.0 ± 0.1	8.1 ± 0.1
Tension/Lamellar Unit (dynes/cm x 10^3)	2.65 ± 0.12	4.5 ± 0.19
Wall Stress (dynes/cm^2 x 10^6)	1.80 ± 0.08	2.09 ± 0.12
Medial Area (mm^2)	1.058 ± 0.030	1.779 ± 0.072

was found that wall stress did not change significantly with aging, either.

The differences between the control and experimental animals' chemical components showed significant increases in aortic dry weight, elastin, collagen, and noncollagenous alkali-soluble proteins. **[Table 5.4]** Remarkable increases in elastin and collagen also occurred during the period between the 2.5 and 16 months of hypertension. It is also interesting to note that sharp increases were seen in the absolute amounts of fibrous proteins were also seen in the aging controls. While the rate of collagen accumulation between the short- and long-term periods appeared similar, the rate of elastin accumulation for the hypertensive vessels was faster than in the controls. When comparing the percentage amounts of the aortic wall components at 16 months, the control and hypertensive cases show no difference for elastin. **[Table 5.5]** While the collagen content increased in the control and hypertensive rats over the period inbetween 2.5 and 16 months, the hypertensive vessels show a collagen percentage slightly less than the controls after 16 months. For the alkali-soluble proteins, the percentage decreased slightly with aging in the controls, but a larger decrease in percent occurred with duration of hypertension reflecting an absolute amount of this component combined with a

Table 5.4: Total Aortic and Wall Component Weights. [Wolinsky 1971, 1972]

Short-Term (2.5 mo.) Hypertension	Control	Hypertensive
Total Aortic Dry Weight	7.61 ± 0.50	12.37 ± 0.41
Elastin	3.13 ± 0.19	4.25 ± 0.22
Collagen	1.04 ± 0.08	1.71 ± 0.11
Alkali-Soluable Protein	1.39 ± 0.07	3.83 ± 0.12

Long-Term (16 mo.) Hypertension	Control	Hypertensive
Total Aortic Dry Weight	10.78 ± 0.57	16.52 ± 0.77
Elastin	4.43 ± 0.31	6.75 ± 0.31
Collagen	2.7 ± 0.17	3.50 ± 0.15
Alkali-Soluable Protein	1.73 ± 0.070	3.60 ± 0.39

Table 5.5: Percents of Aortic Wall Components. [Wolinsky 1971, 1972]

Short-Term (2.5 mo.) Hypertension	Control	Hypertensive
Elastin	41.24 ± 0.60	34.32 ± 0.91
Collagen	13.79 ± 0.74	13.81 ± 0.59
Alkali-Soluble Protein	18.45 ± 0.96	30.99 ± 0.80
Total	73.48 ± 1.93	79.12 ± 1.44

Long-Term (16 mo.) Hypertension	Control	Hypertensive
Elastin	40.94 ± 0.97	40.94 ± 0.62
Collagen	24.65 ± 1.12	21.27 ± 0.81
Alkali-Soluble Protein	16.15 ± 0.30	21.59 ± 1.70
Total	81.74 ± 1.45	83.80 ± 0.82

continual accumulation of the fibrous proteins. While the percentage of the noncollagenous alkali-soluble proteins of the long-term hypertensive rats was greater than the controls, it was more similar to the controls at 16 months than at 2.5 months.

Looking at these results, it appears that the composition of the aortas with long-term hypertension resemble those of the controls compared to the short-term hypertensive rats. This finding suggests that the response of the aortic wall is biphasic with the early phase consisting of disproportionate increase in noncollagenous alkali-soluble components (attributed to the smooth muscle cell components in the media) and smaller increases in fibrous proteins. The later phase is characterized as a "catch-up" or increase of fibrous elements with no further increase in absolute amounts of noncollagenous alkali-soluble fraction with chronic hypertension. As a result, the increased wall thickness and medial area from elastin and collagen accumulation helps to maintain a constant wall stress in the vessel. Wolinsky's experiment confirms this idea with the end result showing an aortic wall with almost two times the medial area of the control vessel at the same age. These same vessels also display no difference in calculated wall stress while the composition is much closer to that of the control vessel than to that seen in early hypertension. The second major finding of this study was that the aortic wall response to tension increases from a rise in blood pressure and increases in diameter associated with aging is similar to hypertension. The only differences between aging and hypertension were in magnitude. Many changes found previously in vessels during aging include 2-3 fold increases in wall thickness, vessel diameter, and decrease in wall distensibility. For aging, these changes tended to be ascribed to the increased amounts of collagen and not loss of elastin. Wolinsky submits that aging that occurred in the rat aorta was accompanied by the accumulation of both fibrous proteins and that the frayed appearance of elastin is most likely due to newly synthesized fibrils. These compositional changes seemed to reflect the increased levels of calculated tension on the vessel wall which arose from increasing diameter and slowly rising blood pressure. As a result, these increases represent a response to tension as also seen in hypertension, but to a smaller degree. Aging can be considered a muted form of hypertension, or hypertension an accelerated from of aging.

Matsumoto and Hayashi (1994) also examined the mechanical and dimensional adaptation of the aorta to hypertension in rats aged 8-9 weeks by constricting their left renal arteries. Their findings were similar to Wolinsky's study of aortic wall stresses. For this study, the thoracic aortas were excised and used to determine the static pressure-diameter relations and wall dimensions for periods 2, 4, 8, and 16 weeks after hypertension ($P_{sys} \geq 160$ *mmHg*) was induced; systolic blood pressure and heart rate were measured weekly. Data was analyzed by calculating the circumferential stress, σ_θ, calculated by the law of Laplace:

$$\sigma_\theta = \frac{P_i D_i}{(D_o - D_i)}$$

where D_i is the inner diameter of a pressurized specimen, D_o is the outer diameter of the specimen, and P_i is the intraluminal pressure. The incremental elastic modulus, $H_{\theta\theta}$, for orthotropic material was defined as:

$$H_{\theta\theta} = 2\left(\frac{\Delta P_i}{\Delta D_o}\frac{D_o D_i^2}{D_o^2 - D_i^2} + \frac{P_i D_o^2}{D_o^2 - D_i^2}\right)$$

where ΔD_o is the increment of D_o induced by the increment of P_i, ΔP_i. The apparent stiffness of the aorta was expressed by the pressure-strain elastic modulus, E_p:

$$E_p = \frac{\Delta P_i}{(\Delta D_o / D_o)}.$$

The pressure-strain elastic moduli of the aortas were calculated at three different blood pressure levels. **[Table 5.6]** At 100 *mmHg*, the modulus (E_p) was significantly larger in the hypertensive animals than in the control except at 4 weeks. At the higher pressure at 200 *mmHg*, the hypertensive animals had smaller moduli than the controls even though the differences were significant only at 4 weeks. The systolic blood pressure (P_{sys}), which was measured in vivo by tail plethysmography while the animals were conscious, the modulus was significantly larger in the hypertensive animal except at 4 weeks. It was also observed that higher wall stiffness in the hypertensive rats were exhibited at low pressure (100 *mmHg*) while at high pressure (200 *mmHg*), the aortic wall displayed more distensibility compared to the controls. The blood vessel's structural stiffness is

Table 5.6: Pressure-Strain Elastic Modulus (*Ep*) at Three Blood Pressure Levels. [Matsumoto *et al.* 1994]

Weeks after operation	2	4	8	16
CONTROL				
No. of Animals	5	5	7	7
Psys (mmHg)	134 ± 3	134 ± 4	129 ± 3	137 ± 3
Ep (mmHg)				
at 100 mmHg	3.8 ± 0.2	3.4 ± 0.3	3.3 ± 0.1	3.2 ± 0.1
at Psys	14.0 ± 2.3	12.2 ± 2.4	9.4 ± 1.2	9.7 ± 1.7
at 200 mmHg	53.4 ± 5.8	52.4 ± 5.2	55.4 ± 6.1	50.8 ± 6.8
HYPERTENSIVE (Psys > 160 mmHg)				
No. of Animals	8	8	8	5
Psys (mmHg)	199 ± 7	190 ± 9	206 ± 8	192 ± 9
Ep (mmHg)				
at 100 mmHg	4.8 ± 0.3	3.9 ± 0.2	4.3 ± 0.4	4.0 ± 0.3
at Psys	41.1 ± 6.3	26.7 ± 5.3	35.3 ± 4.8	22.4 ± 2.8
at 200 mmHg	40.0 ± 4.3	31.0 ± 2.6	36.9 ± 6.6	31.3 ± 8.0

Table 5.7: Correlation Coefficients Between Systolic Blood Pressure before Sacrifice and Aortic Stiffness Factors. [Matsumoto *et al.* 1994]

Wks. After Operation	2	4	8	16
at 100 mmHg				
T/R_i	0.639	0.842	(0.626)	0.787
$H_{\theta\theta}$	(-0.181)	-0.711	(-0.261)	(-0.574)
at 200 mmHg				
T/R_i	0.682	0.775	(0.588)	0.843
$H_{\theta\theta}$	-0.706	-0.859	-0.673	-0.896

T/R_i = ratio between aortic wall thickness to inner radius.

$H_{\theta\theta}$ = incremental elastic modulus.

Parentheses indicate nonsignificant correlation.

determined by the elastic modulus of the vessel wall's material and the ratio of wall thickness to inner radius (T/R_i). Therefore, E_p increases with the increase of the incremental elastic modulus $H_{\theta\theta}$ and T/R_i. Matsumoto *et al.* calculated the correlation coefficients for T/R_i and $H_{\theta\theta}$ at pressures 100 and 200 *mmHg* with P_{sys} to determine the cause in change in wall stiffness for the hypertensive rats. **Table 5.7** shows that for pressures at both 100 and 200 *mmHg*, there is a significant positive correlation for wall thickness with P_{sys} with the exception of 8 weeks after the operation. The incremental elastic modulus showed a negative correlation with P_{sys} at 4 weeks for pressure of 100 *mmHg* while the rest of the correlation coefficients remained insignificant. At 200 *mmHg*, there was a significant negative correlation of the incremental elastic modulus with the in vivo P_{sys} at all time periods. Looking at the results of this table, it is evident that the stiffness of the blood vessel at low pressure is primarily due to aortic wall thickening. However, as stated previously, the vessel becomes more distensible at high pressures. **Table 5.7** indicates that this increased distensibility is caused by the decrease of elastic modulus compared to the control. The softening of the material in the vessel wall can be regarded as a form of adaptation of the aortic wall.

Relations between P_{sys} and the wall thickness as well as those between the pressure and outer and inner diameters of unloaded aortas were also examined. **Figure 5.14** illustrates these relationships showing a good correlation between wall thickness and P_{sys} as did the outer diameter of the unloaded vessels. The inner diameter, however, did not. This data suggests that the aortic wall thickening caused by hypertension occurs keeping the inner diameter almost constant. From this, it seems that the results indicate that the wall thickening occurs toward the adventitial direction in order to maintain the wall shear stress developed by blood flow at constant level, which is similar to Wolinsky's conclusion.

A comparison of circumferential stress and systolic blood pressure was also done for the three different pressure levels: P_{sys}, and 100 and 200 *mmHg*. The circumferential stress calculated for the systolic blood pressure was almost independent of this pressure, while the stresses varied at 100 and 200 *mmHg* with a negative correlation. **[Figure 5.15]** These results appear to indicate that the aorta wall thickens with the progress of

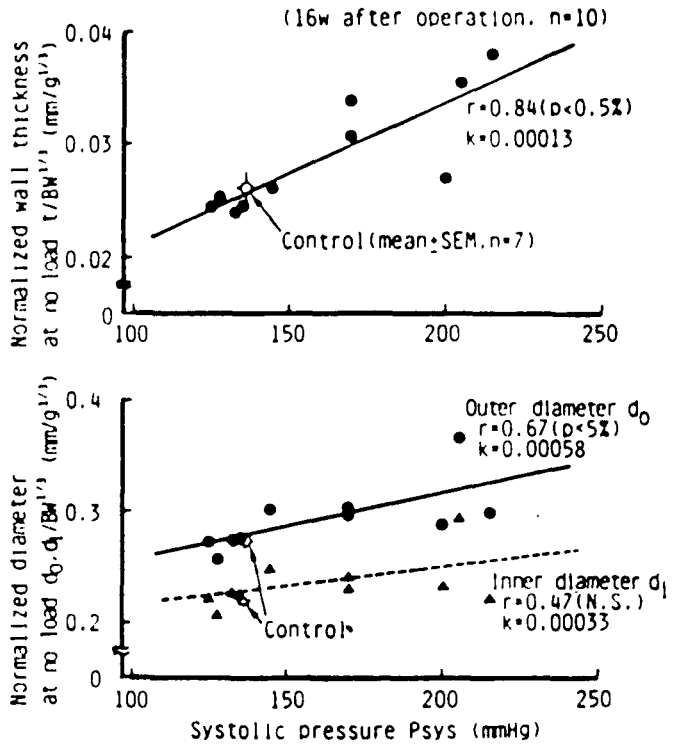

Figure 5.14: Systolic Blood Pressure Before Sacrifice Versus Normalized Wall Thickness and Normalized Diameter of Unloaded Rat Aortas at 16 Weeks. [Matsumoto *et al.* 1994]

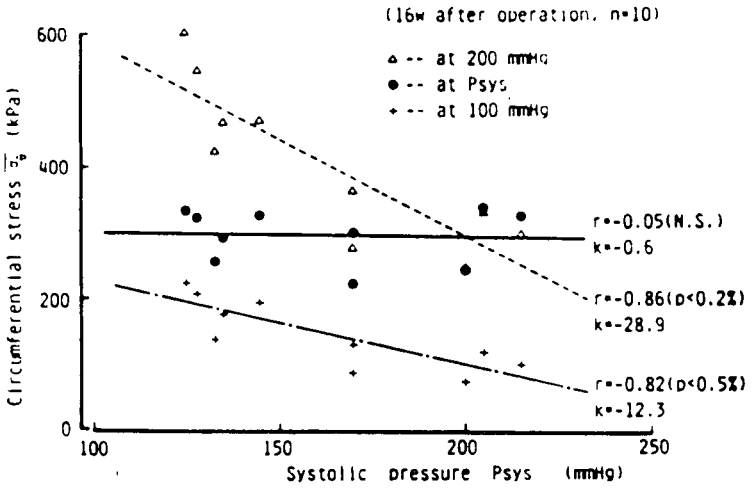

Figure 5.15: Systolic Blood Pressure Versus Circumferential Stress at Three Different Pressure Levels at 16 Weeks. [Matsumoto *et al.* 1994]

hypertension so that the blood vessel maintains a circumferential stress developed by the in situ blood pressure at a constant level. **Figure 5.16** shows the time-related changes of circumferential stress with systolic pressure. These graphs indicate the dimensional adaptation associated with wall thickening which occurs as the vessel wall responds to elevation of blood pressure as a constant circumferential stress is attempting to be maintained. In contrast, the incremental elastic modulus had significant correlation with blood pressure until 8 weeks after the operation; the higher the blood pressure, the stiffer the vessel wall. **[Figure 5.17]** If the blood pressure-wall elasticity relation was similar for all rats, the in vivo elastic modulus in vivo should be greater with higher blood pressure. However, at 16 weeks, the elastic modulus was independent of blood pressure suggesting that the aortic wall of the hypertensive animals wants to restore the in vivo elastic properties to normal after 16 weeks. Thus, it appears that the arterial distensibility is restored in hypertensive patients after a period of time. Nonetheless, the pressure-strain elastic modulus is still higher in the hypertensive animal than in the normotensive one because of wall thickening. From the observations of Matsumoto *et al.* it becomes evident that aortic wall adaptation to mechanical load occurs in two processes: (1) change in the wall thickness to keep stress in an optimal range, and (2) change in the wall elasticity to maintain wall function in an optimal fashion.

Assuming that such organs operate in a manner to achieve optimal performance, such mechanical and morphological changes can be attributed to adapation to a surrounding mechanical environment. From the aforementioned experimental studies, one can see that the biological tissues that compose the blood vessel change in response to the mechanical loading it experiences in order to maintain its normal functioning circumferential stress. Dimensional changes of hypertensive aortas occur to maintain the stresses developed at the same level as that in normal tissues and organs. This form of optimization to a particular stress level appears to be the objective of blood vessel tissue remodeling.

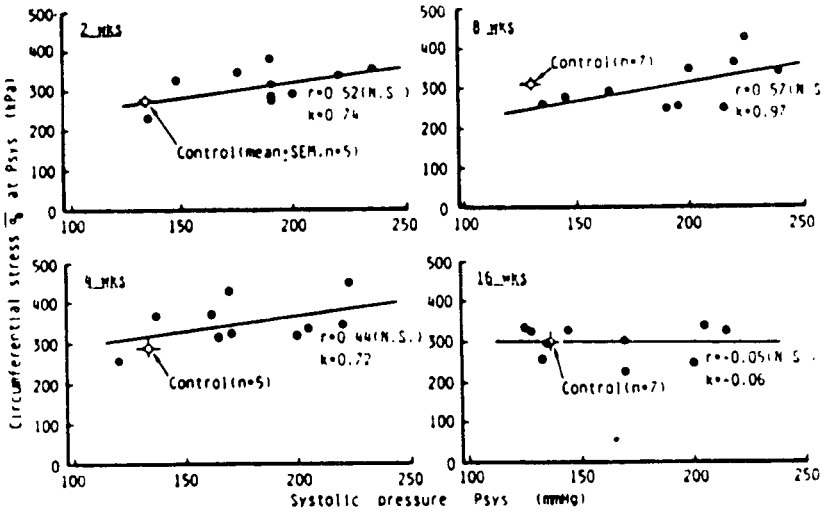

Figure 5.16: Systolic Blood Pressure Before Sacrifice of Each Rat Versus Circumferential Wall Stress at Different Time Periods (2, 4, 8, 16 Weeks). r = Correlation Coefficient, p = Its Significant Level, k (*kPa/mmHg*) = Gradient Regression Line. [Matsumoto *et al.* 1994]

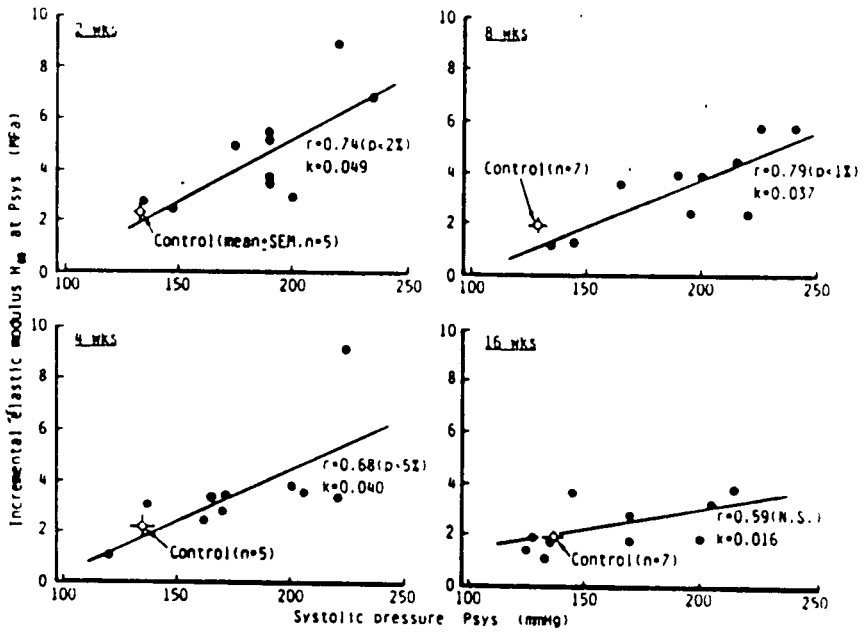

Figure 5.17: Relation Between Systolic Blood Pressure Before Sacrifice and Incremental Elastic Modulus. r = Correlation Coefficient, p = Its Significant Level, k (*kPa/mmHg*) = Gradient Regression Line. [Matsumoto *et al.* 1994]

5.4. *Conclusion*

With the examination of blood vessels, Kanda *et al.* (1993) give insight into the role of vascular cells in the morphological changes within these vessels. The authors show the inclination of SMCs to orient themselves perpendicular to the direction of stress while ECs tend to align themselves with the direction of flow with low turbulence and high shear rate. Experiments involving inducing hypertensive stress in aortic blood vessels by Wolinsky (1971, 1972) also show the remodeling effects of the tissues in the vessels to maintain a constant wall stress. Matsumoto *et al.*'s (1994) experiment on hypertensive rats also concludes the same thing as their findings show that the circumferential stress calculated for systolic blood pressure was independent of pressure. Thus, it seems that the aortic wall thickens with hypertension in order to maintain the vessel's circumferential stress developed by the in situ blood pressure. In addition, vessel wall distensibility was also an objective for remodeling such that optimal wall function could be maintained as the blood vessel transported blood away from the heart.

Other natural materials also appear the display this same phenomenon in order to achieve optimal performance. Remodeling to maintain a particular stress or strain is evident in the materials discussed in the previous chapters, and a comparison of these morphological adaptations will be discussed in the following concluding chapter.

References

Fung, Y.C. 1993. Biomechanics: Mechanical Properties of Living Tissues, 2nd. Ed., Springer-Verlag, New York.

Glagov, S., D.P. Giddens, R. Vito, H. Bassiouny, and C.K. Zarins. 1992. Tissue Reactions to Mechanical Stresses in Relation to Artery Wall Stability. *1992 Advances in Bioengineering*, ed. Martha Warren Bidez, v. 22, pp. 135-137.

Kanda, Keiichi and Takehisa Matsuda. 1993. Behavior of Arterial Wall Cells Cultured on Periodically Stretched Substrates. *Cell Transplantation*, v. 2, pp. 475-484.

Little, Robert C., M.D. 1977. Physiology of the Heart and Circulation, Year Book Medical Publishers, Inc., Chicago.

Matsumoto, T. and K. Hayashi. 1994. Mechanical and Dimensional Adaptation of Rat Aorta to Hypertension. *Journal of Biomechanical Engineering*, v. 113, pp. 278-283.

Rhodin, Johannes A.G. 1981. Anatomy of Microcirculation. In Microcirculation: Current Physiologic, Medical, and Surgical Concepts, eds. Richard M. Effros, Holder Scmid-Shonbein, Jorn Ditzel, Academic Press, New York.

Safar, Michael E. 1996. Arteries in Clinical Hypertension, Lippincott-Raven Publishers, Philadelphia.

Schoen, F.J. 1996. Cardiovascular System. Notes from course HST-030 dated September 24, 1996 for Harvard Medical School, Department of Health, Science, and Technology, Boston, Massachusetts.

Wolinsky, Harvey. 1971. Effects of Hypertension and Its Reversal on the Thoracic Aorta of Male and Female Rats. *Circulation Research*, v. 28, pp. 622-637.

Wolinsky, Harvey. 1972. Long-Term Effects of Hypertension on the Rat Aortic Wall and Their Relation to Concurrent Aging Changes. *Circulation Research*, v. 30, pp. 301-309.

Chapter 6: Conclusion

The major strategic function of structural materials and systems is that of mechanical support. Looking at bone, wood, plant stems, and blood vessels, it is evident that there is a link between structure and mechanical function. The studies of adaptive morphology reviewed in the previous chapters show that these materials are all able to remodel their structure to accommodate the changes in mechanical stresses that they experience. With increased mechanical load, each of these natural materials is able to increase its density, or in the case of plant stems and blood vessels, its wall thickness, through adaptive growth. As the materials are able to remodel their shape by increased growth, they seek a particular *objective* or form of structural optimization. Optimization of a natural material involves the minimization of the mass of the material required for some mechanical support requirement. Some general remodeling objectives or principles for materials include:

(1) Maximum allowable stress per unit weight of material is governed by a specific strength; maximum allowable elastic deformation per unit weight of material is governed by a specific modulus. This is usually seen in cases of simple tension where the cross-sectional shape will be in its simplest form and minimize surface area, i.e. rods and wires.

(2) For other static load types, maximum allowable stress is a function of cross-sectional shape as well as material properties. Maximum allowable deflection in a beam is governed by the flexural modulus (EI) which should be maximized in cases where elastic deformation must be minimized, or where excessive elastic deformation may lead to plastic deformation.

(3) The maximization of cross-sectional area or second moment or area (I) must not be driven to a point of local instability; the wall thickness of cylinder-shaped members should always be great enough to ensure that localized plastic deformation does not take place.

(4) When considering members whose primary need is energy absorption, a uniform cross-section helps eliminate local stress peaks.

(5) For weight and strength considerations, density also plays a role in attaining structural efficiency with materials that generally maintain a fixed modulus. In compressive buckling cases, density is a powered term, and small changes in density are more effective than increases in modulus when enhancing structural efficiency. [Wainwright *et al.* 1976]

Elements should not fail under the working conditions that are imposed upon it. Thus, the idea behind the adaptation of natural materials involves a change in its morphology in order to sustain a particular mechanical support requirement and avoid failure.

Bone is a unique material due to its ability to both deposit and resorb material with alterations in mechanical loading. Studies of hypertrophic activity resulting in increased mechanical stress have indicated an increased cortical bone thickness and cross-sectional area on loaded bones. Experiments which used periodic exercise, disuse with continuous superimposed compressive load, or disuse accompanied by dynamic loading were able to show that bone adaptation may be dependent on magnitude as well as rate of application of the load. This reinforces the notion that the stress and strain histories, which encompass such variations as magnitude, rate, frequency, duration, distribution, and direction, are all sources which regulate the remodeling response of bone. Bone also has the ability to resorb its tissue through its cells, the osteoclasts. Bone cells are sensitive to changes in mechanical loading, and thus tissue can respond with resorption when load is reduced. The common occurrence of bone atrophy is also an example of the remodeling that takes place in bone as long-term decreases in strain cause a reduction in cortical bone thickness and trabecular bone density. Two examples of bone loss due to atrophy are: immobilization studies and stress shielding around prosthetic stems due to the redistribution of loads leading to reduced cortical thickness and increased porosity. As bone undergoes morphological changes with variations in loading, it is able to optimize its shape to accommodate increases or decreases in loading by altering its bone density. This natural occurrence allows for efficient use of its material to maintain the material's factor of safety.

Wood exhibits a similar remodeling process, the only difference being that it cannot resorb tissue like bone. Reaction wood forms on trees in response to abnormal orientations of the tree. Brittle compression wood will push a bent tree into a correct geotropic position while tension wood tends to pull the tree into position. With reaction wood, a tree is able to adapt to any mechanical loading that it might experience to attain the shape which produces constant surface stress. Since a particular species of wood has roughly constant strength, this gives a constant factor of safety. Examining the contours

of trees, it also appears that reaction wood will also form in areas of high stress concentrations such as branch/stem joints and notches. This reinforces the idea that natural materials possess an inherent objective in their remodeling: a constant factor of safety. The shape of the tree stem is altered in such a way as to preserve its constant surface stress in order to reduce the risk of failure due to stress concentrations.

Taking a further look into plant life, we find morphological adaptations have also been described through thigmomorphogenesis, motion-induced inhibition of growth. Plant stems which have been mechanically perturbed by the rubbing of the stem display increased radial growth and inhibited stem elongation in the region of the stimulus. The two biomechanical factors involved in this thigmomorphogenic response include the hormone, ethylene, which is released during perturbation and the growth hormone, auxin, which stimulates ethylene production. Trees have also been influenced by thigmomorphogenic growth as wind loads impose forces that stress the tree stem and promote adaptive growth to produce a more streamlined structure that reduces wind drag. Looking at both plant stems and trees, it is evident that the morphological changes that take place serve to prolong the life of the plant as it undergoes environmental stresses. This response is a strategy for the plants to protect themselves against an antagonistic environment.

The biological tissues that make up the blood vessels are not foreign to adaptive growth as a phenomenon similar to the one seen in plant stems takes place in the aortic wall. Hypertension, which involves blood pressure elevation, acts as a mechanical stress on the vessel wall which produces morphological adaptations. The soft tissues that compose the aortic wall of hypertensive rats have been found to increase their thickness such that the vessel can maintain the circumferential stress at a similar level to a normotensive rat. Such a change in the vessel's dimensions can be attributed to smooth muscle cell hypertrophy and elevated amounts of elastin and collagen. It is apparent in studies of the effects of hypertension on aortic walls that the morphological adaptations which take place act as a means of maintaining a steady-state condition in the tissue. This type of growth is similar to what occurs in bone, wood, and plant stems in that all of these natural materials create more tissue in order to achieve a particular mechanical support

requirement for the material to prevent failure. With the evaluation of these natural materials, the remodeling objectives appear to possess some similarities which can be generalized into two categories: maintenance of stress or strain, and elasticity.

6.1. *Constant Stress and Strain*

Adaptive growth results in the deposition of tissue to the particular material involved, but what regulates the amount of tissue to be deposited? One possible factor is stress or strain. The previous examination of bone reveals that peak strain in bones from functionally equivalent sites are similar during the growth period. Irrespective of bone size and activity, **Table 2.1** shows that the peak strains of bones from different animals were within the range of 2000-3000 με. Studies by Wilson *et al.* (1979) and Mattheck (1989) show that reaction wood grows on trees in order to maintain constant surface stress. At the same time, the investigation of Wolinsky (1971, 1972) and Matsumoto *et al.* (1994) reveal that hypertensive aortic wall thickening occurs to keep the circumferential stress (ε = 0.2-0.3 with E≈1 *MPa*) due to blood flow at the same levels as in normotensive vessels. Unfortunately, the constant surface strain values for the finite-element analysis of the trees that Mattheck examined could not be attained from his study to use for comparison to the bone and blood vessel functional strain values, but it is apparent that these three materials all operate within a strain limit and use this value as their remodeling objective. **Table 6.1** summarizes the findings of these three materials by comparing yield strain (ε^*_y), peak functional strain ($\varepsilon_{functional}$), and safety factor. The values determined for cortical bone and the artery show that adaptive remodeling occurs to keep the material operating within a range of factor of safety.

As the induced loading on each of the different materials increases, dense growth occurs to increase the structure's cross-sectional area. This, in turn, reduces the stress or strain "felt" by the material and keeps the structure functioning within its original capacity before a change in load. Thus bone tissue growth due to hypertrophy is a result of attempting to keep the bone within its peak functional strain with a given safety factor.

Table 1: Summary of Material Strain Values.

Material	ε^{*}_{y}	$\varepsilon_{functional}$	Factor of Safety = $\varepsilon^{*}_{y}/\varepsilon_{functional}$
Cortical Bone[1]	0.004 - 0.011	0.002-0.003	2 - 4
Trabecular Bone[2]	0.008^{C} - 0.011^{T}	-	-
Wood[3]	0.0034	-	-
Artery[4]	2 - 4	0.2 - 0.3	100 - 200

[1] *Currey 1984*

[2] *Keaveny et al. 1994;* *C = Compression, T = Tension*

[3] *Illston 1979*

[4] *Wolinsky 1971, 1972;* *Matsumoto et al. 1994; Mohan et al. 1982*

Likewise, the reaction wood that grows in tree wounds acts to reduce the notch stresses that develop around the border of the wounded area so that a constant surface stress can be maintained. The stress distribution along a tree stem can also be affected by wind and gravity loads, and tree stems will thicken in regions of high bending and axial stress as stem shapes form in response to the time-averaged loads during tree life. The notion of maintaining a constant surface stress also holds for blood vessel remodeling as the increased thickness of the wall reduces the circumferential stress of the artery.

Each of these materials show that stress or strain values serve as mechanical support requirement in order to avoid failure of the material when it is subjected to an increase in loading. Hypertrophic growth prevents the accumulation of high levels of stresses and strains while attempting to preserve the material's mechanical function.

6.2. *Elasticity*

The biomechanical properties of a natural material also give insight into other mechanical support requirements, such as elasticity. Plant stems and blood vessels illustrate the role of elasticity in adaptive growth as each of the these materials alter their morphology and maintain flexibility when subjected to loading.

Jaffe *et al.* (1984) compare control and mechanically-perturbed bean plants and find that there is an increase in diameter and second moment of area for the experimental plant. However, a reduction of the elastic modulus was large enough to overcome the mechanically-perturbed plants' tendency toward stiffness. Thus overall flexibility was increased allowing the plant to continue to sway in such environments as wind without

rupture. The reduction of elastic modulus also occurred for pine saplings subject to rubbing or wind tunnel tests thus creating a more flexible plant stem structure. [Telewski *et al.* 1986b]

For the blood vessels, the elastic modulus was examined at variations of low and high blood pressure in hypertensive rats. [Matsumoto *et al.* 1994] The aortic stiffness of the artery was characterized through the ratio of wall thickness to inner radius and through the incremental elastic modulus. The pressure-strain elastic modulus (E_p) [1] which was used to help describe the stiffness of the aorta (see *Chapter 5: Blood Vessels*) at levels P_{sys} and 100, 200 *mmHg* **[Table 5.6]** and the correlation coefficients for the aortic stiffness factors between P_{sys} and the other two pressure levels **[Table 5.7]** reveal that stiffness at the low blood pressure is attributed to wall thickening. However, as pressure increased, the aortic wall changed its elasticity with decrease in E_p making the wall more distensible and enabling the artery to function as its normal value after a long period of time. Thus, in response to alteration of the applied force, dimensional changes appear much earlier than the change in elastic properties.

6.3. *Conclusion*

Natural materials have the advantage over man-made materials in their efficiency due to the fact that they are composed of living tissues which can remodel with changes in experienced loads. Because of their ability to grow and generate more tissue, they are able to produce the "best" designed structures for the material's particular function. Looking at the four materials discussed previously, it is evident that nature's designs are not random, but rather, possess particular mechanical support objectives in its remodeling and adaptive growth; these objectives attempt to prolong the life of the material and protect it from failure.

The study of natural materials can enhance studies in biomechanics through the examinations of their structures. Nature can provide clues into how to make stronger

---

[1] $E_p = \frac{\Delta P_i}{(\Delta D_o / D_o)}$ where ΔD_o is the increment of D_o (outer diameter) induced by the increment of P_i, (intraluminal pressure), ΔP_i

composites or improved building materials and designs, for example, by investigating materials which experience the same type of loads that the intended man-made material would. Already this discipline of *biomimetics* has been in practice for many years with one of the most notable pioneers, Leonardo da Vinci, who designed "flying machines" patterned after birds. More to date, scientists have also studied abalone, which produces mother-of-pearl. The abalone shell is composed of a chalk-like substance embedded in sticky protein layers, and its strength is achieved through the absorption of stress through tiny cracks. Taking this idea from nature, scientists are experimenting with adding graphite to a protein matrix similar to mother-of-pearl structure, but also having the ability to withstand high temperatures. [Dye 1996]

The studies of bone, wood, plant stems, and blood vessels done here could be useful in understanding the role of morphological adaptation to stresses in shape optimization. As a result, materials or structures which experience similar loading patterns can be modeled after them.

References

Currey, John. 1984. The Mechanical Adaptations of Bones, Princeton University Press, Princeton, New Jersey.

Dye, Lee. 1996. Why Is Wood So Strong? It Listened to Its Mother. *Los Angeles Times*, October 21, 1996, p. D6.

Illston, J.M., J.M. Dinwoodie, and A.A. Smith. 1979. Concrete, Timber and Metals: The Nature and Behavior of Structural Materials, Van Nostrand Reinhold Company, New York.

Jaffe, Mordecai J., Frank W. Telewski, and Paul W. Cooke. 1984. Thigmomorphogenesis: On the Mechanical Properties of Mechanically Perturbed Bean Plants. *Physiol. Plant*, v. 62, pp. 73-78.

Keaveny, Tony M., Edward F. Wachtel, Catherine M. Ford, and Wilson C. Hayes. 1994. Differences Between the Tensile and Compressive Strengths of Bovine Tibial Trabecular Bone Depend on Modulus. *Journal of Biomechanics*, v. 27, no. 9, pp. 1137-1146.

Martin, R. Bruce and David R. Burr. 1989. Structure, Function and Adaptation of Compact Bone, Raven Press, New York.

Matsumoto, T. and K. Hayashi. 1994. Mechanical and Dimensional Adaptation of Rat Aorta to Hypertension. *Journal of Biomechanical Engineering*, v. 113, pp. 278-283.

Mattheck, Claus. 1989. Engineering Components Grow Like Trees.

Mohan, Dinesh and John W. Melvin. 1982. Failure Properties of Passive Human Aortic Tissue: I - Uniaxial Tension Tests. *Journal of Biomechanics*, v. 15, n. 11, pp. 887-902.

Telewski, Frank W. and Mordecai J. Jaffe. 1986b. Thigmomorphogenesis: Anatomical, Morphological and Mechanical Analysis of Genetically Different Sibs of *Pinus taeda* in Response to Mechanical Perturbation. *Physiol. Plant*, v. 66, pp. 219-226.

Wainwright, S.A., W.D. Biggs, J.D. Currey, and J.M. Gosline. 1976. Mechanical Design in Organisms, Princeton University Press, Princeton, New Jersey.

Wilson, Brayton F. and Robert R. Archer. 1979. Tree Design: Some Biological Solutions to Mechanical Problems. *BioScience*, v. 29, no. 5, pp. 293-298.

Wolinsky, Harvey. 1971. Effects of Hypertension and Its Reversal on the Thoracic Aorta of Male and Female Rats. *Circulation Research*, v. 28, pp. 622-637.

Wolinsky, Harvey. 1972. Long-Term Effects of Hypertension on the Rat Aortic Wall and Their Relation to Concurrent Aging Changes. *Circulation Research*, v. 30, pp. 301-309.